2014

Modeling the interaction of complex networks

Wenjia Liu
Iowa State University

Modeling the interaction of complex networks

by

Wenjia Liu

A dissertation submitted to the graduate faculty

in partial fulfillment of the requirements for the degree of

DOCTOR OF PHILOSOPHY

Major: Physics

Program of Study Committee:

Beate Schmittmann, Major Professor

Royce Zia (Virginia Polytechnic Institute and State University)

James W. Evans

Sanjeevi Sivasankar

Alejandro Travesset-Casas

Eve Syrkin Wurtele

Iowa State University

Ames, Iowa

2014

DEDICATION

I would like to dedicate this thesis to my parents, Guangju Liu and Qinghong You, and my husband, Lunan Huang. Without their support, I would not have been able to complete this work.

Don't waste your time looking back on what you've lost. Move on, for life is not meant to be travelled backwards.

TABLE OF CONTENTS

LIST OF FIGURES

ACKNOWLEDGEMENTS

First and foremost, I would like to thank my thesis advisors, Professor Beate Schmittmann and Royce Zia, for accepting me into their scientific family, for their guidance, encouragement and support in the past four years. Their work ethics and passion for science have always stimulated me, and their advice on both research and my career has been priceless. I am also thankful for their understanding and help when I was going through personal difficulties. It is indeed a great honor for me to have worked with them.

I would also like to thank the rest of my thesis committee members, Professor James W. Evans, Sanjeevi Sivasankar, Alejandro Travesset-Casas and Eve Syrkin Wurtele, for their time and advice.

Many thanks to Professor Kevin E. Bassler, Shivakumar Jolad, Michel Pleimling, Leah B. Shaw and Zoltán Toroczkai, and Dr. Hyunju Kim and Thierry Platini for insightful discussions and suggestions.

I would additionally like to thank Lori Hockett and Christa Thomas for their enormous help. I must acknowledge all the friends here and back in China. I am so lucky to have them in my life.

Last but not the least, I would like to thank my family: my parents Guangju Liu and Qinghong You, and my husband Lunan Huang. Their constant support, love and care have gotten me where I am.

ABSTRACT

Many specific networks (e.g., internet, power grid, interstates), have been characterized well, but in isolation from one another. Yet, in the real world, different networks support each other's functions, and so far, little is known about how their interactions affect their structure and functionality. To address this issue, we introduce a stochastically evolving network, namely a preferred degree network, and study the interactions between such two networks. First, a homogeneous preferred degree network is studied. The resultant degree distribution is consistent with a Laplacian distribution, and an approximate theory provides good explanations. Second, another preferred degree network is introduced and coupled to the first following some specific rules. When the interaction is present, this system exhibits both interesting and puzzling features. Generalizing the theory for the homogeneous network, we are able to explain the total degree distributions well, but not the intra- or inter-group degree distributions. To develop a better understanding, we perform a systematic study of the number of inter-group links. We find that the interactions between networks have a profound effect. In certain regime of parameter space, mean-field approximations provide good insight into observed behaviors. Third, reminiscent of introverts and extroverts in a population, we consider an extreme limit of our two-network model. Using a self-consistent mean-field approximation, we are able to predict its degree distributions. Monitoring the total number of inter-group links between the two communities, we find an unusual transition, and succeed in predicting its key features. Finally, we present results for models involving several other forms of interaction.

CHAPTER 1. INTRODUCTION

1.1 Introduction to complex networks

In the past few years, studies on network systems have received extensive attention. Many real-world systems, e.g., the World Wide Web and the internet, have been examined in the context of a mapping to complex networks, which consist of a set of interconnected components that interact in various ways. For example, the World Wide Web [1, 2, 3] is essentially a set of web pages that interact through hyperlinks. The physical internet is built up by routers and computers, connected by wires. Not limited to the above two real-world examples, network structures can be recognized everywhere, in natural structures as well as man-made artifacts [4, 5, 6, 7, 8]. The former range from the microscopic, e.g., neuron architectures, to the cosmic, e.g., galactic filaments. For the latter, they include critical infrastructures, e.g., power grids and interstate systems, as well as virtual webs, such as Facebook and LinkedIn. Understanding their characteristics and behaviors is clearly important. Exploring these complex systems requires access to large scale data and powerful analysis methods. Thanks to the rapid pace of development in information technology, we are able to collect and analyze considerable amounts of data, to describe various features of these systems. At the same time, an interdisciplinary academic field, network science, is rapidly developing to study the network representation of physical, biological, and infrastructure systems, providing important concepts and tools to characterize and understand complex networks. This field has involved researchers from various areas, i.e., physics, mathematics, engineering, computer science, statistics, biology and sociology. Particularly, the underlying dynamic nature of these large size complex networks has attracted the attention of the statistical physics community. Among different methods and techniques used in network science, the statistical physics approach has been considered

as a useful and convenient strategy, due to its ability of dealing with large numbers of coupled degrees of freedom, and connecting the microscopic properties of individual components of a system to the macroscopic characteristics.

Dramatic advances have been made by the statistical physics community, in understanding the dynamics associated with complex networks. A network consists of a set of nodes connected by links, where the nodes represent elementary components and links represent some kind of interactions between pairs of components. For example, in a food web, the nodes are species and the links represent predator-prey relationships [9, 10, 11]. The topology of a network is specified by its pattern of connections. Studies on networks start from probing properties of the static networks, and then curiosity shifts to the dynamics coupled to network. Depending on the focus of network model, the dynamics is often classified into two patterns, dynamics of networks (e.g., the growth of the World Wide Web) and dynamics on networks (e.g., the disease spreading). According to different patterns of dynamics, in physics community, studies on complex networks are often arranged into three directions: (1) *Network topology (static networks and dynamics of networks)*: The earliest research on networks concentrates on the topological properties of static networks, e.g., study of Leonhard Euler on the Seven Bridges of Königsberg problem. More recently, the focus shifts to the topology of dynamic networks, i.e., the change of topological structure of network induced by the underlying, local laws. Studies in this field have unfolded that certain network topologies are invoked by specific evolution rules. Particularly, notable examples are small-world network [27, 17] and scale-free network [2] (see Chapter 2 for details for these two classes of networks). (2) *Dynamical processes on networks*: This aspect of network research has focused on the degrees of freedom on nodes (or links), and only the networks with static topology are under consideration. In such a network, each node can exist in different states, and its state can change dynamically (or variant flows are associated with links). For example, in a voter model, any given node (voter) can take one of two values on some issue, and its value can change under the influence of opinions of neighboring nodes. (3) *Adaptive coevolving networks*: The previous two lines of research treat dynamics of networks distinctly from the dynamics on networks. However, in real-world, the dynamics of networks depends on the topological properties of networks. As a result, attention

has been attracted to the merge of (1) and (2), leading to a new branch of study, dynamics of adaptive network. Take the epidemic spreading on a population for example. The topology of network (human contacts) influences the dynamic states of nodes (individuals), i.e., susceptible, infected, and recovered. On the other hand, the state of a node affects its connections, e.g., it is likely that a susceptible will avoid making contact with an infected, and this results in a decrease of links in the network. In that sense, a mutual interaction is established between topological evolution of the network and the dynamics of the nodes.

The above work within the physics community has successfully characterized the properties of many real-world networks [4, 5, 6, 7, 8], e.g., physical, social, biological, but in the context of a single, isolated network. Yet, in nature, different networks support the functions of one another, and are closely coupled together. For instance, electrical power grids serve internet communications, which in turn, rely on information exchange between power stations; highway use affects both air and rail traffic, and as a result, directly affects communication networks. More examples include the bank network and the network of commercial firms, food webs with common species, and protein networks with common proteins. In a word, complex networks are highly coupled to one another, and therefore, should be modeled as interdependent networks, or even in the context of a network of networks. In more recent years, the significance of interdependent networks has begun to be noticed by the physics community, and some aspects have been explored. Notable examples include the investigation of critical infrastructure interdependencies [96, 97, 98, 99], and approaches such as the multilayer method to couple traffic flows to physical infrastructures [87].

So far, relatively little work has been done on interdependent networks and many fundamental issues remain to be probed. A key issue is to model interactions between networks, i.e., to define a reliable model of interdependent networks, based on which one can pursue the same research program that was established for a single network, examining (1) *Network topology*, (2) *Dynamical processes on networks*, and (3) *Adaptive coevolving networks*, but on a model of interdependent networks. Of course, the final goal of this study is to answer the question of how to model a network of networks, and how it functions, but as a first step towards the goal, we focus on a simpler case, a system of *two* interdependent networks. Our work presented in

this dissertation aims at exploring several possible approaches to model the interaction between two networks, and further, understanding how the interactions affect the topological properties of each individual network. Specifically, this thesis is devoted to establishing a model of two interdependent networks, and analyzing (1) *Network topology.*

1.2 Outline of the dissertation

As mentioned before, so far, in the physics community, the understanding of interdependent networks remains limited, and little is known about how their interactions affect their structure and functionality. To address this issue, we introduce a sufficiently simple network model and study the interactions between such networks, using the language of social networks. The thesis consists of eight chapters. The first chapter is the current introductory chapter. This chapter starts with a brief introduction to complex networks and network science, followed by a thesis outline. Chapter 2 presents a description of several basic concepts and classical models of network science, and then provides a review of main results of earlier studies on complex networks, as well as a more detailed introduction of interdependent networks. In the following chapters, we introduce the idea of a stochastically evolving network, characterized by a set preferred degree κ. Based on this model, we introduce the interactions between two networks. In Chapter 3, we first focus on a single homogeneous isolated network. This chapter concentrates on the model description of a single preferred degree network. Each node with degree k can add (cut) its links with probability $w(k)$ $(1 - w(k))$, to reach and maintain κ. We examine the degree distribution in steady state with different forms of $w(k)$. Chapter 4 describes the quantities of interest for the two-network models and their notations (e.g., degree distributions ρ and the total number of cross links X). More importantly, Chapter 4 introduces a reference model of interdependent networks, by partitioning the single network into two identical sectors. This model establishes a baseline for our study of two-network models. Chapter 5 to 7 focus on different models of interdependent networks. Chapter 5 introduces a second preferred degree network and defines an interaction between the two networks, which allows for the formation of cross links. When the interaction is present, this model exhibits both interesting and puzzling features. Monitoring the total number of cross links between the two

communities, we find a very slow dynamics, as well as large fluctuations. This chapter presents a systematic study of the statistical properties of ρ and X as a function of the parameters of the two preferred degree networks. Chapter 6 studies an extreme case, dynamic network involving two networks: One set of nodes, labeled introverts (I), prefers no contacts, while the other, labeled extroverts (E), seek to maximize their degrees. With "maximal frustration" present, an unusual transition is observed in the system, as the ratio of network sizes N_1/N_2 is varied through unity. Remarkably, the system can be described in terms of a Hamiltonian, and some of its behaviors can be understood analytically. Chapter 7 presents simulation results and analytical explanations for two models involving other forms of interaction. Finally, Chapter 8 summarizes our work and ends with an outlook.

CHAPTER 2. LITERATURE REVIEW

While our studies focus on the topological properties (mainly the degree distribution) of interdependent networks, this chapter is devoted to *a much broader tour* of work having been done in the field of complex networks, including typical characteristics of network structures, classical models of networks, empirical studies on complex networks, and previous investigations of interdependent networks. Information in this chapter is based on several review papers and books [5, 6, 7, 8, 77].

2.1 Typical characteristics of complex networks

Complex networks are normally described in the language of graph theory. A graph is composed of a collection of mathematically abstract nodes (or vertices) which are connected by links (or edges). The two components of a graph, $G(V, E)$, are a set of nodes, V, and a set of links, E. Nodes in set V are assigned an index labeled i = 1, 2, 3,..., N, and links in E are represented by the two indexes associated with their end nodes, i.e., for i,$j \in V$, $E = (i, j) \in V \times V$. An adjacency matrix representation of a graph with N nodes is an $N \times N$ matrix, $\mathbb{A}$, specifying which nodes are connected to which other nodes. The non-diagonal entry A_{ij} is the number of edges from node i to node j, and the diagonal entry A_{ii}, is either once or twice the number of edges (loops) from node i to itself. Though multiple edges (more than one link having the same starting and ending nodes) exist in some real-world systems, e.g., collaboration networks [14, 15], most networks we will discuss later are simple graphs, where multiple edges or self-loops are not allowed. Therefore, we can narrow down the possible values

of A_{ij}:

$$A_{ij} = \begin{cases} 1 & \text{if there is a link from node } i \text{ to node } j, \\ 0 & \text{otherwise.} \end{cases} \tag{2.1}$$

Clearly, $A_{ii} = 0$ for all $i \in [1, N]$ when self-loops are prohibited. An asymmetric adjacency matrix can represent a directed graph, consisting edges carry a direction. In contrast, the adjacency matrix representation of an undirected graph is always symmetric.

With a mathematical representation of complex networks, let us turn our attention to the network properties. In the following, we introduce several structural characteristics usually considered, such as, degrees, their distribution, clustering coefficient, and average path length.

Degree and degree distribution

The degree is the simplest and most intensively studied single-node feature. In an undirected simple graph (without multiple edges or self-loops), the degree, k, of a node i, is defined as the total number of its links. Recall that the elements $A_{ij} = 0$ (1) indicate the absence (presence) of the link between nodes i and j. Then, the mathematical representation of k is simply $\Sigma_{j=1}^{N} A_{ij}$. For the case of a directed graph, where $A_{ij} \neq A_{ji}$ in general, the definition can be easily generalized. We coin the links merging into (going out from) node i as its incoming (outgoing) links. The associated degrees are in-degree, $k^{in} = \Sigma_{j=1}^{N} A_{ji}$, and out-degree, $k^{out} = \Sigma_{j=1}^{N} A_{ij}$. Clearly, the total degree is $k = k^{in} + k^{out}$.

The degree distribution, denoted by $\rho(k)$, is the normalized number of nodes with degree k. In other words, $\rho(k)$ is the probability that a randomly selected node has degree k. Clearly, an undirected graph can be described by a single degree distribution, for the total degree k. A directed graph, however, is characterized by four different degree distributions: The total degree distribution $\rho(k)$, the in-degree distribution $\rho^{in}(k^{in})$, the out-degree distribution $\rho^{out}(k^{out})$, and the joint degree distribution $P(k^{in}, k^{out})$. However, these distributions are not independent; they satisfy the following equations:

$$\rho(k) = \sum_{k^{in}} P(k^{in}, k - k^{in}) = \sum_{k^{out}} P(k - k^{out}, k^{out}), \tag{2.2}$$

$$\rho^{in}(k^{in}) = \sum_{k^{out}} P(k^{in}, k^{out}), \tag{2.3}$$

$$\rho^{out}(k^{out}) = \sum_{k^{in}} P(k^{in}, k^{out}). \tag{2.4}$$

Thus, the average degree is obtained easily: $\langle k \rangle = \sum_k k\rho(k)$. Accordingly, $\langle k^{in} \rangle = \sum_{k^{in}} k^{in}\rho^{in}(k^{in})$, and $\langle k^{out} \rangle = \sum_{k^{out}} k^{out}\rho^{out}(k^{out})$.

Clustering coefficient

To reflect the connections in the neighborhood of a node, the clustering coefficient is introduced. This quantity is noted in sociology first [16], as it is common to see that if individuals A and B are friends, and B and C are friends, then normally A and C are also friends. For undirected graphs, the degree to which nodes tend to group together is quantified by the clustering coefficient, which is high if the neighbors of a node have a high probability to be connected. Different definitions for this quantity exist, and here we present the one introduced by Watts and Strogatz [17]. For a node i with k_i neighbors, the maximum possible number of links within its neighborhood is $k_i(k_i - 1)/2$. Denoting by d_i the number of links among i's neighbors, the clustering coefficient of node i is given by,

$$C_i = \frac{2d_i}{k_i(k_i - 1)}. \tag{2.5}$$

for an undirected graph. With the definition of C_i for a node, the clustering coefficient of the network is defined as the average of C_i over all nodes i:

$$C = \frac{1}{N}\sum_i C_i. \tag{2.6}$$

Average path length

The average path length is a measure of average distance between any two nodes in a network. It answers questions like: What is the average number of clicks which leads us from one webpage to another? How many new connections we have to make, on average, to reach a stranger on Facebook? To define the average path length, l, which is a global measure, we need to introduce a local quantity first, the shortest path length between nodes i,j, l_{ij}. Given that the process

of going from a node to one of its neighbors is treated as one step, l_{ij} describes the minimum number of steps needed to reach node j from node i (or from j to i in case of undirected graphs). Based on l_{ij}, the average path length of a network is defined as

$$l = \frac{1}{N(N-1)} \sum_{i \neq j} l_{ij}, \tag{2.7}$$

where the average here is over all pairs of nodes, and $l_{ij} = 0$ if j can not be reached from i. Another similar measure of distance in a network is *diameter* of a network, D, which is the maximum shortest path in the network.

Degree distribution, clustering coefficient, and average path length are the three most frequently studied characteristics of networks. Fig. 2.1 shows some characteristics of several real networks, including but not limited to the three introduced above. In the following section, we will present a few representative network models that are frequently used, as well as their properties.

2.2 Network models

Models of networks provide a useful framework to understand empirical complex networks. Various models have been considered to generate network structures similar to real-world complex networks. The earliest model is the Erdős-Rényi random graph model. Two other well-known and much studied examples of network models are those of the Watts-Strogatz small-world and Barabási-Albert scale-free models. This section serves to introduce these three commonly cited models, as well as their key characteristics. In later chapters, we will see that the model we are introducing is distinct from the three.

Erdős-Rényi random graph model

In the 1960s, Erdős and Rényi published a series of papers [18, 19, 20], introducing the random graph model and its properties. The random graph is denoted by $G(N, p)$, where N is the number of nodes in the network, and p serves as the probability with which a pair of nodes is connected. The same p applies to all $N(N-1)/2$ pairs of nodes. Clearly, on average, this

Network	Size	$\langle k \rangle$	ℓ	ℓ_{rand}	C	C_{rand}	Reference
WWW, site level, undir.	153 127	35.21	3.1	3.35	0.1078	0.00023	Adamic, 1999
Internet, domain level	3015–6209	3.52–4.11	3.7–3.76	6.36–6.18	0.18–0.3	0.001	Yook *et al.*, 2001a, Pastor-Satorras *et al.*, 2001
Movie actors	225 226	61	3.65	2.99	0.79	0.00027	Watts and Strogatz, 1998
LANL co-authorship	52 909	9.7	5.9	4.79	0.43	1.8×10^{-4}	Newman, 2001a, 2001b, 2001c
MEDLINE co-authorship	1 520 251	18.1	4.6	4.91	0.066	1.1×10^{-5}	Newman, 2001a, 2001b, 2001c
SPIRES co-authorship	56 627	173	4.0	2.12	0.726	0.003	Newman, 2001a, 2001b, 2001c
NCSTRL co-authorship	11 994	3.59	9.7	7.34	0.496	3×10^{-4}	Newman, 2001a, 2001b, 2001c
Math. co-authorship	70 975	3.9	9.5	8.2	0.59	5.4×10^{-5}	Barabási *et al.*, 2001
Neurosci. co-authorship	209 293	11.5	6	5.01	0.76	5.5×10^{-5}	Barabási *et al.*, 2001
E. coli, substrate graph	282	7.35	2.9	3.04	0.32	0.026	Wagner and Fell, 2000
E. coli, reaction graph	315	28.3	2.62	1.98	0.59	0.09	Wagner and Fell, 2000
Ythan estuary food web	134	8.7	2.43	2.26	0.22	0.06	Montoya and Solé, 2000
Silwood Park food web	154	4.75	3.40	3.23	0.15	0.03	Montoya and Solé, 2000
Words, co-occurrence	460.902	70.13	2.67	3.03	0.437	0.0001	Ferrer i Cancho and Solé, 2001
Words, synonyms	22 311	13.48	4.5	3.84	0.7	0.0006	Yook *et al.*, 2001b
Power grid	4941	2.67	18.7	12.4	0.08	0.005	Watts and Strogatz, 1998
C. Elegans	282	14	2.65	2.25	0.28	0.05	Watts and Strogatz, 1998

Figure 2.1 This figure shows information of structural properties of several real networks. For each network, the number of nodes, the average degree, the average path length, and the clustering coefficient are denoted by size, $\langle k \rangle$, l, and C, respectively. l_{rand} and C_{rand} indicate the average path length and clustering coefficient of a random graph of the same size and average degree. Image is taken from [5] with permission of the American Physical Society.

model has $\binom{N}{2}p$ links, and the degree distribution is a binomial distribution,

$$\rho_{ER}(k) = \binom{N-1}{k} p^k (1-p)^{N-1-k}. \tag{2.8}$$

In the limit of $N \to \infty$, the above distribution reduces to a Poisson distribution,

$$\rho_{ER}(k) \to \frac{(Np)^k e^{-Np}}{k!}, \text{ as } N \to \infty \text{ and } Np = const. \tag{2.9}$$

Therefore, most nodes of the graph have average degree $\langle k \rangle = (N-1)p \simeq Np$. It is easy to see that the random graph model has a low clustering coefficient: The probability of two nodes being connected is p, regardless of whether they share a common neighbor, and therefore, $C = p$, which decreases to 0 as $N \to \infty$ and $Np = const.$ The average path length of the Erdős-Rényi random graph is estimated as $l \simeq lnN/ln(Np)$ [21]. It can be roughly understood by the following arguments: Within d steps, the number of nodes can be reached from a node is $\langle k \rangle^d$. Suppose within $\tilde{l}$ steps, a node can reach all the nodes of the graph, then $\langle k \rangle^{\tilde{l}} \simeq N$. Thus, the distance through the network is $\tilde{l} = lnN/ln\langle k \rangle \simeq lnN/ln(Np)$.

Due to its simplicity and understandable properties, the random graph model of Erdős-Rényi remains one of the most important models. However, with low clustering coefficient and Poisson degree distribution, it fails to capture some characteristics of real-world networks. For instance, many social networks [22, 23, 24, 16] are highly clustered, and possess a small average shortest path between nodes. Moreover, most real-world networks, including the World Wide Web and the internet, exhibit power-law degree distributions instead of Poisson distributions [2, 25, 26]. For that reason, two other popular models have been developed and much studied.

Watts-Strogatz small-world model

The key feature of small-world network models is that, most nodes in the network are not neighbors of one another, but there is a relatively short path between any pair of nodes, despite the large graph size. The most widely studied small-world model was proposed by Watts and Strogatz in 1998 [27, 17]. The model is built as follows. It starts with a ring of N nodes, each connected to $2e$ nearest nodes (e nodes clockwise and counterclockwise, respectively). This results in a ring lattice with Ne links. Then, for each node, every link (connected to a clockwise neighbor) is rewired with probability p, or preserved with probability $1-p$. For the

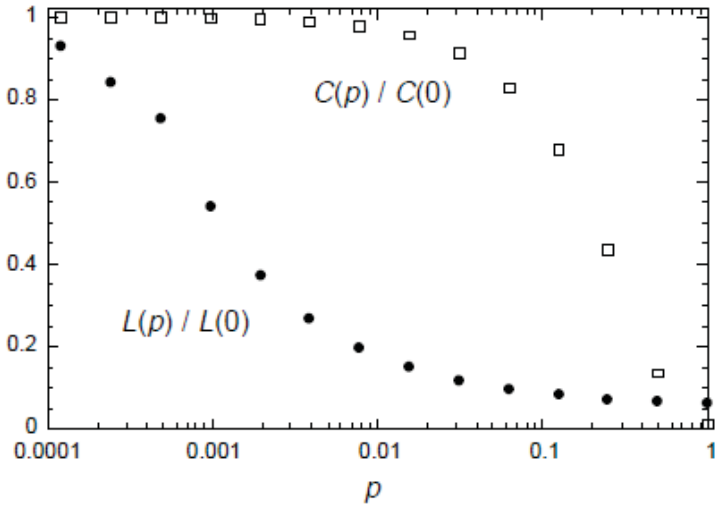

Figure 2.2 This figure shows path length $l(p)/l(0)$ and clustering coefficient $C(p)/C(0)$ as a function of p, for the Watts-Strogatz model. Image is taken from [17] with permission of the Nature Publishing Group.

case of rewiring, the link is reconnected to a randomly chosen node, such that no multiple edges or self-loops are allowed. This process introduces pNe far connections, and makes it possible to interpolate between a regular lattice ($p = 0$), and a classical random graph ($p = 1$). As $p \to 0$, $l(p) \sim N/4e \gg 1$ and the clustering coefficient is $C(p) \sim 3/4$. As $p \to 1$, $l(p) \sim lnN/ln(2e)$ and $C(p) \sim 2e/N \ll 1$, attaining the value for classical random graphs. In the intermediate region (see Fig. 2.2), $l(p)$ falls very rapidly due to the appearance of shortcuts between nodes, while $C(p)$ remains quite close to the high value for the regular lattice, only falling at relatively high p, and this is the so called small-world property.

Barabási-Albert scale-free model

The scale-free models describe the class of networks that exhibit a power-law degree distribution, and so far, many observed networks fall into this class [28]. In the late 1990s, Barabási and Albert proposed a model to explain the appearance of power-law distributions [2], where the key underlying mechanism is growth and preferential attachment of nodes [2, 29, 30]. The model is established as follows:

- *Growth*: The network starts with a small number, m_0, of nodes, connected to one another.

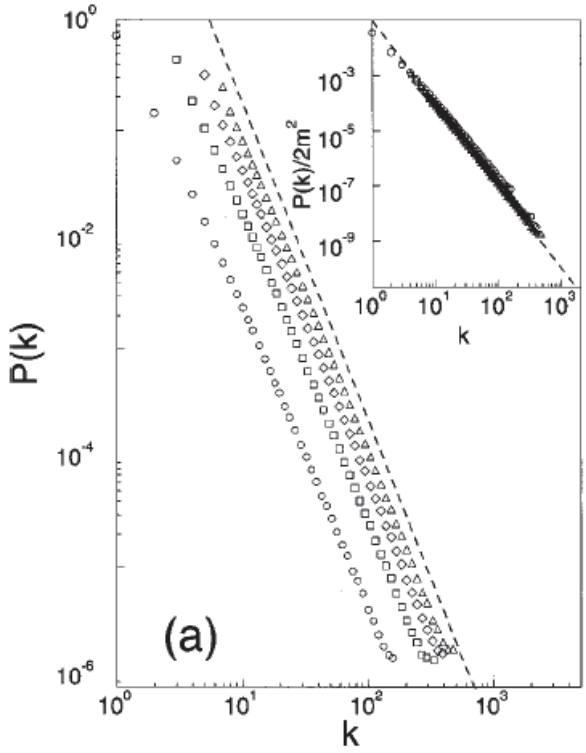

Figure 2.3 This figure shows degree distribution of the Barabási-Albert model: $N = m_0 + t = 300000$ and $m_0 = m = 1$ (circles), $m_0 = m = 3$ (squares), $m_0 = m = 5$ (diamonds), and $m_0 = m = 7$ (triangles). The slope of the dashed line is $\gamma = 2.9$. The inset shows the rescaled distribution $P(k)/2m^2$ for the same values of m, the slope of the dashed line being $\gamma = 3$. Image is taken from [29] with permission of the Elsevier.

At each time step, a new node with m ($\leq m_0$) links is added in, and it is connected to m nodes already existing in the network.

- *Preferential attachment*: The probability, Π, that an old node i will be selected to make a connection with the new node is determined by its degree k_i, and Π is given by

$$\Pi = \frac{k_i}{\sum_j k_j}. \tag{2.10}$$

After t time steps, the resultant network contains $N = m_0 + t$ nodes and $mt + m_0(m_0 - 1)/2$ links. The numerical simulations indicate that the graph generated with this algorithm evolves into a power-law with the form $\sim k^{-3}$ (see Fig. 2.3).

2.3 Overview of studies on complex networks

Though complex networks have been widely studied by researchers from different disciplines, their interest lies in three aspects: topological properties of networks, network evolution (growth), and dynamical processes on networks. In this section, we present the main contributions and results in the three fields.

Network topology of select real networks

Social networks. A social network describes a group of individuals/organizations with interactions among them [16]. The forms of interaction vary from friendship between individuals [33] to business cooperation between companies [31, 32]. Examples of the earlier studies on social networks include, Moreno's graphical depictions of networks of friendships within small groups [33], the social network study of factory workers in the late 1930s in Chicago [34], and the important "small-world" experiment of Milgram [22, 23], often associated with the phrase "six degrees of separation." Besides that, more recently, the web of human sexual contacts [35] and business communities also have received particular attention. Due to lack of storage technology and inability to collect large scale data, earlier studies of social networks often had drawbacks, e.g., inaccuracy and small data samples. Thanks to the rapid pace of development in information technology, nowadays, researchers are enabled to access considerable amounts of reliable data, and therefore, they turn attention to the type of networks with good records, e.g., coauthorship of scientists [36, 37, 38, 39, 14, 15, 40, 41] and movie actor collaboration network [17, 42, 43, 21], where nodes and links stand for individual authors/actors and collaboration, respectively. Both networks are found to have power-law degree distributions $\rho(k) \sim k^{-\gamma}$, where γ varies between 2.1 to 2.5. Besides, the movie actor collaboration exhibits a high clustering coefficient, more than 100 times higher than a random graph [17]. *Information networks.* The citation network of scientific publications belongs to this category. The reason for that is when an old article is cited by later articles, the information of the old one is shared and spread on the network. A citation network should be a directed graph, where academic articles are nodes and the references to previously published papers are represented by directed links [44, 45, 46, 47, 48, 49, 50, 51, 52, 53]. Redner's study on papers published in 1981 in journals,

catalogued by the Institute for Scientific Information, and 20 years of publications in Physical Review D, suggests that the in-degree distribution follows a power-law with exponent $\gamma \simeq 3$ [47]. Another much studied information network is the World Wide Web (WWW), which is the largest network with available topological information [1, 2, 3, 30, 54, 55, 56]. Though the WWW has a large number of nodes, it is reported to display small-world property, with low average shortest length. Moreover, a lot of attention has been paid to its evolution, which is well explained by the Barabási-Albert scale-free model [2]. *Biological networks.* Examples of biological networks include metabolic networks [57, 58, 59, 60, 61], food webs [9, 62, 10, 63, 64, 11, 65], neural networks [66, 67], and so on. In a network of metabolic pathways, nodes are metabolic substrates and products, joined by links of directed chemical reaction, that involve given substrates and products. Its degree distributions, both in- and out-degree, follow power laws for all organisms, and the degree exponent varies between 2.0 and 2.4. A food web represents predator-prey relationships between various species. It also indicates energy flow from prey to predator when the prey is eaten. Studies of food webs have focused on their topology [9, 11, 10]. Particularly, their degree distribution is found to be consistent with a power-law with a small exponent of $\gamma \simeq 1.1$. Neural networks are also a class of biological networks of considerable importance. Studies have concentrated on their topology, functional areas and pathways.

Dynamical processes on networks

While the above studies have focused on the topological evolution of networks, often referred as "dynamics of networks," another major trend of research on complex networks has concentrated on "dynamics on networks" [68]. In this study, the network under consideration is static, i.e., topology of the network remains unchanged, while the state of nodes changes dynamically. Typical examples of this study are opinion formation and epidemic spreading. Many models, e.g., voter models, or epidemic models (such as susceptible-infected-susceptible (SIS) model and the susceptible-infected-recovered (SIR) model), have been widely studied on regular lattices [69], and random [70], scale-free [71, 72], or small-world [73, 74, 75] networks.

Adaptive coevolving networks

An assumption of the above studies is that the contact process takes place on a static network. In more recent works, more realistic situations are considered, where the dynamics *of* networks

and dynamics *on* networks are coupled together. A non-trivial feedback loop connects the two features, which in turn, gives rise to a mutual interaction between the state and topology of the network [76, 77]. Naturally, the coupling of dynamical processes on networks and the evolution of the underlying topological structure, namely, coevolution of adaptive networks, starts to attract increasing attention. Some examples of such studies are the opinion dynamics on an adaptively changing network [78, 79, 80, 81, 82, 83], and adaptive epidemic network models [76, 84]. (A review on the adaptive coevolving networks can be found at [77].)

2.4 Interdependent networks

In the previous sections, we have briefly overviewed the work on biological, social, infrastructure, or technological networks. Almost all these studies have focused on a particular case, where the network under consideration is isolated from the rest of the world. However, such a situation rarely exists in nature, and instead, individual networks are often elements of a large system, where several coexisting networks interact and support the function of one another [85, 86, 87, 88, 89, 90]. So far, there is one class of interdependent networks, the protein interaction networks, that have been widely investigated in the biology community [91, 92, 93, 94, 95]. These networks represent biological processes regulated by a number of proteins. Since one given protein participates in different processes, the networks are interdependent. Other than this class of networks, other modern systems are becoming more and more mutually coupled, and little is known about their interaction. For instance, smartphones can help drivers avoid heavy traffic. This situation cannot be fully described in terms of a single network, whether we focus on cellular communication or the transportation (road) network. An even more complicated example of interdependent networks is the whole system of infrastructure networks, containing airlines, ground transportation, power grids, and telecommunications, all highly coupled to each other. Meanwhile, the internet plays a critical role by interacting with all of them. It is clear that the significant, mutual dependence of real-world networks can not be ignored, and therefore, models of interdependent networks are desired, culminating perhaps, in a "theory of networks of networks."

In recent years, the significance of interacting networks is coming onto center-stage, and

many scientists and engineers turn their attention to various aspects of such interactions. Notable contributions include the following. To study the load distribution in three transportation systems, Kurant and Thiran introduce a layered model, coupling traffic flows to physical infrastructures [87]. Buldyrev et al. first propose a model of two-interdependent networks, where the nodes in either network require support from another, and in turn, the failure of nodes in one network can cause the failure of neighboring nodes in the other network. This process can happen recursively, and then, lead to a cascade of failures. Based on that model, they study the robustness of critical infrastructure networks with interactions [96, 97, 98, 99]. Besides, they take further steps towards the cascading failures of other type of networks, e.g., a financial system modeled by a bi-partite banking network [100]. At the same time, similar work on the failures in interconnected networks has been published by other authors, Leicht and D'Souza [101], and Vespignani [102]. In [103], Parshani et al. claim that real interdependent networks are usually not randomly interdependent, and instead the coupled nodes crossing networks are connected according to some regularity, which is coined inter-similarity by the authors. Based on simulation and analysis of the port-airport system, they report that, as the networks become more inter-similar, the system becomes significantly more robust to random failure. Another recent work on robustness and restoration of interaction networks, focusing on ecological networks, reported by Pocock et al. [104], is to understand the effects of species' declines and extinctions.

CHAPTER 3. HOMOGENEOUS PREFERRED DEGREE NETWORKS AND THEIR STATISTICAL PROPERTIES

To model the interaction between two networks, we start with a single homogeneous network, so that a baseline can be established. In this chapter, a new type of network model is introduced, followed by a discussion of its statistical properties. Accordingly, this chapter consists of two sections: The model description of a single-network model, and simulation results and theoretical explanations for its degree distribution.

3.1 Model specifications

Our single-network model consists of N nodes (with no degrees of freedom), and a set of dynamically evolving links. A single network is a homogeneous population, each node preassigned the same preferred degree, κ [12, 13, 105, 106, 107, 108]. By adding/cutting links, all nodes tend to reach and maintain their number of links (degree), k, at κ. Given that a node has k links, the probability for it to add (cut) a link is $w(k)$ $(1-w(k))$. $w(k) \in [0,1]$ is referred to as a *rate function*. Clearly, we can choose different rate functions, w_+ and w_-, to describe the preference of adding and cutting a link, respectively, but for the sake of simplicity, here we only consider the case where $w_- = 1 - w_+$. To reach the preferred degree, the nodes are supposed to add links when they have fewer links, while they should cut links when they have more links than κ. That is, we need a $w(k)$ which has larger values at lower k and smaller values at larger k. Clearly, the rate functions $w(k)$ plays a role of describing the tolerance level (or flexibility) of an individual. For example, if $w(k) = \Theta(\kappa - k)$ (Heavyside step function), this model represents an extremely rigorous population, which restrictively keep κ contacts and are unhappy with one more/less friend. On the other hand, if $w(k)$ changes its value from 1 to 0

more slowly, this model describes a more flexible population, which prefers to have κ contacts though, having a few more/less friends will also be fine. Of course, there are many possible ways to define $w(k)$, and we choose the form of the well-known Fermi-Dirac function:

$$w(k) = \frac{1 + e^{-\beta\kappa}}{1 + e^{\beta(k-\kappa)}}. \tag{3.1}$$

In this form, the flexibility of individuals is reflected by a parameter β. For the most rigid population, we choose $\beta \to \infty$, so that w becomes a step function: $w = 1$ if $k \leq \kappa$, and 0 otherwise. For more flexible population, finite β is selected. (In simulations, κ is chosen to be a half integer, so that no ambiguity should arise.)

Given the form of the rate function, the network is updated according to the following steps. All simulations start with an empty network, where every node is isolated from one another. In each time step (attempt), a node is randomly selected from the N nodes, and its degree, k, is noted. Next, a random number, r, valued between 0 and 1, is generated. If $r < w(k)$, the chosen node will create a new link to a randomly chosen node not already connected to it. Otherwise, it breaks an existing link at random. The partner node has no control of the updating actions. Additionally, multiple edges or self-loops are not allowed.

3.2 Simulation results and theoretical considerations

With the stochastic rules above, we perform Monte Carlo simulations on the network with the following selected parameters: reasonably large $N = 1000$, $\kappa = 250$ (which is not too small or too large compared to the network size), and three different rate functions with $\beta = 0.1$, 0.2 and ∞, respectively (see Fig. 3.1(a)). In the simulation, we update one link and generate a new configuration at each attempt. One Monte Carlo step (MCS) is defined as N such attempts, so that, on average, each node is ensured to have the chance to be picked once and update its links. For a single-network model, we discard the first $1K$ MCS, which appears to be sufficient here for the system to reach steady state. Thereafter, we measure the quantities of interest every 100 MCS and compile averages from 10^4 measurements (i.e., runs of $1M$ MCS).

To characterize the structure of the network and find out how individuals are connected in a preferred degree network, an immediate quantity to examine is the degree distribution in

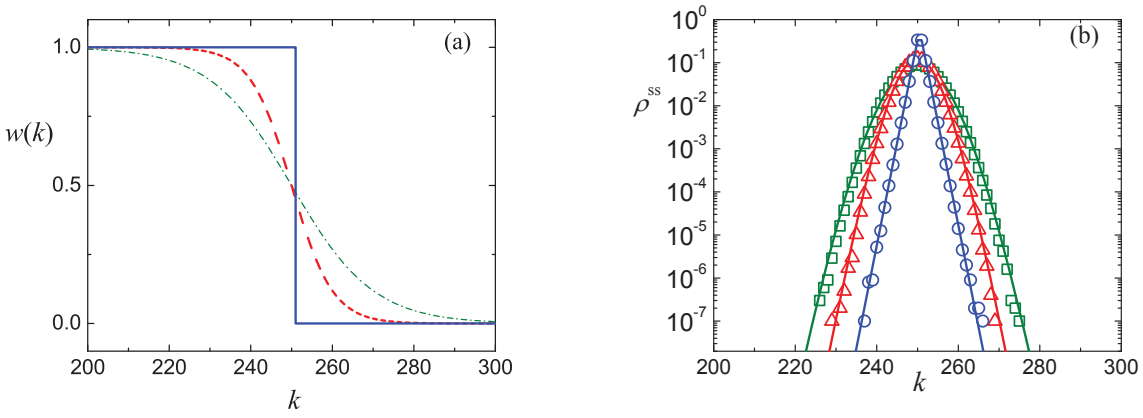

Figure 3.1 (a) shows different $w(k)$'s for $\kappa = 250$: Fermi-Dirac functions $w(k) = (1 + e^{-\beta\kappa})/(1 + e^{\beta(k-\kappa)})$, with $\beta = 0.1$ (green), 0.2 (red) and ∞ (blue). (b) shows corresponding degree distributions of the system with $N = 1000$, $\kappa = 250$, and different $w(k)$'s: $\beta = 0.1$ (green squares), 0.2 (red triangles) and ∞ (blue circles). The solid lines in (b) are theoretical predictions.

steady state, which is the average fraction of nodes with k links. Denoting by n_k the number of nodes with k links in each measurement, we define the degree distribution $\rho(k)$ by:

$$\rho(k) = \frac{\langle n_k \rangle}{N}. \tag{3.2}$$

Typical simulation results of $\rho^{ss}(k)$ (with superscript ss denoting "steady state") of the single-network model are shown in Fig. 3.1(b). As expected, $\rho^{ss}(k)$ is centered at κ. However, unlike the Erdős-Rényi random network, our simulations show that $\rho^{ss}(k)$ does not, in general, follow the Poisson distribution. Instead, the form of $\rho^{ss}(k)$ varies depending on the details of $w(k)$: As $w(k)$ is reduced to a Heavyside step function by letting $\beta \to \infty$, $\rho^{ss}(k)$ is consistent with a symmetric exponential distribution, $\propto e^{-\mu|k-\kappa|}$ (blue circles in Fig. 3.1(b)). Our data indicate $\mu = 1.08 \pm 0.01$. If $w(k)$ differs from the extreme case ($0 < \beta < \infty$), $\rho^{ss}(k)$ is Poisson like in $k \sim \kappa$, crossing over to the same exponential tails (green squares and red triangles).

To understand the behavior of the degree distribution, let us turn to a theoretical description of the model. Though the dynamics of this model is very simple, the process of link updates does not obey detailed balance. As a result, solving the exact master equation (6.7) is challenging

(see Appendix A for details). However, instead of working with the exact master equation, we find the behaviors of degree distribution can be explained well in the context of an approximate master equation:

$$\begin{aligned}\Delta\rho(k,t) &\equiv \rho(k,t+1) - \rho(k,t) \\ &= W[k,k+1]\rho(k+1,t) + W[k,k-1]\rho(k-1,t) \\ &- (W[k+1,k] + W[k-1,k])\rho(k,t)\end{aligned} \tag{3.3}$$

where $W[k,k+1]$ specifies the probability for a node with degree $k+1$ to change to the state with degree k, $k \in [0, N-1]$. The right hand side of this equation can be written as difference of two currents, i.e., $\Delta\rho(k,t) = (W[k,k+1]\rho(k+1,t) - W[k+1,k]\rho(k,t)) - ([W[k-1,k])\rho(k,t) - W[k,k-1]\rho(k-1,t))$. For $k \geq 0$, of course, we impose the boundary condition: $\rho(-1,t) = 0, W[0,-1] = W[-1,0] = 0$. In the steady state, the distribution $\rho^{ss}(k)$ satisfies $\Delta\rho^{ss}(k) = 0$, as well as all currents being vanishing. Therefore, we obtain

$$W[k-1,k]\rho^{ss}(k) = W[k,k-1]\rho^{ss}(k-1). \tag{3.4}$$

To solve this equation, our next step is to determine the rates, $W[k,k-1]$ and $W[k-1,k]$. Focusing on a randomly chosen node i with degree k_i, we notice that, in each attempt, the probability to select node i is $1/N$, and the rate for the node itself to create (destroy) a link is just $w(k_i)\ (1 - w(k_i))$. Besides, the remaining $N-1$ nodes also contribute to updating links of i, i.e., the degree of i can be changed by the other $N-1$ nodes taking action on a link to i. Of these nodes, there are k_i nodes already connected to node i (group A) and $N-1-k_i$ ones disconnected (group B). In all cases, approximately half of them have degree less than κ, so that the probability that any one among those $N-1$ nodes will create or break a link is $1/2$. Now, consider a node j, with degree $\tilde{k}_j$, in group A, which is selected with probability $1/N$. With probability $1/2$, j will cut one of its links, and the probability that this is the link to node i is $1/\tilde{k}_j$. We approximate $k_i \simeq \kappa$, and $\tilde{k}_j \simeq \kappa$, so the rate for any of the links attached to i to be cut by other nodes is $k_i \times 1/2 \times 1/\tilde{k}_j \times 1/N \simeq 1/(2N)$. Similarly, the rate for the group B nodes to create a link to our node is also $1/(2N)$. Thus, we get the rates $W[k,k-1] \simeq (w(k-1)+1/2)/N$ and $W[k-1,k] \simeq (1-w(k)+1/2)/N$, which leads Eqn. (3.4)

to:

$$\frac{\rho^{ss}(k)}{\rho^{ss}(k-1)} = \frac{w(k-1)+1/2}{1-w(k)+1/2} \tag{3.5}$$

(shown as solid lines in Fig. 3.1(b)), which is in excellent agreement with our simulation results.

CHAPTER 4. QUANTITIES OF INTEREST AND A BASELINE MODEL OF INTERDEPENDENT NETWORKS

The knowledge of a single homogeneous preferred degree network provides a baseline for our study of interdependent networks. In the real world, we rarely observe single isolated networks with distinct topology. What is more common is the coexistence of multiple networks, interacting and supporting the function of one another. We take a first step towards the study of topological properties of interdependent networks, by looking at a model of *two* interacting networks. In this chapter, we will introduce several quantities of interest and their notations for the interacting networks model. We will also introduce a very simple model for two coupled networks, which will serve as a baseline for our studies of more sophisticated models. These models will be discussed in the following three chapters.

4.1 Quantities of interest

With one more network in the system, more quantities need to characterize the networks. Here, let us leave the details of the model description to the next section, and start with an introduction of quantities of interest and their notations. Suppose we have two preferred degree networks of size N_1 and N_2, respectively. Each network represents a homogeneous population, having its own preferred degree κ_1 (κ_2). For each node in the system, there are two types of links, the links to nodes in the same network (internal links or intra-group links) and the links across two networks (cross links or inter-group links). Accordingly, besides a total degree, k_α ($\alpha = 1, 2$), which has been well described in our study of a single-network model, in the two-network model, there are two more types of degrees, namely the internal degree, k^*_α, and the cross degree, $k^\times_\alpha$. By definition, for each node, its degrees obey the relation $k_\alpha = k^*_\alpha + k^\times_\alpha$.

A specific example of $(k_1^*, k_1^\times, k_2^*, k_2^\times)$ is provided in Fig. 4.1. Different types of degrees lead to more degree distributions. We refer to the degree distribution discussed for the single-network model as total (or global) degree distribution, ρ_α, which is associated with the total degree k_α. In addition, there are four more detailed degree distributions, $\rho_{\alpha\gamma}$ $(\gamma = 1, 2)$, representing the links from network α to γ. To minimize confusion, instead of $\rho_{\alpha\gamma}$, we use the following notation: ρ_1^*, $\rho_1^\times$, ρ_2^* and $\rho_2^\times$, to represent the internal and cross degree distributions of network 1 and 2, respectively. Again, we refer the readers to Fig. 4.1 for a specific example of degree distributions. Clearly, ρ_1^* and ρ_2^* are two distinct distributions. Here, we should emphasize that even though $\rho_1^\times$ and $\rho_2^\times$ provide distributions of the same set of links, they contain distinct information about these links. Specifically, the total number of cross links satisfies $X = \Sigma k_1^\times = \Sigma k_2^\times$; but the two networks differ in how the X cross links are distributed over the respective nodes. This can also be observed in Fig. 4.1. Therefore, generally, $\rho_1^\times$ differs from $\rho_2^\times$.

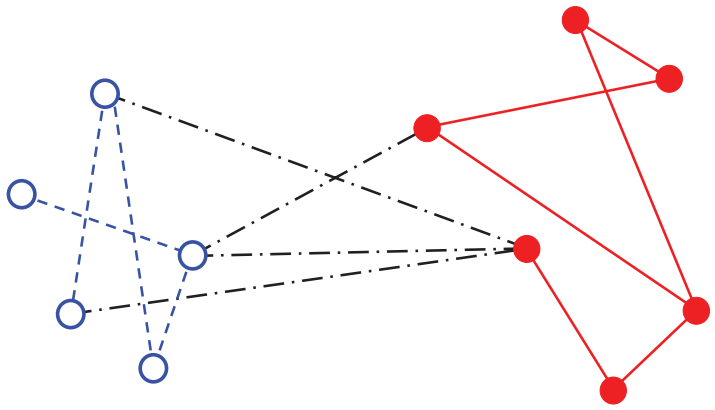

Figure 4.1 The nodes of the two groups are denoted by open blue (1) and closed red (2) circles. The intra-group links are shown as blue dashed and red solid lines, while the inter-group links are dot-dashed lines (black). For this network, the sets of k's are: $k_1^* = \{2, 1, 2, 1, 2\}$, $k_1^\times = \{1, 0, 2, 1, 0\}$, $k_2^\times = \{0, 0, 1, 3, 0, 0\}$, and $k_2^* = \{2, 2, 2, 1, 3, 2\}$. Thus, the non-vanishing contributions to the distributions are $\rho_1^*(1) = 2, \rho_1^*(2) = 3, \rho_1^\times(1) = 2, \rho_1^\times(2) = 1$ and $\rho_2^\times(0) = 4, \rho_2^\times(1) = 1, \rho_2^\times(3) = 1, \rho_2^*(1) = 1, \rho_2^*(2) = 4, \rho_2^*(3) = 1$.

While the degree distributions provide us with detailed knowledge about the topology of

the two-network model, a simpler global measure, which captures the coupling strength, is the total number of cross links, X. Moreover, the time trace of X, $X(t)$, serves to describe how tightly the two networks are coupled at any time. Given $X(t)$, we can compile the distribution of X, which is denoted by $P(X)$. When the system reaches stationary state, the mean of the distribution, $\langle X\rangle$, is given by $\Sigma X P^{ss}(X)$, where P^{ss} represents the distribution in "steady state." Clearly, $\langle X\rangle$ and $\langle k\rangle$ must obey the following condition: $\langle X\rangle = N_\alpha \langle k_\alpha^\times\rangle$. In addition to the distribution of X, it is also possible to explore its frequency content by measuring the power spectrum, $I(\omega)$. Given the time trace $X(t)$, a Fourier transformation is defined as $\tilde{X}(\omega) \equiv \sum_{t=1}^{T} X(t) e^{i\omega t}$ where $\omega = 2\pi m/T$, T is the number of data points of $X(t)$. The power spectrum is obtained by averaging over several Fourier transformation series: $I(\omega) = \langle |\tilde{X}(\omega)^2| \rangle$.

4.2 A simple two-network model

With a second network present, there are numerous possibilities to construct interaction between them. If no cross link exists, we end up with two isolated single networks. Therefore, a key issue we face is how to establish the cross links, and of course, different rules of introducing cross links result in different models. Before we examine more involved two-network models, let us first present a very naive approach to construct interactions between two networks. Here we reuse the single-network model discussed in the last chapter, and partition the set of nodes into two distinct subsets, by randomly relabeling them with red and blue, respectively. The links are updated according to the following rules. We start with a single preferred degree network consisting of $2N$ nodes, each assigned the same κ. Amongst the $2N$ nodes, we arbitrarily label N of them as red and the rest as blue, but we do not distinguish red and blue nodes when updating links. Hence we use the same link update rules as in the single-network model, and specifically, for simplicity, we choose $w(k)$ as $\Theta(\kappa - k)$, where Θ is the Heavyside step function. In each attempt, a node is selected from $2N$ nodes at random, and its degree k is noted. If $k > \kappa$, the node cuts one of its existing link. If $k < \kappa$, the node adds a link to an unconnected node. Its partner is selected at random from all the remaining $2N - 1$ nodes. So far, this is just the single-network model of the previous chapter. However, when we take measurements, we distinguish between red and blue nodes. Therefore, in fact, we have a two-network model,

each network consisting of nodes of one color (red or blue), as well as different types of links, namely $red-blue$, $red-red$, $blue-red$ and $blue-blue$ connections.

Given the updating rules above, effectively, the $red-red$ and $blue-blue$ links are internal links, while the $red-blue$ and $blue-red$ links are cross links. Clearly, in this simple model, the total degree distribution is exactly the same as the degree distribution in a single preferred degree network model. Therefore, let us focus on the internal and cross degree distributions. $2N$ is chosen to be 2000 and κ to be 250, so that each group in the system has 1000 nodes and the same κ, which is comparable to the single-network model. The simulation results are shown in Fig. 4.2. All the four degree distributions (associated with $red-blue$, $red-red$, $blue-red$ and $blue-blue$ links, respectively) are on top of each other. They are Gaussian like and centered at $\kappa/2$.

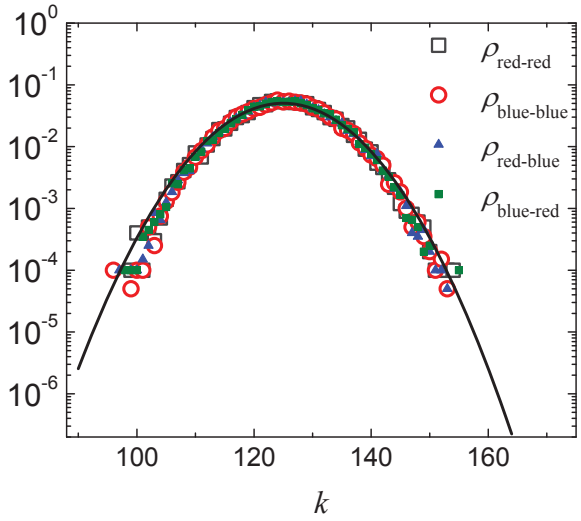

Figure 4.2 Degree distributions of the relabeling two-network model, with $2N = 2000$ and $\kappa = 250$. The markers and solid line represent the simulation results and theoretical prediction, respectively.

The behavior of the degree distributions can be explained by a binomial distribution. From the discussion of the single-network model, we know that in a preferred degree network, the total degree distribution is sharply peaked at κ, that is, the average degree of each node is approximately κ. In this simple two-network model, κ is 250, and therefore, in the steady state,

on average, each node has 250 links. In other words, each node is approximately connected to 250 other nodes (neighbors). As we arbitrarily partition the nodes into two equal groups, the chance that a node is labeled as red or blue is the same. Therefore, amongst 250 neighbors of a node, any of them is marked as red (blue) with probability 1/2. Thus, the probability, that k neighbors of a randomly selected node are labeled as red (blue), is $\binom{\kappa}{k}(1/2)^k(1-1/2)^{\kappa-k}$, indicating a binomial distribution (shown as a solid line in Fig. 4.2).

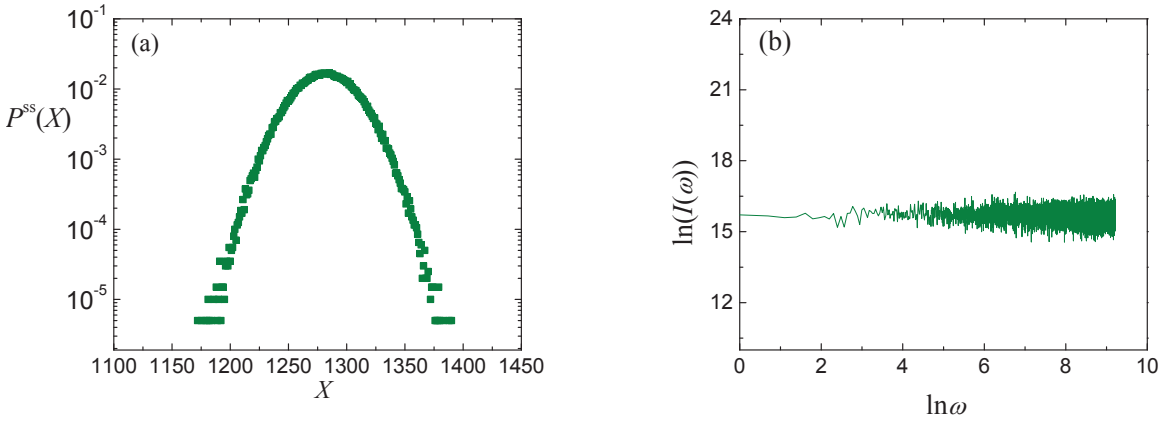

Figure 4.3 This figure shows (a) $P^{ss}(X)$ and (b) $I(\omega)$ for the simple relabeling model with $2N = 200$, $\kappa = 25$.

Another simple quantity used to characterize two-network models is the total number of cross links X, describing how strongly two networks are coupled each other. In this model, specifically, X is the number of $red - blue$ (or $blue - red$) links. To make our data more comparable to our studies reported in the next chapters, when measuring X, we choose a smaller system, where $2N = 200$ and $\kappa = 25$. To obtain the distribution of X, we run the simulation for 10^7 MCS, and measure X once every 100 MCS to record its time trace $X(t)$. Its distribution $P^{ss}(X)$ is compiled from $X(t)$ (see Fig. 4.3(a)). The resultant $P^{ss}(X)$ is a Gaussian distribution with mean $\langle X\rangle$ close to 1275 and standard deviation $\sigma \simeq 25$. This distribution can be explained by the central limit theorem. Suppose the random variable associated is x, which in our case is the number of cross links any node has. Given x, X can be written as $\Sigma_{red}x$ (or $\Sigma_{blue}x$). As discussed in the previous paragraph, in the stationary state, the

distribution of x can be explained by a binomial distribution $\binom{\kappa}{x}(1/2)^x(1-1/2)^{\kappa-x}$ with mean $\langle x\rangle = \kappa/2 = 25.5/2 = 12.75$ and standard deviation $\sigma_x = \sqrt{25.5(1-1/2)/2} = \sqrt{25.5}/2$. Since there are 100 red nodes (or 100 blue nodes), the mean of X is simply $\langle X\rangle = 100\langle x\rangle = 1275$, and the standard deviation is $\sigma_X = \sqrt{100}\sigma_x \simeq 25$.

Finally, we study the power spectrum of X. To calculate the power spectrum, we measure a series of time traces $\{X(t)\}$, each 2×10^6 MCS long. In each run, X is measured every 100 MCS, so that the number of data points T is 2×10^4. $I(\omega)$ is obtained by averaging over 20 Fourier transformation series, shown in Fig. 4.3(b), with the first 10^4 points of the power spectrum plotted. As expected the dynamics of $X(t)$ is governed by white noise.

As expected, with such simple dynamical rules, the features of this relabeled two-network model are trivial. This work provides us with a baseline for our study of interdependent network models. In the following chapters, we will introduce different methods to model the interaction of networks, and present both simulation results and analytical considerations.

CHAPTER 5. INTERACTING DYNAMIC NETWORKS I: A GENERAL MODEL

In this chapter, we introduce interactions between two preferred degree networks by a new parameter controlling the preference of updating cross links. We start with a detailed model description, followed by discussions of the degree distributions and the number of cross links. In this system, we deal with a much larger parameter space, each network involving three parameters. To characterize the network model well, we explore the parameter space systematically, providing simulation results with selections of different parameter sets. We find both understandable and puzzling features. Generalizing the prediction for the homogeneous population, we are able to explain the total degree distributions well, but not the intra- or inter-group degree distributions. When monitoring the total number of inter-group links, X, we find very surprising behavior. Remarkably, a simple self-consistent mean-field approach works well to predict the distribution of X in a special regime.

5.1 Model description

This section provides an introduction of a method to couple two preferred degree networks [12, 13, 108]. We start with two isolated preferred degree networks, each of size N_α and preferred degree κ_α ($\alpha = 1, 2$ distinguishing between network 1 and 2). The total number of nodes in the system is defined as $N \equiv N_1 + N_2$. In general, $N_1 \neq N_2$ and $\kappa_1 \neq \kappa_2$. To reduce complexity, in all two-network models, we only consider the most rigid population, where the rate function $w(k)$ is a Heavyside step function, $\Theta(\kappa - k)$. As we stated in the discussion of the baseline model for the interdependent networks, the key step to construct a two-network model is to establish the cross links, so now we focus on the formation of cross links in this model. In this

chapter, we restrict ourselves to only one mechanism of establishing interaction, and leave other possibilities to later chapters. When a node is selected to update its links, e.g., add a contact, we have to specify whether to add an intra- or inter-group connection. To make this decision, a very simple method is to introduce an interaction strength $\chi \in [0, 1]$, which is the probability that a cross link is selected to update. Accordingly, the dynamics is modified as follows. In an attempt, a node is selected from the entire population at random, and its degree, k, is noted. If $k > \kappa$, the node will cut one of its existing links, and otherwise, it will add a new link to a neighbor not yet connected to it. Regardless of adding or cutting, the action will be executed on a cross link with probability χ. Similarly, $1-\chi$ is the probability that the action is taken on an internal link. In that sense, the fraction of cross links depends on χ, i.e., $\chi = 0$ results in two isolated networks, while with $\chi = 1$, the system describes two networks updating inter-group connections only. However, we will see later that χ does not control the exact number of cross links, but plays a role as the preference of updating cross links. In general, the two networks may have different preference of interacting with the other group, i.e. $\chi_1 \neq \chi_2$.

5.2 Statistical properties and theoretical understanding

5.2.1 Degree distributions

Similar to the single-network model, we first concentrate on the degree distributions. In the two-network model, each network is associated with three parameters, N, κ and χ, and this results in a 6-dimensional parameter space. To effectively explore the effect of each parameter on the system, we restrict ourselves to keeping two pairs of parameters fixed and letting the third vary, i.e., equal N's and κ's, but $\chi_1 \neq \chi_2$, equal N's and χ's, but $\kappa_1 \neq \kappa_2$, and equal κ's and χ's, but $N_1 \neq N_2$. In our simulations, one MCS is defined as N $(= N_1 + N_2)$ attempts of updating a link, such that we can insure that each node has the chance to be picked once.

5.2.1.1 Equal N's and κ's, but $\chi_1 \neq \chi_2$

With equal N's and κ's, clearly, we have two identical preferred degree networks when there is no interaction. When they are coupled, the only difference between them is the preference of

updating cross links. To make the simulation results comparable to the single-network model, we also choose $N_1 = N_2 = 1000$ and $\kappa_1 = \kappa_2 = 250$. Similarly, in our simulations, we discard the first $2K$ MCS and obtain the simulation results by averaging over 10^4 measurements, separated by 100 MCS. As mentioned in the previous chapter, we can consider different classes of degree distributions, the total degree distribution ρ, and the detailed degree distributions ρ^* and $\rho^\times$. Let us first consider the total degree distributions in the steady state, ρ_α^{ss}. With a new parameter introduced, the two-network model does not generate a brand new type of total degree distribution. Like the degree distribution of the homogeneous population, ρ_α^{ss} is also a symmetric, two tailed exponential distribution ($\propto e^{-\mu|k-\kappa|}$). Meanwhile, we find the tail is ε-dependent, where $\varepsilon \equiv \chi_1 - \chi_2$. Simulation results are presented in Fig. 5.1(a). It shows three systems with $\varepsilon = 0.2$, but different set of χ_α's. Clearly, for the three systems studied, ρ_1^{ss} and ρ_2^{ss} collapse onto two curves. Additionally, when the two networks have equal χ's ($\varepsilon = 0$), ρ_α^{ss} is identical to the degree distribution of a single network model. These observations indicate that though it does not dramatically change the topological properties of networks, χ affects the structure of the two-network model by changing the slope of the exponential tails. Next, let us provide a theoretical analysis of how the interaction strength χ influences the distribution by developing a mean-field theory for ρ_α^{ss}.

Here, we reuse the approach from the single-network model, following the line of thought which led to Eqn. (3.4). First, we have to determine $W[k-1,k]$ and $W[k,k-1]$. Note that $W[k-1,k]$ specifies the probability for a node to change its degree from k to $k-1$. Let us first focus on $W[k-1,k]$, and suppose we are looking at a node i in network 1. The contributions to this rate come from, (1) node i itself cutting a link, and (2) other k nodes already connected to i cutting the link to i. Recall that the rate for a node itself to cut a link is just $(1-w(k))/N$, as discussed in the single-network model. In the two-network model, no change is needed for (1). For contribution (2), instead of treating all other nodes the same, now we have to distinguish neighbors of node i by their groups (in network 1 or in network 2). Let us point out that in Eq. (3.5), 1/2 accounts for the remaining nodes taking actions on the selected node. A neighbor of i in network 1 will choose to update a link to a node in network 1 with probability $1-\chi_1$, and this rate is χ_2 for a node in network 2. Therefore, the probability

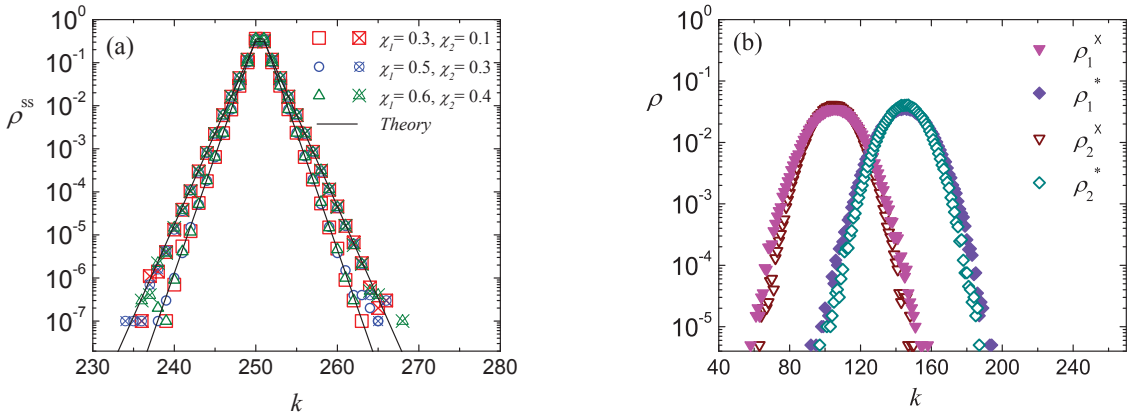

Figure 5.1 (a) The markers without and with cross show simulation data for ρ_1^{ss} and ρ_2^{ss}, respectively. The system parameters are: $N_1 = N_2 = N/2 = 1000$, $\kappa_1 = \kappa_2 = 250$ and fixed $\varepsilon = \chi_1 - \chi_2 = 0.2$. The solid lines represent the theory. (b) Simulation results of internal and cross degree distributions for the system with $\chi_1 = 0.5$ and $\chi_2 = 0.3$.

for (2) is $(1 - \chi_1 + \chi_2)/(2N)$, where $1/N$ accounts for choosing a node from N nodes. Now we have found that $W[k-1, k] = (1 - w(k) + (1-\varepsilon)/2)/N$. Following a similar analysis, we can find $W[k, k-1]$, which is $(w(k-1) + (1-\varepsilon)/2)/N$. A recursive equation for ρ_1^{ss} follows as

$$\frac{\rho_1^{ss}(k)}{\rho_1^{ss}(k-1)} = \frac{w(k-1) + (1-\varepsilon)/2}{1 - w(k) + (1-\varepsilon)/2} \tag{5.1}$$

and a similar equation can be established for ρ_2^{ss}. The above equation of ρ_α^{ss} leads to

$$\mu_1 = ln\frac{3-\varepsilon}{1-\varepsilon}; \quad \mu_2 = ln\frac{3+\varepsilon}{1+\varepsilon} \tag{5.2}$$

which provides information about how the exponential tail deviates from $ln3$. Remarkably, this simple generalized argument gives a good explanation for the degree distributions. The prediction from Eqn. (5.1) is shown as solid lines in Fig. 5.1(a).

With a global picture of the network structure, let us now turn to to more specific description of its topology, by measuring distributions ρ^* and $\rho^\times$. The resultant ρ_α^* and $\rho_\alpha^\times$ are shown in Fig. 5.1(b). Surprisingly, though the total degree distributions are symmetric exponential distributions, these distributions appear to be Gaussian like. We expect that $\langle k_1^\times \rangle = \langle k_2^\times \rangle$, since at any time $\Sigma k_1^\times = \Sigma k_2^\times$ and here $N_1 = N_2$. Our simulation results agree with this

expectation, where both $\rho_1^\times$ and $\rho_2^\times$ have means around 100. On the other hand, ρ_1^* and ρ_2^* are almost on top of each other, with means around 150. All of these distributions are much broader, $O(10)$, than the symmetric exponential distribution. Additionally, both ρ_α^* and $\rho_\alpha^\times$ can also be roughly described by the binomial distributions. To see that, let us reuse the same argument for the simple relabeling network model (in Chapter 3): In the stationary state, each node has approximately κ (= 250 in this case) connections. A naive picture is that 0.4 (average of χ_1 and χ_2, as a rough guess) of the neighbors are cross links, and 0.6 of them are internal links. Therefore, we arrive at the following binomial distributions $\binom{250}{k}(0.4)^k(0.6)^{250-k} \simeq \rho^\times$ and $\binom{250}{k}(0.6)^k(0.4)^{250-k} \simeq \rho^*$. This rough argument captures the right mean: $\langle k^\times \rangle = 0.4\kappa = 0.4 \times 250 = 100$ and $\langle k^* \rangle = 0.6\kappa = 0.6 \times 250 = 150$. We should clarify that even though we repeatedly use the terms binomials and Gaussians, these distributions are not precisely so, but how they deviate from such binomials or Gaussians is beyond the scope of this work.

We should point out to our readers that the Gaussian like ρ^* and $\rho^\times$ only characterize the properties of internal and cross links over a short time scale ($O\left(10^4\right)$ MCS), which is denoted by τ_{short}. As we measure the detailed degree distributions at much later times, e.g., $O(10^5)$ or $O(10^6)$ MCS, different features appear. We discover two different time scales associated with our system. In this subsection, let us focus on the description of this model over τ_{short}, and leave the discussions of the features over the longer time scales to the next subsection.

5.2.1.2 Equal N's and χ's, but $\kappa_1 \neq \kappa_2$

In this section, we examine two networks with same size and interaction strength, but different preferred number of contacts. When two groups of nodes are assigned different κ, i.e., $\kappa_1 < \kappa_2$, it is natural to refer to the two networks as introverts and extroverts, respectively. In other words, this simple two-network model simulates the interaction between an introvert population (I's) and an extrovert population (E's). With different κ's, a new feature appears in the system. E's have larger κ so that they prefer to have more inter- and intra-group contacts, while I's with smaller κ tend to maintain fewer internal and cross links. Thus, I's may receive more connections than wanted, and they keep cutting unwanted links. We term the competition between I's and E's as *frustration*. In this chapter, we will only look at systems with moderate

difference between κ_1 and κ_2, leaving the discussions of maximal frustration to Chapter 6. In Fig. 5.2(a), we show ρ_α^{ss} of the system with $\kappa_1 = 100$ and $\kappa_2 = 250$ ($N_1 = N_2 = 1000$, $\chi_1 = \chi_2 = 0.5$). Both ρ_α^{ss}'s are consistent with a Laplacian distribution with $\mu \cong ln3$, centered at their own κ_α's. ρ_α^{ss} here can also be explained by Eqn. (5.1) by setting ϵ to 0, which is reduced to Eqn. (3.5), the theory for degree distribution in a single-network model. Therefore, with moderate difference in κ_α, the interaction between two networks introduces no new behaviors in ρ_α^{ss}. However, if we keep increasing $|\kappa_1 - \kappa_2|$, ρ_α^{ss} will eventually deviate from Laplacian distributions (see next chapter). Next, we turn our focus to the four detailed distributions ρ_α^* and $\rho_\alpha^\times$, which are shown in Fig. 5.2(b). They are also measured at τ_{short}. Again, they are Gaussian like distributions, but appear to have different means and widths. As mentioned before, the means of $k_\alpha^\times$ should obey $N_1\langle k_1^\times\rangle = N_2\langle k_2^\times\rangle$, and since here $N_1 = N_2$, we should also get $\langle k_1^\times\rangle = \langle k_2^\times\rangle$, which agrees with the simulation result. A simple estimate for $\langle k_\alpha^\times\rangle$, namely $\langle k_\alpha^\times\rangle \simeq (\kappa_1\chi_1 + \kappa_2\chi_2)/2 = 87.5$, provides some insight into its numerical value. The simple scheme produces a good fit to simulation results. In addition, we have another identity, $\langle k_\alpha\rangle = \langle k_\alpha^\times\rangle + \langle k_\alpha^*\rangle$. Thus, the mean of internal links is $100-87.5 = 12.5$ and $250-87.5 = 162.5$, respectively, which also roughly agrees with the simulation data.

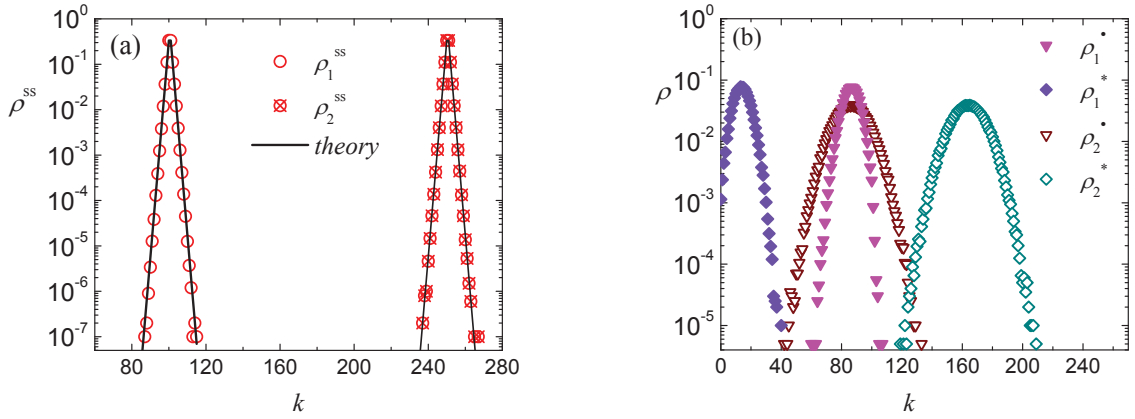

Figure 5.2 (a) ρ^{ss}, (b) ρ^* and $\rho^\times$ for network 1 and network 2, with parameters $N_1 = N_2 = N/2 = 1000$, $\kappa_1 = 100$, $\kappa_2 = 250$, and $\chi_1 = \chi_2 = 0.5$. Solid lines are theoretical predictions.

5.2.1.3 Equal κ's and χ's, but $N_1 \neq N_2$

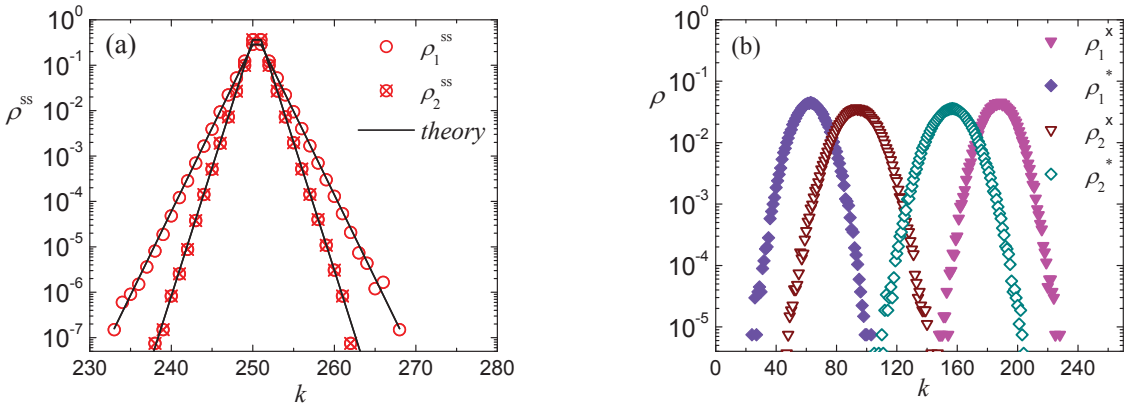

Figure 5.3 (a) ρ^{ss}, (b) ρ^* and $\rho^\times$ for network one and network two, with parameters $N_1 = 500$, $N_2 = 1000$, $\kappa_1 = \kappa_2 = 250$, and $\chi_1 = \chi_2 = 0.5$. Solid squares and triangles represent ρ_1^* and $\rho_1^\times$. Empty squares and triangles stand for ρ_2^* and $\rho_2^\times$.

In the last part of this section, let us change the third system control parameter N and check how it affects the properties of our model. Now we consider two networks with same preference but different sizes, specifically, $\kappa_\alpha = 250$, $\chi_\alpha = 0.5$, $N_1 = 500$ and $N_2 = 1000$. The simulation results are presented in Fig. 5.3. Again, we may also expect frustration between networks. Though they are both assigned the same κ $(= 250)$, the total amount of links each group demands is $250N_1$ and $250N_2$, respectively, and therefore, the larger group wants more links than the smaller group. However, similar to the system with moderate difference in κ_α, with modest difference between the sizes, ρ_α^{ss} presents no distinct characteristics from the distributions we have seen before. We should also point out that in the extreme cases (i.e. $N_1 \ll N_2$), the smaller group may have no internal link, i.e., all of its links are cross links coming from the larger group. Thus, ρ_1^{ss} is essentially $\rho_1^\times$, which is certainly not a Laplacian distribution. Even though ρ_α^{ss} displays no new features when different system sizes are chosen, it is clear that the Laplacian distribution is N_α-dependent (see Fig. 5.3(a)). To explain the changes induced by system size, we turn to theoretical analysis. We reuse Eqn. (3.4), and as before, we have to determine $w[k-1,k]$ and $w[k,k-1]$. Again, we focus on $w[k-1,k]$ and

consider a chosen node i in network 1. $w[k-1,k]$ consists of two contributions: (1) node i itself cutting a link (with rate $(1-w(k))/N$), and (2) other k nodes already connected to i destroying the edge to i. From our previous discussion, we know that in a single-network model, the probability for (2) is 1/2. In a two-network model, we have to consider both N_α and χ_α. Suppose that i has $k_1^\times$ cross links, and any neighbor of i in network 2 has $k_2^\times$ cross links. We approximate $k_1^\times$ and $k_2^\times$ by their averages, and recall that $\langle k_1^\times\rangle N_1 = \langle k_2^\times\rangle N_2$. A relation between $k_1^\times$ and $k_2^\times$ is found, i.e., $k_1^\times = k_2^\times N_2/N_1$. Therefore, the probability that neighbors of i in network 2 will cut a link to i, is enhanced by a factor of N_2/N_1. Including this factor, we find that i's neighbors in network 2 will cut a link to i with rate $\chi_2 N_2/(2N_1)$. On the other hand, this rate for neighbors of i in network 1 is unchanged, still $(1-\chi_1)/2$. Now the 1/2 in Eqn. (3.5) has been modified to

$$\frac{1}{2}\left\{\frac{N_2}{N_1}\chi_2 + (1-\chi_1)\right\}, \tag{5.3}$$

and we can get the same form for the rate of adding links. In fact, this is a general expression for the rate, with which other nodes take actions on a chosen node in the two-network model. Here, we can further simplify the above expression, by plugging $\chi_1 = \chi_2$ into Eqn. (3.5), and finally reach the equation

$$\frac{\rho_\alpha^{ss}(k)}{\rho_\alpha^{ss}(k-1)} = \frac{w(k-1) + N/4N_\alpha}{1 - w(k) + N/4N_\alpha} \tag{5.4}$$

to predict degree distributions (solid lines in Fig. 5.3(a)). Again, the theory provides good agreement with simulation data.

Not surprisingly, the four detailed degree distributions, ρ_α^* and $\rho_\alpha^\times$, are Gaussian like. Their means are located at different values. Of course, the means should also obey $\langle k_1^\times\rangle N_1 = \langle k_2^\times\rangle N_2$ and $\langle k_\alpha^*\rangle + \langle k_\alpha^\times\rangle = \langle k_\alpha\rangle$. In our simulation, network 2 is twice as large as network 1. Therefore, it is understandable that $\rho_1^\times$ is centered at ~ 185, which is twice of $\langle k_2^\times\rangle$, valued ~ 90. Additionally, the corresponding internal degree is ~ 65 and 160, respectively. Again, these ρ's are measured at τ_{short}.

Although exploration of these three types of systems (unequal χ's, κ's, N's) is not sufficient to provide us with a complete picture of interacting networks model, they do point to some common themes. In the limited parameter range that we have explored here, the total

degree distributions in the steady state, $\rho_\alpha^{ss}(k)$, can be reasonably well described by a simple approximation scheme for their master equations, which leads to recursive solutions. To examine further details, such as how the degree k is partitioned between intra-group connections (k^*) and cross links ($k^\times$), we study four other specific degree distributions, $\rho_\alpha^{*,\times}$ by simulations and find them to be Gaussian like distributions. A very crude estimate, based on binomials, appears to be adequate, especially for describing their properties over relatively short time scales, τ_{short}.

5.2.2 The total number of cross links, X

As mentioned before, there are two different time scales associated with this system, and the features over τ_{short} are examined in the previous subsection. Recall that when we measure the total degree distribution, $2K$ MCS is enough to let the system relax into the stationary state, that is, $O\left(10^3\right)$ MCS is sufficient for the system to reach the state where each node has approximately κ links, from an empty network. Besides, it only takes $O\left(10^4\right)$ MCS (τ_{short}) for us to collect enough data and get a good measurement for the total degree distribution. During τ_{short}, the specific degree distributions $\rho^\times$ and ρ^* settle into Gaussian like distributions. However, we observe that the centers of these detailed distributions appear to wander slowly over longer time scales. That is, if we let the system continue to evolve till much later times, e.g., $O(10^5)$ or $O(10^6)$ MCS, and then measure $\rho^\times$ and ρ^* over τ_{short} again, they are still Gaussian like distributions with unchanged width, but their means have shifted. In other words, there is a much larger time scale, τ_{long}, after which the system finally relaxes into the true steady state. In this subsection, we will discuss the features of the system measured over τ_{long}.

As discussed above, the means of $\rho_\alpha^{*,\times}$ are slowly wandering. Note that, for either network, their means obey $\langle k_\alpha^* \rangle + \langle k_\alpha^\times \rangle = \langle k_\alpha \rangle$. Therefore, with pre-assigned κ_α, instead of studying all the means, we can focus on either cross links or internal links, and the other is automatically found. For convenience, let us concentrate on cross links only. We believe that the slow wandering of the means can be traced to similar behaviors of X: While at shorter time scale, X is relatively constant, and the value may slowly vary on the longer time scales. This subsection provides a systematic investigation of how X depends on the various aspects of the two groups.

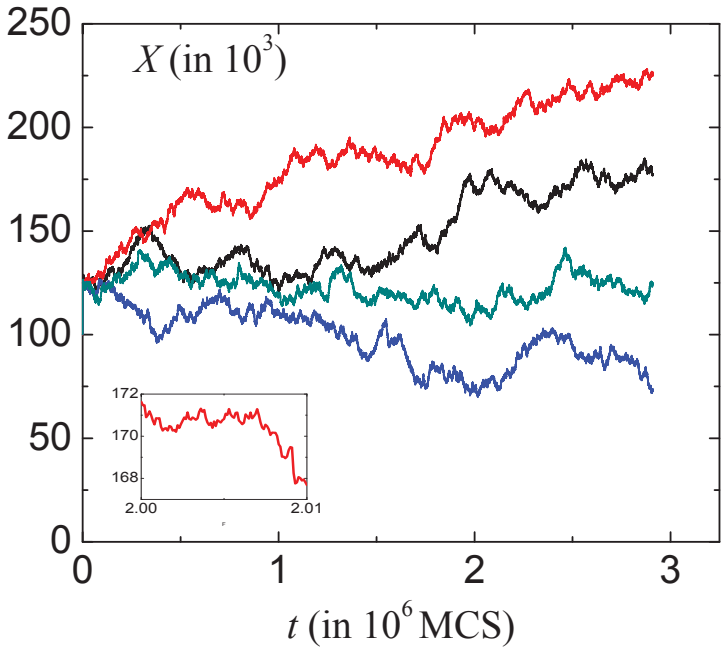

Figure 5.4 Four independent time traces $X(t)$ for a system with $N_1 = N_2 = N/2 = 1000$, $\kappa_1 = \kappa_2 = 250$ and $\chi_1 = \chi_2 = 0.5$. In the inset, we show a small section (10^4 MCS) of the red trace, to illustrate how little X varies at this time scale. Note the scale for X here spans just $4K$, compared to the $250K$ in the main figure.

To make connection with the results for the degree distributions, we first present the simulation results of a symmetric system with parameters comparable to studies in the previous subsection ($N_\alpha = 1000$, $\kappa_\alpha == 250$, $\chi_\alpha = 0.5$). In Fig. 5.4, we show four independent runs of $X(t)$ over $3M$ MCS, and they are similar to random walks. All four runs start from empty networks, so that the initial value $X(0)$ is 0. Even though the four runs wander widely after $\sim 10^5$ MCS, it is notable that for all of them, at the beginning of simulations, X increases rapidly to a certain value ($\sim 125K$) and stays there for a short while. The value $125K$ can be estimated by $N_\alpha\kappa_\alpha\chi_\alpha$. In the figure, clearly, one can tell that none of the runs have reached their boundaries yet, and they just start to "walk." A reasonable estimate of the allowed range for X is $0 \leq X \lesssim N_\alpha\kappa_\alpha$. The lower bound is obvious, which represents the situation where there are no cross links, while the upper bound is achieved when each node has the maximally allowed number of links and all the links are cross links. The figure illustrates that $\tau_{long} \gg 3M$

MCS for this system to finally reach its stationary state. Here, we should also point out that within the short time scale $\tau_{short} \sim 10^4$ MCS, X is relatively constant (shown as an inset in Fig. 5.4). Note that, within the interval of τ_{short}, the degree distribution of cross links, $\rho_\alpha^\times$, is Gaussian like. These distributions can also be explained by the following simple arguments: Within τ_{short}, X can be treated as a constant. Since all the updates of links are done at random, we may assume that the X cross links are distributed randomly among N_α nodes in each group. Therefore, this question is simplified to a problem of throwing X links arbitrarily on N_α nodes, which is well characterized by a binomial distribution, $\binom{X}{k}\left(N_\alpha^{-1}\right)^k\left(1-N_\alpha^{-1}\right)^{X-k}$.

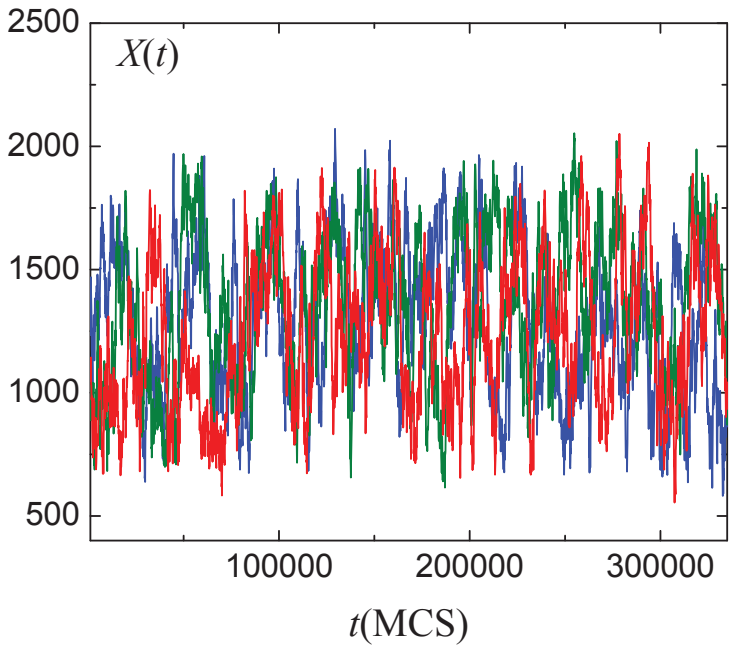

Figure 5.5 Three time traces of X (red, green, and black), for a system with $N_1 = N_2 = N/2 = 100$, $\kappa_1 = \kappa_2 = 25$ and $\chi_1 = \chi_2 = 0.5$.

We have seen that for a large system ($N_\alpha = 1000$) to settle down to the stationary state, it will take $\tau_{long} \gg 3M$ MCS, which is computationally expensive. To make our further exploration of X easier, we have to consider smaller systems, accordingly, with smaller κ's. Thus, in the following discussions on X, only smaller systems with $N_1 + N_2 = 200$ will be examined. To connect with the large system, let us first study the symmetric system, where

$N_1 = N_2 = 100$, $\kappa_1 = \kappa_2 = 25$ and $\chi_1 = \chi_2 = 0.5$. With a similar analysis, we can argue that the allowed range for X is from 0 to roughly $\sim N_\alpha \kappa_\alpha = 2.5K$ for the smaller system. In Fig. 5.5, we display three short sections (each 10^5 MCS long), obtained from partitioning a single long run (10^7 MCS). Note that for this small system, $X(t)$ indeed traverses the full range in each case. Besides, none of them wander closely to their minimum or maximum allowed value, and instead, they all fluctuate between ~ 500 and ~ 2000. The time trace is much like an unbiased random walk confined between two "walls." To probe deeper into the hypothesis and illustrate the distinct features of X, let us turn to more measurable quantities of X, and meanwhile make comparisons to the simple relabeling model.

5.2.2.1 Comparison between homogeneous and heterogeneous populations

Let us first briefly remind our readers of the relabeling model. This model updates its links following the same steps as in a single network model, and therefore, essentially this simple model has no difference from a homogeneous population. To define cross links in a single network, we arbitrarily partition the nodes into halves, relabeled as red and blue, and treat the $red - blue$ links as cross links. Significantly, in this model, only when taking measurements, we distinguish between red and blue nodes, so that the relabeling does not affect the link updates. Therefore, the comparison between this model and the two-network model is in fact a comparison between homogeneous and heterogeneous populations. In this subsubsection, we will show that the interaction between networks brings substantial changes to the topology of a network.

To get the distribution of X, with confidence that the system has reached steady state, we compile a histogram, $P^{ss}(X)$, from the time trace and show the results in Fig. 5.6. The green curve is $P^{ss}(X)$ for the simple relabeling model. It can be well described by a Gaussian, with mean close to 1275 and standard deviation $\sigma \sim 25$. As discussed before, this distribution can be well explained by the central limit theorem (see Chapter 3). By contrast, the simulation results of the two-network model paint a completely different picture. Unlike the $P^{ss}(X)$ of a single network, $P^{ss}(X)$ is not a Gaussian; instead, it is a broad and flat distribution, around the mean of approximately 1250 (i.e., $N_\alpha \kappa_\alpha \chi_\alpha$) with soft cutoffs at both ends. Such a distribution

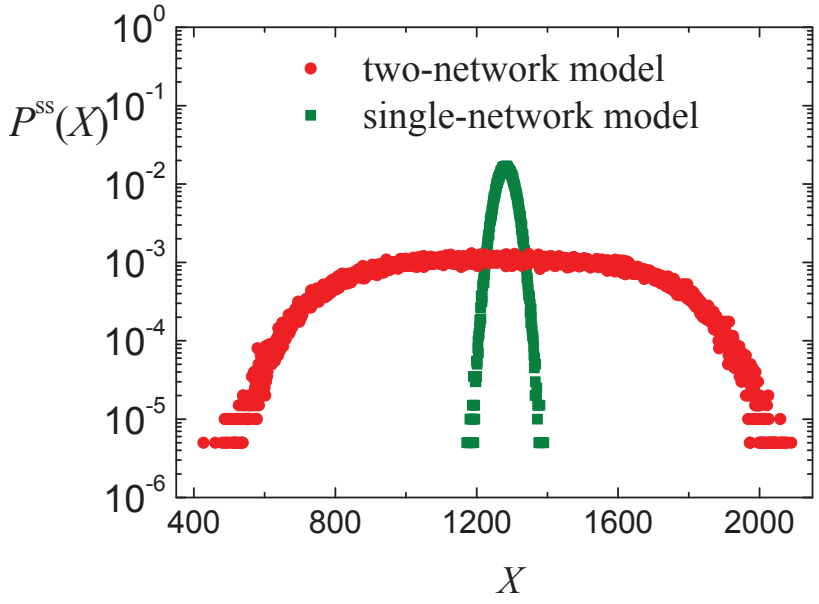

Figure 5.6 This figure shows $P^{ss}(X)$ for two-network model (red) with $N_1 = N_2 = 100$, $\kappa_1 = \kappa_2 = 25$ and $\chi_1 = \chi_2 = 0.5$, as well as $P^{ss}(X)$ for a base relabeling model (green) with $N = 200$ and $\kappa = 25$.

is consistent with the idea that $X(t)$ executes a simple random walk between two soft walls, located approximately at $X_{\min} \sim 500$ and $X_{\max} \sim 2000$. However, in the following discussion, we will see that in principle, X is not constrained between these two values. Clearly, for any two networks system, the lowest possible value of X is 0, when all the links are only distributed inside each network. As for the upper bound, a rough estimate is $\kappa_\alpha N_\alpha$, where every node in the system has κ_α cross links. Other than these two boundaries, there is no constraints on X. In principle, X can explore the whole range. However, as we have seen in the figure, X only explores from $\sim$ 20% to $\sim$ 80% of its allowed range. Later in this chapter, we will systematically study how the range of X depends on the parameters. But now let us continue the comparison between one- and two-network models.

To confirm our expectation, we construct the power spectrum of X and explore the frequency content of X. With the time trace $\{X(t)\}$, each 2×10^6 MCS long, we define a Fourier transformation as $\tilde{X}(\omega) \equiv \sum_{t=1}^{T} X(t) e^{i\omega t}$ where $\omega = 2\pi m/T$, and T is the number of data points of $X(t)$, 2×10^4 ($m \in [0, T]$). The power spectrum is obtained by averaging over 20

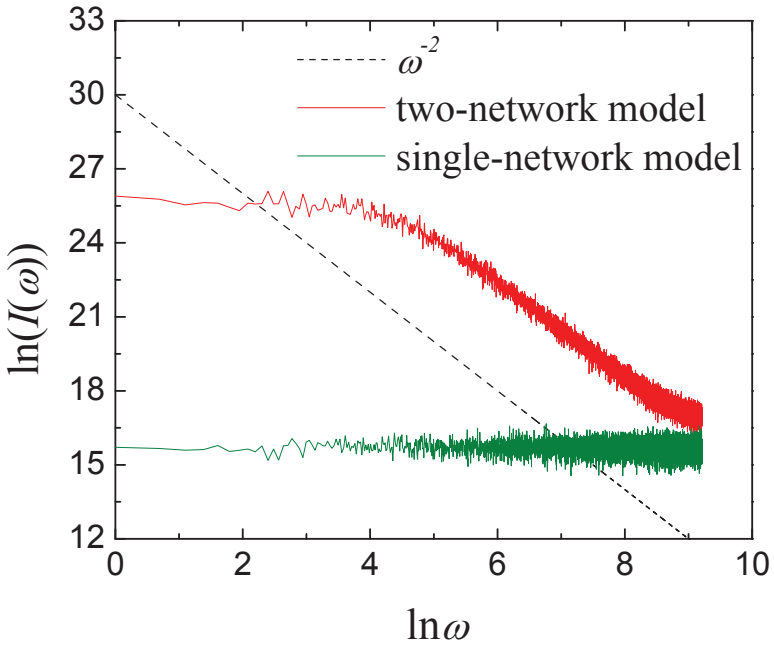

Figure 5.7 This figure shows $I(\omega)$ for two systems: the red line represents $I(\omega)$ of two-network model with $N_\alpha = 100$, $\kappa_\alpha = 25$ and $\chi_\alpha = 0.5$, and the green line represents $I(\omega)$ of single-network model with $N = 200$, $\kappa = 25$. The dashed line is $\propto 1/\omega^2$.

Fourier transformation series: $I(\omega) = \langle|\tilde{X}(\omega)^2|\rangle$. In Fig. 5.7, we plot the first 10^4 points of the power spectrum, and find that $I(\omega)$ of the two-network model (red line) is consistent with $1/\omega^2$ (dashed line) beyond some ω_0. $1/\omega_0$ corresponds to the time that it takes for X to explore the whole range before it notices the wall. By contrast, $I(\omega)$ for the single-network model (green line) is a flat spectrum, containing equal power of any frequencies.

Let us have a short summary about what we have found from the comparison between the single- and two-network models. When the two models have comparable sets of system parameters, their degree distributions have no significant difference. (The total degree distributions of the two-network model are also symmetric exponential distribution, but the width depends on the system parameters.) With more careful examinations, however, we discover that X exhibits remarkably different behavior when two networks are coupled. We have shown that $X(t)$ reflects an unbiased random walk confined between two walls. But it is puzzling where the walls are and how their locations depend on the parameters. To answer these questions,

we have to investigate X more systematically.

5.2.2.2 Systematic study of the statistical properties of X

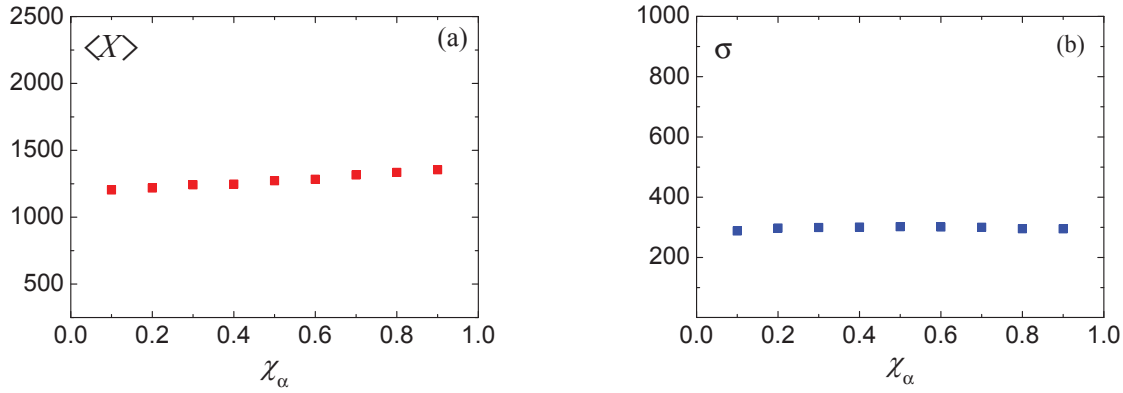

Figure 5.8 The (a) means and (b) standard deviations of $P^{ss}(X)$ for two-network model with $N_\alpha = 100$, $\kappa_\alpha = 25$, and different χ_α's, as a function of χ_α.

In this subsubsection, we will study the statistical properties of X as a function of the parameters of the two-network model: N_α, κ_α, and χ_α ($\alpha = 1, 2$). As a start, we only consider two symmetric networks, where $N_1 = N_2$, $\kappa_1 = \kappa_2$ and $\chi_1 = \chi_2$. Thereafter, we move forward to a more general two-network model, where $N_1 \neq N_2$ and $\kappa_1 \neq \kappa_2$. For all selected parameter sets, we measure the mean, $\langle X \rangle$, and the standard deviation, σ, of $P^{ss}(X)$, the distribution of X. We believe these two quantities characterize $P^{ss}(X)$ well, since the former describes the center of $P^{ss}(X)$ and the latter specifies the width. Therefore, to compare $P^{ss}(X)$ of different systems, instead of displaying the whole distribution, we focus on $\langle X \rangle$ and σ, and explore the statistical properties of X in the following cases: Each time, two of the three pairs of system parameters are fixed, and the third one varies. In the simulations, we always start with empty systems, and run two independent simulations, each 10^7 MCS long. X is measured once every 100 MCS, so that there are 2×10^5 data points in total for each system parameter set. We then calculate the means and standard deviations.

5.2.2.3 Symmetric networks: Fixed N's and κ's, but varied χ's.

To have comparable parameters to our previous study, we choose the value of N_α and κ_α to be 100 and 25, respectively, and vary χ_α (with $\chi_1 = \chi_2$). Recall that χ_α controls how closely two networks are coupled: The larger χ is, the more often the two networks update their cross links. As mentioned before, in the extreme case, $\chi_\alpha = 0$ results in two isolated networks, while if we set $\chi_\alpha = 1$, the internal links are frozen and only cross links are updated. Other than these two cases, the networks can choose to update either internal or cross links, and the preference is determined by χ_α. Here, we will avoid the extreme cases, and only study more general values, $\chi_\alpha \in (0, 1)$. We should emphasize that χ_α specifies the preference of updating cross links though it does not directly reflect the fraction of cross links. As the same χ_α is applied to both adding and cutting actions, the preference of a node to add or cut a cross link is the same: If a node is highly likely to add cross links, it is just as likely to cut them. In that sense, clearly χ_α is not directly related to the value of X, but to the frequency with which X changes. Therefore, our expectation is that changing χ_α will not affect $\langle X \rangle$ or σ. In Fig. 5.8, we present our simulation results. The simulation paints a picture similar to our expectation, especially for σ. A slow rising trend of $\langle X \rangle$ is observed (in (a)) though there is no huge change in $\langle X \rangle$: Its value changes from ~ 1190 to ~ 1370 (a change of $\sim 15\%$) along with the increase of χ_α from 0.1 to 0.9. It is difficult to explain these variations in detail, though the typical values deviate little from $\langle X \rangle \sim 1272$ in the symmetric case ($\chi_\alpha = 0.5$), as predicted above. Furthermore, the plot of Fig. 5.8(b) confirms our expectation of σ's, which are more or less the same, all valued at ~ 300, for different χ_α's. We will next see that more interesting behavior appears when we vary the other two control parameters. Changing χ_α (between 0 and 1) does not affect the distribution of X too much, so in the rest of this chapter, we will always keep χ_α unchanged.

5.2.2.4 Symmetric networks: Fixed N's and χ's, but varied κ's.

In this part, we will consider two networks with same size and χ_α, but different κ_α. In our preferred degree network, κ_α is the key system parameter, which determines the average degree

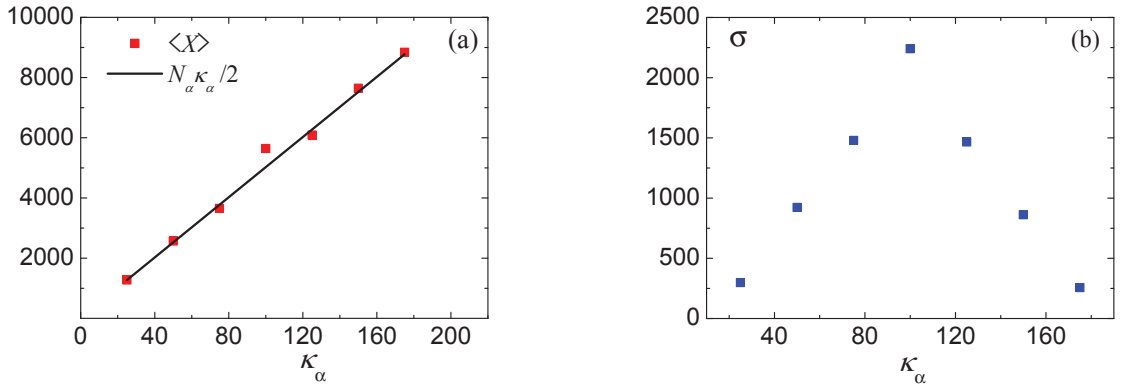

Figure 5.9 The (a) means and (b) standard deviations of $P^{ss}(X)$ for the two-network model with $N_\alpha = 100$, $\chi_\alpha = 0.5$, and different κ_α's, as a function of κ_α.

of each node. Therefore, the change of κ_α is supposed to have significant influence on X. To confirm this conjecture, we now vary κ_α , and keep $N_\alpha = 100$ and $\chi_\alpha = 0.5$. The resultant $\langle X \rangle$ and σ are shown in Fig. 5.9.

Not surprisingly, $\langle X \rangle$ increases along with κ_α. This can be understood by the following arguments. In the Section 5.2.1, we have seen that in the steady state, $\rho_\alpha(k)$ is sharply peaked at κ_α, and the distribution is symmetric around κ_α. Therefore, we can roughly assume that in the steady state, each node has approximately κ_α links. Besides, since the two networks are symmetric and particularly, their preference of updating cross links, χ_α, is 0.5, we may expect that the internal and cross degrees of any node are equal. Thus, we can approximate $\langle X \rangle$ by $\kappa_\alpha N_\alpha/2$, which is plotted as a solid line in Fig. 5.9(a). Clearly, this simple argument provides a reasonably good prediction of $\langle X \rangle$.

Next, let us move on to the other quantity, σ, which is associated with the lower and upper bounds of X. As discussed before, in this two-network model, the two bounds of X are 0 and $\kappa_\alpha N_\alpha$. Other than these two boundaries, in principle, there are no constraints on X. Therefore, X is supposed to be able to explore the whole range. If this is true, we expect that σ should be positively correlated with κ_α. However, our simulation again displays a different picture. It turns out that the distribution of σ is symmetric around κ_α, and σ_{max} appears when $\kappa_\alpha = N_\alpha$. If we continue increasing κ_α beyond that point, σ instead decreases. Besides, we also

run similar simulations on other system sizes, and all the results reflect the same observation: Instead of increasing along with κ_α, σ achives its maximum when $\kappa_\alpha = N_\alpha$. That is, X has the largest fluctuation in the most symmetric system. In this case ($\kappa_\alpha = N_\alpha = 100$), $P^{ss}(X)$ has the largest width, and X wanders from $\sim 5\%$ to $\sim 95\%$. When κ_α differs from N_α, the actual allowed range of X is narrowed down, e.g., when $\kappa_\alpha = 25$, X can only explore from approximately 20% to 80% of its allowed range.

5.2.2.5 Symmetric networks: Fixed κ's and χ's, but varied N's.

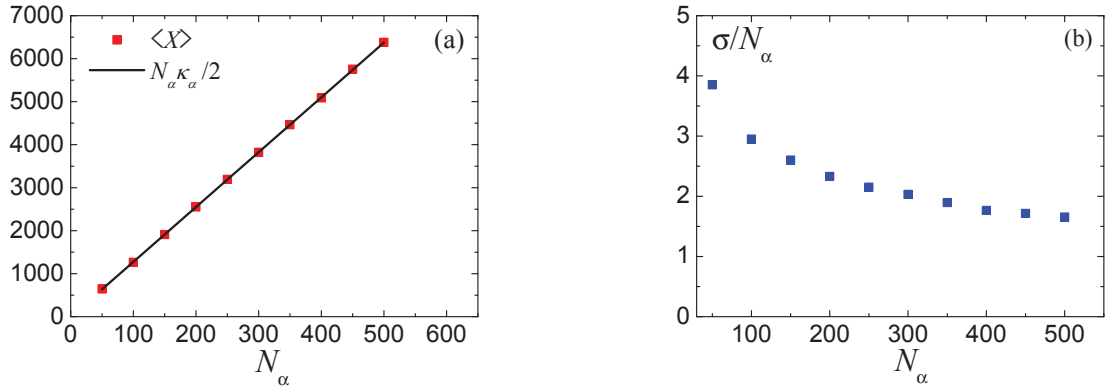

Figure 5.10 The (a) means and (b) standard deviations of $P^{ss}(X)$ for the two-network model with $\kappa_\alpha = 25$, $\chi_\alpha = 0.5$, and different N_α's, as a function of N_α.

In this subsubsection, we vary the system size N_α, while fixing $\kappa_\alpha = 25$ and $\chi_\alpha = 0.5$. When the number of nodes is larger, an immediate guess is that $\langle X \rangle$ will also increase. Recall that in the previous subsubsection, $\langle X \rangle$ can be roughly predicted by $\kappa_\alpha N_\alpha/2$. Here we only change N_α and keep κ_α fixed, and so we should arrive at the same prediction. In Fig. 5.10(a), we plot the comparison between $\langle X \rangle$ (red squares) and $\kappa_\alpha N_\alpha/2$ (solid lines). The simulation results are indeed consistent with our prediction. We also present the results for the standard deviation, σ, in Fig. 5.10(b). To compare σ's of systems with different sizes, we actually plot the "normalized" standard deviation, which is σ/N_α. While the system size increases by a factor of 10, from $N_\alpha = 50$ to 500, σ/N_α decreases from ~ 3.85 to ~ 1.65, by a factor of ~ 2.3. That is, the normalized width of X slowly declines when the system gets larger.

5.2.2.6 More general networks: Fixed χ's, but varied N's and κ's.

In the previous discussions, we have investigated the simplest cases, where the parameters of two networks are always kept to be symmetric. Here we will turn our attention to a more general case, in which each network has its unique parameters. However, as mentioned before, for a system with 6 independent controlling parameters, the parameter space can be very large. Therefore, it would be very difficult for us to explore the whole parameter space. To make our study doable, as well as have comparable simulation results to the previous sections, we apply three constraints on the parameters. That is, we fix the sum of the parameters: $N_1 + N_2 = 200$, $\kappa_1 + \kappa_2 = 50$, and $\chi_1 + \chi_2 = 1$. Moreover, after the discussion of the symmetric networks with fixed N's and κ's, but varied χ's, we notice that the distribution of X is not dramatically influenced by χ_α. Therefore, we can further reduce the space by letting χ_α equal 0.5. Finally, we arrive at a confined parameter space, where N_α and κ_α are varied, but with constraints $N_1 + N_2 = 200$, $\kappa_1 + \kappa_2 = 50$, and χ_α is fixed at 0.5. In Fig. 5.11, we show the results for three different pairs of κ's: ($\kappa_1 = 5$, $\kappa_2 = 45$), ($\kappa_1 = 15$, $\kappa_2 = 35$), and ($\kappa_1 = 25$, $\kappa_2 = 25$), partly for convenience and partly for having κ_1's ratios at $1 : 3 : 5$. Naturally, we refer to the network with larger κ as extroverts, and the other group as introverts. For each κ set, we measure how $\langle X \rangle$ and σ change when the number of extroverts (N_2) varies, and plot the $\langle X \rangle$'s and σ's as a function of N_2.

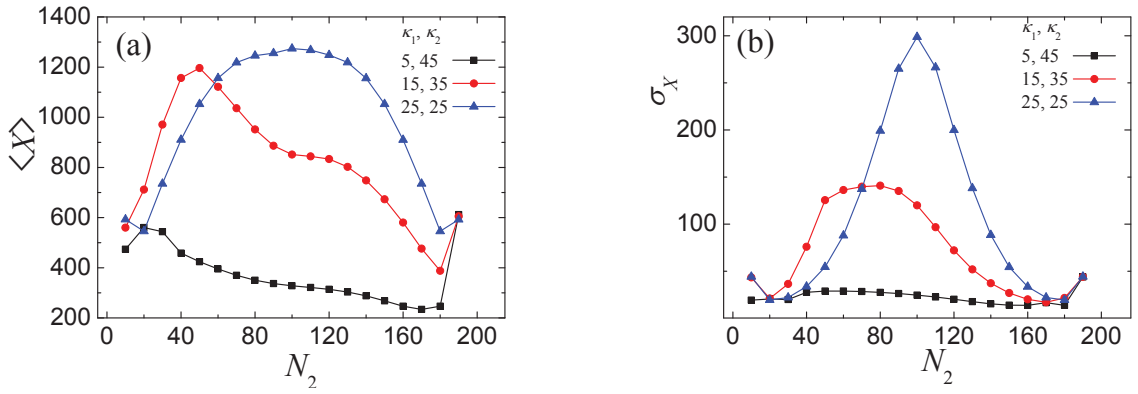

Figure 5.11 The (a) means and (b) standard deviations of $P^{ss}(X)$ for the two-network model with $\kappa_1 + \kappa_2 = 50$, $N_1 + N_2 = 200$, and $\chi_\alpha = 0.5$, as a function of N_2.

With more general parameter sets, we cannot consider N_α or κ_α alone, since both are changing now. For convenience, we coin the product of the two parameters the *network preferred degree*, $\kappa_\alpha^{network} \equiv N_\alpha \kappa_\alpha$. This quantity provides information about how many links each network would like to achieve, and it can affect the number of cross links. For example, if $\kappa_1^{network}$ is much larger than $\kappa_2^{network}$, then we can observe "frustration" in such system: One network always tries to cut the unwanted cross links, while the other one seeks to add links to reach its network preferred degree. Therefore, we may expect that when the two networks have equal $\kappa^{network}$, both networks are "happy."

Let us look at the plot of $\langle X \rangle$ first in Fig. 5.11(a). Not surprisingly, when the two networks have same κ ($= 25$), the distribution of $\langle X \rangle$ is also symmetric. Remarkably, though the change of $\kappa_\alpha^{network}$ is the same between any neighboring data points, the change of $\langle X \rangle$ is not linear. Recalling that when we have a system with $\kappa_\alpha = 25$, $N_\alpha = 100$, and $\chi_\alpha = 0.5$, $\langle X \rangle$ is observed to be ~ 1272, here we also find the same $\langle X \rangle$ value, not only in the symmetric system, but also in the range between $N_2 = 90$ to 110. When N_2 further differs from 100, $\langle X \rangle$ firstly decreases very slowly: At $N_2 = 60$ and $N_2 = 140$, $\langle X \rangle$ only reduces by ~ 100. When N_2 varies beyond that range, $\langle X \rangle$ decreases much faster, changing by ~ 200 when N_2 differs by 10.

For the other cases where κ's are not symmetric, we are not surprised by the lack of symmetry in the curves. The plots exhibit decreasing trends in general, peaking at lower N_2's. It may look unreasonable at first glance that $\langle X \rangle$ decreases when the population of extroverts grows. If we think more carefully, however, we can understand why this can happen. It is true that when N_2 gets larger, the $\kappa^{network}$ of the extroverts is greater. But at the same time, N_1 is smaller, so that the introverts prefer a smaller number of links. When the two groups are coupled, there is large frustration between them, and the trend of $\langle X \rangle$ should depend on who "wins." Therefore, it is possible for $\langle X \rangle$ to decrease. (Of course, it would be highly desirable to formulate an analytic and more convincing approximation scheme. However, to describe how strong the frustration is, or how to predict which group plays the leading role is beyond our goal in this study. Therefore, we only provide some qualitative analysis instead of quantitive solutions.) Moreover, we observe that the maximal value is achieved when the two groups prefer to have approximately the same network preferred degree, $\kappa_1^{network} \simeq \kappa_2^{network}$. This

balance occurs at $N_2 = 4\kappa_1$ for our parameters, 100 for the symmetric case, and 20 and 60 for the systems with ($\kappa_1 = 5$, $\kappa_2 = 45$) and ($\kappa_1 = 15$, $\kappa_2 = 35$), respectively. While such arguments produce a rough understanding of the data, more quantitative improvements are clearly needed.

σ has a similar trend as the distribution of $\langle X \rangle$ (Fig. 5.11(b)). We obseve that when the system parameters of the two networks are mostly symmetric, the system exhibits the largest fluctuations. That is, in the figure, the systems with $\kappa_1 = \kappa_2 = 25$ and $N_1 \sim N_2$, have much larger σ than the other systems: The largest σ is ~ 300, which is more than 10 times larger than its smallest value. In addtion, this is true not only for the systems with $N_1 + N_2 = 200$, but also for two-network models in other sizes. For the system with $\kappa_\alpha = 25$, the distribution of $\langle X \rangle$ reaches its maximum value at $N_2 = 100$, and the peak of the distribution of σ also appears at the same N_2. However, for the other two systems with asymmetric κ's, compared to the distribution of $\langle X \rangle$, the largest σ appears at larger N_2's, which is around 70 for the system with $\kappa_1 = 15$ and $\kappa_2 = 35$ and 40 for the system with $\kappa_1 = 5$ and $\kappa_2 = 45$.

Based on our discussion of two-network models with general parameters, we find it is very involved to analytically explain the means and standard deviations of $P^{ss}(X)$, let alone the whole distribution. The difficulties arise from the fact that the process of updating links violates detailed balance, and moreover, for each node, it has two possible action options (adding and cutting). Even though it is difficult to understand the whole plot of Fig. 5.11, one can ask if there is a special regime that is governed by simpler rules, so that we can explain part of the plot. Fortunately, such a regime exists. By examining Fig. 5.11(a) carefully, we notice that in the high N_2 corner, the three plots tend to merge. In that regime, the population of extroverts is much larger than that of the introverts, and also $\kappa_2^{network} \gg \kappa_1^{network}$. That can result in the introverts always getting more links than they want, and therefore introverts always cut links. In that sense, in the stationary state, the extroverts either add or cut links, while the introverts are only allowed to cut links. Clearly, this regime is distinguished from the general case, where all the nodes can choose to add or cut links. Note that, a similar argument does not necessarily exists in the low N_2 corner, where $N_1 > N_2$ and $\kappa_1 < \kappa_2$, and it is not clear if $\kappa_1^{network} \gg \kappa_2^{network}$ or $\ll \kappa_2^{network}$. In the following subsubsection, we will present an analytical

understanding of X in this distinct regime.

5.2.2.7 Theoretical understanding of X in a special regime.

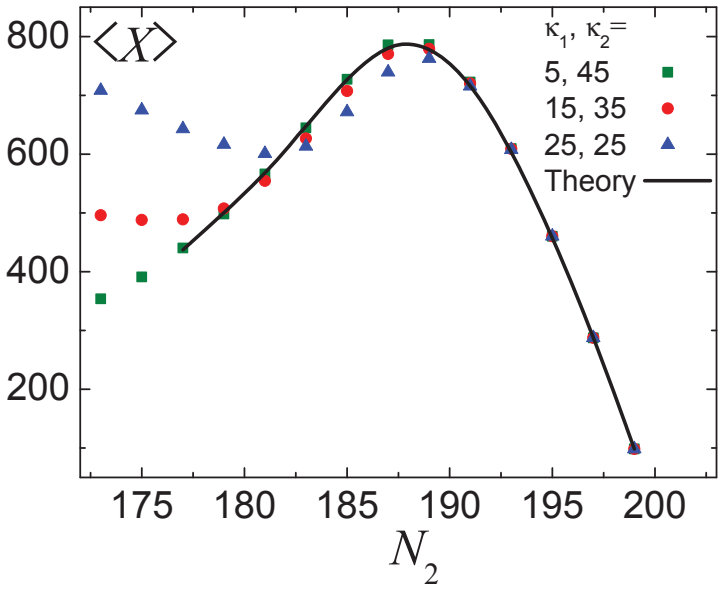

Figure 5.12 The means of $P^{ss}(X)$ for two-network model with $\kappa_1 + \kappa_2 = 50$, $N_1 + N_2 = 200$, and $\chi_\alpha = 0.5$.

As discussed above, there is a distinct regime in Fig. 5.11, where $\kappa_1^{network} \ll \kappa_2^{network}$ ($N_1 \ll N_2$). In this special range of N_2, three curves merge into one point at $N_2 = 190$. To get a better observation, we "zoom in" on that regime, and examine more data points with large N_2's (from 173 to 199). The simulation results are shown in Fig. 5.12. Even though the three plots differ significantly outside the special regime, surprisingly, a universal pattern is observed for all the three systems, i.e., the three plots of $\langle X \rangle$ are exactly the same in the extreme large N_2 regime, from $\sim$ 190 to 199. Here, the average degree of introverts, $\langle k_1 \rangle$, is typically far larger than κ_1, and perhaps a more general characterization is $\kappa_1^{network} \ll \kappa_2^{network}$. Therefore, introverts (I's) always cut their links when picked to update links, so that there are no I-I links. Moreover, with different κ sets, the value of N_2, at which the system enters that regime, is different, i.e., the plots of systems with $\kappa_1 = 5$, $\kappa_2 = 45$ and with $\kappa_1 = 15$, $\kappa_2 = 35$ merge at

$N_2 \sim 180$, while the plot of system with $\kappa_1 = \kappa_2 = 25$ merges at $N_2 \sim 190$.

To confirm our expectation that the I's only cut links, let us look at the degree distributions in the special regime. A plot of typical total degree distributions in that regime is shown in Fig. 5.13(a). The total degree distribution of extroverts (E's) exhibits no unexpected feature. The nodes of E's are "content," and the degree distribution is still consistent with a symmetric exponential distribution around κ_2, which has been well explained earlier. On the other hand, the total degree distribution of I's is not a symmetric exponential distribution any more, but a Gaussian like one, peaked at ~ 78, which is $\gg \kappa_1$ ($\kappa_1 = 5$ in figure). Moreover, the internal degrees (green squares) of all I's are 0. This indicates that all I's have no internal links at all, and all of their degrees come from cross links, and therefore the total degree distribution is exactly their cross degree distribution. These findings support our assumption: The I's get too many cross links from E's, and their degrees are much higher than the preferred degree, so they keep cutting links (internal and cross), which eventually results in zero internal degrees.

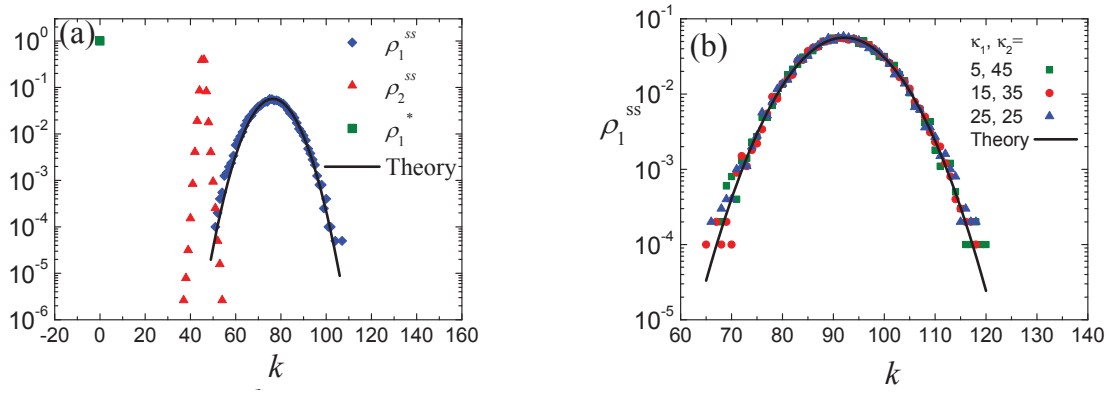

Figure 5.13 (a) The total degree distributions ρ_1^{ss}, ρ_2^{ss} for the two-network model ($N_1 = 10$, $N_2 = 190$, $\kappa_1 = 5$, $\kappa_2 = 45$ and $\chi_\alpha = 0.5$) are represented by blue diamonds and red triangles, respectively. The green squares represent the internal degree distribution of network one, ρ_1^*. (b) The total degree distributions ρ_1^{ss} for two-network models with three sets of κ_1, κ_2. The other associated parameters are $N_1 = 5$, $N_2 = 195$, and $\chi_\alpha = 0.5$. In both figures, solid lines represent theoretical predictions.

Thanks to the feature that there are no I-I links, the two-network model is reduced to a simpler one: one group of nodes can add and cut links, and the other one is allowed to cut links only. For I's, since they have no internal links, once we can understand their total degree distribution, we indeed interpret their cross degree distribution. Furthermore, with the relation $\langle X\rangle = \langle k_1\rangle N_1$, $\langle X\rangle$ can be explained once we understand $\langle k_1\rangle$. Therefore, to find a prediction for $\langle X\rangle$, let us start with formulating an approximation for the degree distribution of I's. Recalling our approach from Section 3.2, here we follow the same idea. Let us use Eq. (3.4), and rewrite it as:

$$\frac{\rho^{ss}(k+1)}{\rho^{ss}(k)} = \frac{W[k+1,k]}{W[k,k+1]}. \tag{5.5}$$

Just to remind our readers, $W[k,k']$ specifies the rate for a node with degree k' to change to k. Once W's are given, with the recursive relation, the stationary $\rho^{ss}(k)$ can be found explicitly. W can be approximated by using the following arguments. Focusing on a particular I node i, with degree k, the only possibility for it to gain one link is by an E node, e, not already connected to it choosing to add a cross link to i. In this process, several rates are involved and should be specified: $(N_2-k)/N$ (the probability to choose an E node not linked to i), w_{+2} (the probability that e wants to add a link), χ_2 (the probability for e to add a cross link), and p (the probability that this cross link is added to i). We can estimate p as follows: On average, each I has $\langle k\rangle = X/N_1$ cross links. If these $\langle k\rangle$ links are evenly distributed on N_2 E's, the fraction of cross links on any E is $\langle k\rangle/N_2 = X/(N_1N_2)$, denoted by f. Thus, the number of I's unconnected to our node e is

$$\frac{1}{p} \simeq 1 + (N_1-1)(1-f), \tag{5.6}$$

where 1 is the contribution from i, and the other N_1-1 introverts each contribute $1-f$. Therefore, the rate p is simply $1/(1+(N_1-1)(1-f))$. As a result, we can write

$$W[k+1,k] = \frac{1}{N}\frac{(N_2-k)\,w_{+2}\chi_2}{1+(N_1-1)(1-f)} \simeq \frac{1}{N}\frac{(N_2-k)/4}{1+(N_1-1)(1-f)}, \tag{5.7}$$

where w_{+2} is approximated by $1/2$, since the degree distribution of the E's is a symmetric exponential distribution around κ_2. On the other hand, the contributions to $W[k,k+1]$ come from two processes. In one process, node i itself chooses to cut a cross link: i is chosen with rate $1/N$ and it cuts a cross link with probability $(1-w_{+1})\chi_1$. As I's always have degrees

larger that κ_1 in our case, w_{+1} is 0, and in turn, this probability is simplified to χ_1 $(= 1/2)$. In the other process, one of the E nodes, l, already connected to i chooses to cut the cross link to i: l is selected with rate $(k+1)/N$ and cuts one of its cross links with probability $(1 - w_{+2})\chi_2 \cong 1/4$. Following a similar argument, we find the number of cross links that l can see is

$$1 + (N_1 - 1) f. \tag{5.8}$$

Given these rates, $W[k, k+1]$ can be written as

$$W[k, k+1] = \frac{1}{N}\left[\frac{1}{2} + \frac{(k+1)/4}{1 + (N_1 - 1) f}\right]. \tag{5.9}$$

Finally, a recursion relation of ρ^{ss} is found to be

$$\rho(k)\left\{\frac{(N_2 - k)/4}{1 + (N_1 - 1)(1 - f)}\right\} = \rho(k+1)\left\{\frac{1}{2} + \frac{(k+1)/4}{1 + (N_1 - 1) f}\right\}. \tag{5.10}$$

We can write the above recursion relation as

$$\rho(k+1) = \rho(k) R(k), \tag{5.11}$$

where

$$R(k) = \frac{N_2 - k}{1 + (N_1 - 1)(1 - f)}\left\{2 + \frac{k+1}{1 + (N_1 - 1) f}\right\}^{-1} \tag{5.12}$$

With normalization, $\rho(k)$ is completely determined, with$N_{1,2}$ as control parameters and f determined self consistently, through the equation:

$$f = \frac{\langle X\rangle}{N_1 N_2} = \frac{\langle k\rangle}{N_2} = \frac{1}{N_2}\sum_{0}^{N_2} k\rho_1^{ss}(k). \tag{5.13}$$

Note that this is independent of the κ's, and in that limited sense, "universal." In Fig. 5.13(a), we present the theory and simulation data for the degree distribution of I's. Fig. 5.13(b) displays ρ_1^{ss} of more extreme systems with $N_1 = 5$ and $N_2 = 195$. Clearly, in the $N_1 \ll N_2$ regime, Fig. 5.13(b) shows that ρ_1^{ss} of different systems are on top of each other, and are fitted well by the theory from Eqn. (5.11) and (5.12). We can conclude that this approximation scheme captures the essentials of the system within this regime. As a result, we can now use the relationship $\langle X\rangle = \langle k\rangle / N_2$ to get $\langle X\rangle$ in the regime, shown as a solid line in Fig. 5.12, and again it provides a good approximation.

CHAPTER 6. INTERACTING DYNAMIC NETWORKS II: THE XIE MODEL

In the previous chapter, we introduced a general two-network model, explored its statistical properties, and discussed some difficulties we are facing. The complexity of the model arises from the fact that in either network, each node can take two possible actions, adding or cutting links, and each has two choices of links, inter- or intra-group links, to update. In the last part of the previous chapter, we have seen that the features of cross links can be understood in a special regime, where one group of population can only cut links so that its internal links are frozen. This gives us a hint that we may have a chance to further understand the two-network model by allowing each group to only add or cut links, but not both. In this chapter, we focus on a simplified interacting networks model, where one group of nodes only adds links and the other group only cuts links. To make the model description simple and easy to understand, we still use the language of social networks, where nodes and links represent individuals and contacts (between pairs of individuals), respectively.

6.1 Model description

The simplified model is defined as follows. As before, we consider two preferred degree networks, labelled "introverts" (I's) and "extroverts" (E's), with $\kappa_I < \kappa_E$. They are of size N_I and N_E, respectively. The total number of nodes is denoted by N ($= N_I + N_E$). In our previous model, the nodes in both networks can take two actions, adding and cutting. In this simpler version, we minimize κ_I and maximize κ_E ($\kappa_I = 0$ and $\kappa_E = \infty$), so that the I's (E's) only cut (add) links. In each attempt, we choose a node at random amongst the N nodes. If it is an I node, it always cuts an existing link selected at random. If an E node is picked, it

always adds a new connection to a randomly chosen neighbor. We refer to this model as the XIE (eXtreme Introverts and Extroverts) model [106, 107]. In such a model, $I-I$ (or $E-E$) and $I-E$ connections are treated as internal and cross links, respectively.

Implementing the rules in simulations, one significant simplification of the XIE model is observed, which enables a bipartite graph description of this model. Since the I's (E's) always cut (add) links, soon after the simulation starts, our system quickly evolves into a special state, where all the $I-I$ ($E-E$) connections are absent (present) and only $I-E$ connections are actively updated. In other words, all the links inside the I network and E network are "frozen," while only the cross links are "active," so that the internal links can be ignored, resulting in a bipartite graph. Therefore, instead of considering all the $2^{N(N-1)/2}$ possible configurations of this model, we are allowed to focus only on the $\mathcal{N}$ ($\equiv N_I N_E$) cross links with $2^{\mathcal{N}}$ configurations. Clearly, the XIE model is a particular case of our previous model by setting $\kappa_1 = 0$, $\kappa_2 = \infty$ and $\chi_1 = \chi_2 = 1$ in the original two-network model, and starting the simulation with network one empty and network two fully connected.

Given the evolution rules, clearly, there are only two control parameters, N_I and N_E. Only the cross links are allowed to be added or cut, depending on which one of its associated nodes are picked. With only two control parameters, exploration of the parameter space is straight forward, by changing the ratio of N_I and N_E. Although when $N_I = N_E$, the model seems simple at first glance, many surprising results arise in this case.

As before, a natural first step is to investigate the degree distribution, denoted by ρ. Again, there are several types of $\rho(k)$'s for the XIE model, depending on what type of links (internal or cross) $\rho(k)$ is associated with. However, as we have discussed above, the internal links of I's (E's) are all absent (present), so it is sufficient to describe each population by one single degree distribution, denoted by $\rho_I(k_I)$ and $\rho_E(k_E)$, respectively (see an example of ρ_I and ρ_E in Fig. 6.1). Here we need to emphasize that, even though the set of cross links is the same for the two groups, the distributions can be different. Therefore, $\rho_I(k_I)$ is not simply equal to $\rho_E(k_I + N_E - 1)$ in general. Beyond the degree distributions, we are also interested in a macroscopic quantity, the total number of cross links, X, defined as Σk_I (or Σk_E). Unlike the degree distributions, which focus on the details of the distribution of links, this simple quantity

directly reflects how strongly the two networks are coupled.

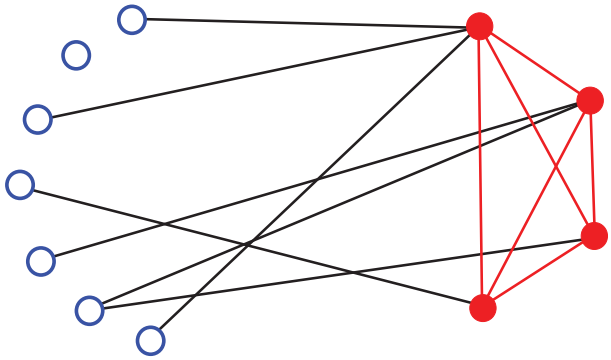

Figure 6.1 The nodes of the two groups, I's and E's, are denoted by open blue and closed red circles, respectively. The cross links and internal links are shown as black and red solid lines, respectively. For this network, the sets of k's are: $k_I = \{1, 0, 1, 1, 1, 2, 1\}$, and $k_E = \{6, 5, 4, 4\}$. Thus, the non-vanishing contributions to the distributions are $\rho_I(0) = 1/7, \rho_I(1) = 5/7, \rho_I(2) = 1/7$ and $\rho_E(4) = 2/4, \rho_E(5) = 1/4, \rho_E(6) = 1/4$.

6.2 Statistical properties of the degree distributions

In the following, we present the details on the Monte Carlo simulation results for the XIE model, as well as the analytical approximations which capture the main features of this model. To save us some computational expenses, in the XIE model, we always look at a relatively small system with $N = 200$. To explore the parameter space, in the simulations, we vary N_I and N_E while fixing $N = 200$, and the associated preferred degree κ_I (κ_E) is set at its minimum (maximum) value 0 (199). The simulations are always started from empty networks (no links) and follow the stochastic rules given above to generate links. One MCS is defined as N attempts (of adding or cutting links), so that, on the average, each node is picked once to update its links.

6.2.1 Nonequal N_I and N_E

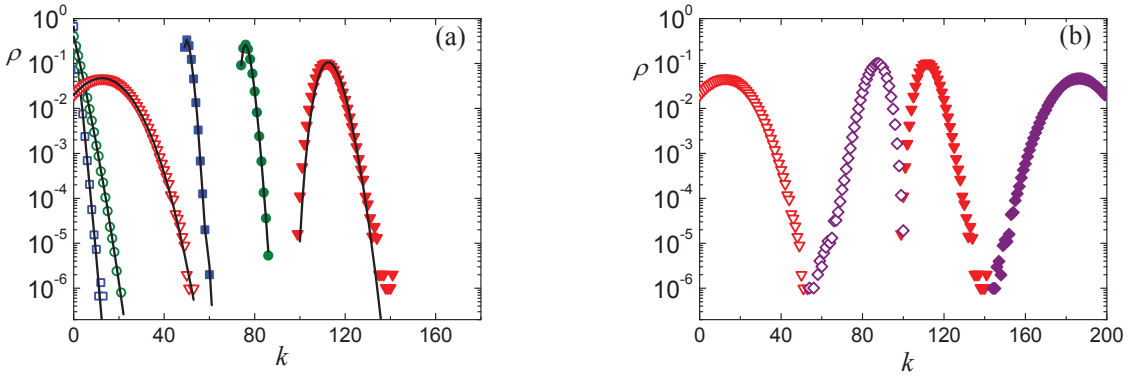

Figure 6.2 Simulation results of degree distributions for XIE model. (a) shows the degree distribution of the network with (N_I, N_E)=(150,50) (blue), (125,75) (green), and (101, 99) (red). (b) shows the comparison of the degree distribution for the systems with (N_I, N_E)=(101,99) (red), and (99, 101) (purple). The open and closed markers represent ρ_I and ρ_E, respectively. Solid lines represent theoretical predictions.

Let us first discuss the cases when the two groups are of different sizes. After we start the simulation, all the $E-E$ links are quickly formed within N MCS. It is sufficient to discard the first $1K$ MCS to let a system of size $N = 200$ reach the stationary state. Thereafter, we obtain the degree distributions by taking the average over 2×10^4 measurements, separated by 100 MCS. The resultant ρ_I and ρ_E for systems with $N_I > N_E$ are shown in Fig. 6.2(a). Some features can be understood easily. Since all E's are connected to each other, the degree of any E, k_E, is at least $N_E - 1$. For all the systems in the figure, the average of the I's degrees, $\langle k_I \rangle$, is smaller than the E's average degree, $\langle k_E \rangle$, since κ_E is larger than κ_I. When there are more E nodes in the system, more links are desired. Therefore, both $\langle k_I \rangle$ and $\langle k_E \rangle$ increase when N_E increases, which is consistent with the resultant distributions. Moreover, the two groups should have equal number of cross links, resulting in the following relation, $\langle k_I \rangle N_I = (\langle k_E \rangle - N_E + 1)N_E$, from which we can get the ratio between $\langle k_I \rangle$ and $\langle k_E \rangle - N_E + 1$ if given N_E/N_I. For convenience, we define a new quantity $\bar{k}_E \equiv k_E - N_E + 1$, which stands for the cross degree of E nodes, and accordingly, the average of $\bar{k}_E$ is $\langle \bar{k}_E \rangle$ ($\equiv \langle k_E \rangle - N_E + 1$). Now, the

relation between the average degrees can be written as $\langle k_I \rangle / \langle \bar{k}_E \rangle = N_E/N_I$, and our simulation results well agree with it. For example, in the system with $N_I = 150$ and $N_E = 50$, from the simulation, we get $\langle k_I \rangle / \langle \bar{k}_E \rangle = 1/3$, which is exactly the value of $N_E/N_I = 50/150 = 1/3$. Clearly, however, this is not sufficient to explain the whole distributions, and some other features remain puzzling: In contrast to the degree distribution of the homogeneous population which is centered at κ, ρ_E here is not centered at its own preferred degree. For all the systems in the figure, κ_E is 199, but the maximum k_E of each system is much less than 199. Before going any deeper in this puzzling feature, it is natural to first find out how the system behaves in the opposite case, where $N_I < N_E$: Will k_E remain much less than κ_E?

To proceed, let us consider a comparison between two systems, one with more I's and the other with more E's. The simulation results are shown in Fig. 6.2(b). The two systems are similar and symmetric, $(N_I, N_E) = (101, 99)$ and $(99, 101)$, respectively. Interesting features are observed: (1) Though the control parameters of the two systems are quite close, their average degrees significantly differ from each other. Take $\langle k_I \rangle$ for instance. In the system with 101 I's and 99 E's, $\langle k_I \rangle$ is around 14, while $\langle k_I \rangle$ is approximately 86 in the other system. (2) By just two nodes changing sides from introverts to extroverts, the whole degree distribution is flipped, i.e., the degree distributions of the two systems exhibits symmetry, to be discussed below. Besides, the same features can also be observed in other pairs of systems with symmetric N_I and N_E (excluding $N_I = N_E$), e.g., between the systems with $(N_I, N_E) = (150, 50)$ and $(50, 150)$, $(125, 75)$ and $(75, 125)$. Moreover, the symmetric systems which differ only in one I and E from each other have also been examined, e.g., $(N_I, N_E) = (100, 99)$ and $(99, 100)$, and they exhibit the same features. Based on these observations, two immediate issues are to be considered: How do we understand the flip of the degree distribution between the symmetric pair of systems? Suppose this observation is true for any symmetric pair of XIE systems, then is the degree distribution of system with parameters $(N_I, N_E) = (100, 100)$ symmetric, since it is paired to itself? We will leave the second question to the next subsection, and try to answer the first one here.

To explain the degree distributions, we introduce an alternative representation to describe the degrees of nodes, and the symmetry will be easily seen under the new description. The

connections of the XIE model can be represented by a $N \times N$ adjacency matrix $\mathbb{A}$, where the elements $a_{ij} = 0$ (1) indicate the absence (presence) of the link between nodes i and j. Since self loops are not allowed, $a_{ii} = 0$ for all i's$\in [1, N]$. Moreover, only the cross links (I-E) are active. Thus, we can consider $\mathbb{N}$ only, the appropriate rectangular sector of $\mathbb{A}$. Let us denote the elements of this $N_I \times N_E$ matrix by n_{ij}. Note that the first (second) index is associated with an I (E) node, so that $i \in [1, N_I]$, $j \in [1, N_E]$. The degree of an I (E) node, can be obtained by summing up all entries along row i (column j). To specify the state of a node, so far, we have always used its degree. In the new description, the states of I's are still characterized by their degrees, but we use a new quantity p, which is the complement of the degree, to describe the state of an E. For simplicity, we suppress the subscript I on k_I from now on. Letting $\bar{n} \equiv 1-n$, we define the degree of an introvert i, and the complement of the degree of an extrovert j, as

$$k_i \equiv \Sigma_j n_{ij}; \quad p_j \equiv \Sigma_i \bar{n}_{ij}. \tag{6.1}$$

By definition, clearly $k_i \in [0, N_E]$ and $p_j \in [0, N_I]$. Additionally, a key symmetry here is $n_{ij} \Leftrightarrow \bar{n}_{ji} \oplus N_I \Leftrightarrow N_E$, which we will refer to as "particle-hole symmetry." This explains the symmetry of the degree distributions qualitatively.

6.2.1.1 Self-consistent mean-field approximation

The major step to understand a stochastic dynamic process involves writing down the master equation and solving it for each configuration. For the XIE model, we find a simple self-consistent mean-field approach sufficient to provide a good explanation to the degree distributions. Thus, we directly work on an approximate expression for ρ. We first write down a general expression for the change of $\rho_I(k,t)$ and $\rho_E(p,t)$ for one attempt, and here we use q to represent the degree (complement of degree) for an I (E). Invoking the approach from the single-network model, and following the line of thought which led to Eqn. (3.4), we obtain a similar expression

$$W[q-1,q]\rho^{ss}(q) = W[q,q-1]\rho^{ss}(q-1). \tag{6.2}$$

where $W[q,q-1]$ specifies the rate for an I (E) with $q-1$ "particles" ("holes") to change to the state with q "particles" ("holes"). To solve this equation, our next step is to determine

the rates, $W[q-1,q]$ and $W[q,q-1]$. (For simplicity, we drop the superscript ss for the degree distribution.) Focusing on the degree distribution of the introverts, ρ_I, we note that for a chosen I node i, only i itself contributes to $W_I[k-1,k]$. That is, only when i is picked to update a link, i can cut one of its links and decrease its degree by one, and the rate for choosing node i is $1/N$. Thus, rate $W_I[k-1,k]$ is $1/N$. On the other hand, the contribution to $W_I[k,k-1]$ is from the process that one of the extroverts j, with "holes" p_j, not connected to i, is selected and creates a link to node i. In this process, a j is picked with rate $(N_E-k+1)/N$. The probability that j creates the connection to i is $1/p_j$. Since there are N_E-k+1 such E nodes, with different p's, finding out exact $W_I[k,k-1]$ is quite involved. Thus, we approximate the number of "holes" of each E by the average, $\langle p\rangle'$. Note that this average is not simply the average value of p over all E's, but over those E's having non-vanishing p's. $\langle p\rangle'$ is given by

$$\langle p\rangle' \equiv \frac{\sum_{p>0} p\rho_E(p)}{\sum_{p>0}\rho_E(p)} = \frac{\sum_{p\geq 0} p\rho_E(p)}{1-\rho_E(0)} = \frac{\langle p\rangle}{1-\rho_E(0)}. \tag{6.3}$$

With the above $\langle p\rangle'$, the expression for $W_I[k,k-1]$ can be written as $(N_E-k+1)/(N\langle p\rangle')$. Thus, Eqn. (6.2) for ρ_I evolves to the form of

$$\frac{1}{N}\rho_I(k) = \frac{N_E-k+1}{N}\left(\frac{1}{\langle p\rangle'}\right)\rho_I(k-1). \tag{6.4}$$

Following the above analysis, a similar argument leads to $W_E[p-1,p]=1/N$ and $W_E[p,p-1] = (N_I-p+1)/(N\langle k\rangle')$, with $\langle k\rangle' = \langle k\rangle/(1-\rho_I(0))$, so that we obtain

$$\frac{1}{N}\rho_E(p) = \frac{N_I-p+1}{N}\left(\frac{1}{\langle k\rangle'}\right)\rho_E(p-1). \tag{6.5}$$

Clearly, if $\langle p\rangle'$ and $\langle k\rangle'$ are given, we can solve for $\rho_I(k)$ and $\rho_E(p)$ by repeatedly using Eqn. (6.4) and (6.5). However, to obtain the value of $\langle p\rangle'$ and $\langle k\rangle'$, we have to know $\rho_I(k)$ and $\rho_E(p)$ first, which seems to lead us to an endless loop. To avoid that circumstance, let us pretend that we already know either of $\langle p\rangle'$ and $\langle k\rangle'$, say now we assume that we know $\langle p\rangle'$ and assign it with a reasonable value between 0 and N_I. With a given $\langle p\rangle'$, we can calculate $\rho_I(k)$ explicitly using Eqn. (6.4), and get a specific average $\langle k\rangle'$ from $\rho_I(k)$. Thereafter, we plug in the resultant $\langle k\rangle'$ to Eqn. (6.5) and find out $\rho_E(p)$. With known $\rho_E(p)$, thereafter, we can follow Eqn. (6.3) to get an output of $\langle p\rangle'$. In this process, we input a $\langle p\rangle'$ and get an output $\langle p\rangle'$. To get the

right degree distributions, we adjust the input $\langle p \rangle'$, until the difference between the input and output is $O(10^{-5})$. Consequently, the corresponding degree distributions are considered to be the mean-field approximation for $\rho_I(k)$ and $\rho_E(p)$. This method is referred to as *self-consistent mean-field approximation*. Here, we have to remind our readers that even though we have obtained $\rho_E(p)$, it is not the originally defined degree distribution of extroverts, but the "hole" distribution. To recover this, we can simply replace p by $N-1-k_E$, and then get the right $\rho_E(k_E)$. On the other hand, $\rho_I(k)$ itself is the degree distribution of introverts, $\rho_I(k_I)$. This approach works quite well to predict the degree distributions and is shown as solid lines in Fig. 6.2(a). Moreover, clearly, in Eqn. (6.4) and (6.5), if we switch N_I and N_E, the new $\rho_I(k_I)$ and $\rho_E(k_E)$ are essentially the old $\rho_E(k_E)$ and $\rho_I(k_I)$, respectively. That is, the symmetry also appears in the mean-field approximation. So far, we have shown both the simulation results and theoretical considerations for the stationary distribution of the network with *non*-equal N_I and N_E. In the following subsection, we move on to the very special case of our model, where $N_I = N_E$.

6.2.2 $N_I = N_E$

In this subsection, we aim to answer the question: What is the degree distribution for the case $(N_I, N_E) = (100, 100)$? In this case, the whole network is symmetric. In the "particle-hole" description of XIE model, now there are 100 I nodes demanding no "particles" and 100 E nodes preferring 0 "holes," for which Eqn. (6.4) and (6.5) are exactly the same. As a result, $\rho_I(k)$ and $\rho_E(p)$ have the same form. Note that the relation between the "holes" and degrees of E's is $p = N-1-k_E$, so the degree distributions $\rho_I(k_I)$ and $\rho_E(k_E)$ should be symmetric around $(N-1)/2$, i.e., 99.5 in our case. The simulation results are shown in Fig. 6.3. As expected, the distributions are symmetric around 99.5. However, surprisingly, the distributions are flat and broad, quite different from the sharp ones seen before. Even if compared to the distributions of systems with $(N_I, N_E) = (101, 99)$ or $(N_I, N_E) = (99, 101)$, where the only difference is one node, the distribution of $(100, 100)$ is still peculiar. Besides, the distribution takes much longer time ($O(10^7$ MCS)) to reach its steady state, while all other cases ($N_I \neq N_E$) only take $O(10^5$ MCS). As a consequence of the broad distribution, the self-consistent mean-field approach

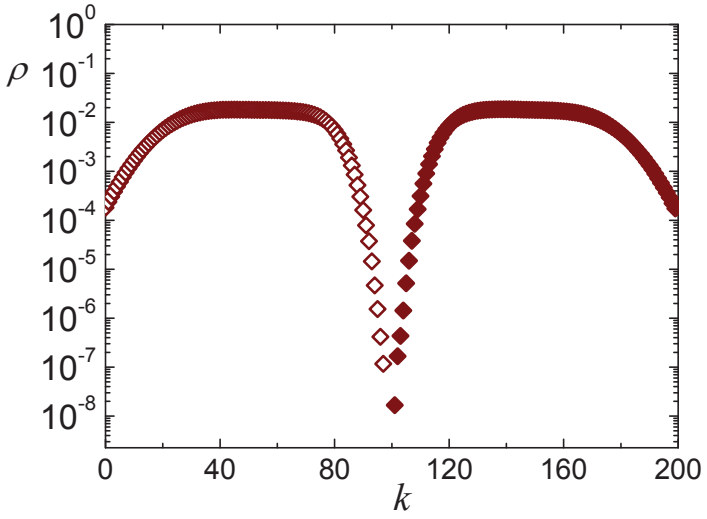

Figure 6.3 Simulation results of degree distributions for the network with 100 introverts and 100 extroverts. The empty and solid diamonds represent ρ_I and ρ_E, respectively.

does not work any more, since the degree of each individual node cannot be well approximated by the average degree. However, we can understand the distributions qualitatively. In the XIE model, the introverts (extroverts) always cut (add) links, and so the number of cross links is determined by which group has more chance to update links. In the networks with *non*-equal N_I and N_E, on the average, the majority nodes are picked and update their links more often, so that the majority "wins" the "frustration," and the whole network will have fewer (more) links if it has fewer (more) extroverts than introverts. In the special $N_I = N_E$ case, however, the introverts and extroverts are equally likely to be selected. Thus, in each attempt, the probability for a link to be formed or destroyed is equal, and therefore neither of the two populations will "beat" the other, which results in "maximal frustration." To look into the behavior of the network in the special case more carefully, we turn our attention to a simpler quantity, namely X, the total number of cross links.

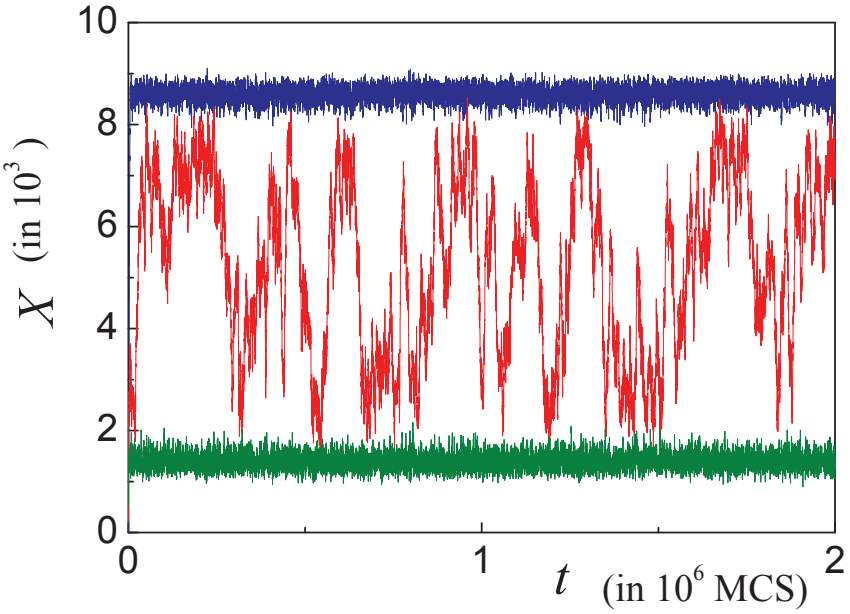

Figure 6.4 Time traces of X for three cases: $N_I = 101$ (green), 100 (red), and 99 (blue).

6.3 Statistical properties of the total number of cross links

Though the networks are typically characterized by the degree distributions, we have seen that, for the special case $N_I = N_E$, the degree distributions are peculiar, and our mean-field approach for the degree distributions fails. Recalling that the only dynamics is on the cross links, we believe that the puzzle can be traced to the behaviors of a simple quantity, X. Particularly, the broad degree distributions of (100, 100) should be associated with a broad distribution of X, and the "flip" of the degree distributions of (101, 99) and (99, 101) should be related to a "jump" of X.

To see how X behaves, we first show the time traces $X(t)$ for $(N_I, N_E) = (101, 99)$, $(100, 100)$, and $(99, 101)$ in Fig. 6.4 (green, red and blue). Clearly, $X(t)$ for $(100, 100)$ displays quite different behaviors from the other two systems. The data for $N_I - N_E = \pm 2$ (green and blue lines) show that X settles down very quickly, and hovers around its own average $\langle X \rangle$ with fluctuations of $O(100)$. When only two nodes "change sides" from introverts to extroverts $(101, 99) \to (99, 101)$, $\langle X \rangle$ displays a large jump, and this observation is consistent with the

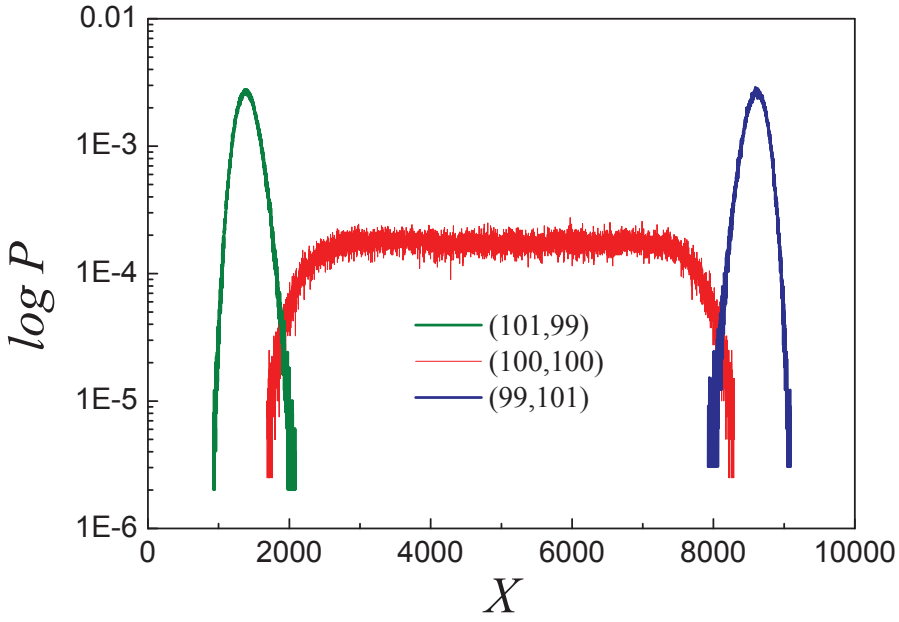

Figure 6.5 Histograms of X for three cases: $N_I = 101$ (green), 100 (red), and 99 (blue).

degree distribution: The whole distribution is flipped as $(101, 99) \to (99, 101)$. In particular, the fraction $\langle X \rangle / \mathcal{N}$ changes from $\sim 15\%$ to $\sim 85\%$, a jump of 70%. On the other hand, $X(t)$ of $(100, 100)$ wanders widely, evolving very slowly.

From the time traces in the stationary state, we compile the histograms for X, $P^{ss}(X)$, and show the results in Fig. 6.5. The resultant $P^{ss}(X)$ for $(101, 99)$ and $(99, 101)$ are Gaussian like, sharp distributions, while $P^{ss}(X)$ for $(100, 100)$ is essentially a flat distribution exploring most of its full range, with soft cutoffs at both ends. This reminds us of an unbiased random walk, confined between two "walls." To confirm our expectation, we have constructed the power spectrum from $X(t)$ and found that it is indeed consistent with $1/f^2$ for $1/f \lesssim 10^6$ MCS. The 10^6 MCS is the time for X to traverse the observed range, and it can be roughly explained as follows. Recall that in the $N_I = N_E$ situation, the rate for X to increase and decrease by one is equal at each update attempt. Considering the traverse as an unbiased random walk, we can treat each attempt as a random variable x, with two values ± 1, corresponding to adding and cutting a cross link, respectively. Accordingly, we obtain $\langle x \rangle = 0$ and $\langle x^2 \rangle = 1$. Thus, the

expected value of the distance after n steps walking is

$$\sqrt{\langle(\sum_{i=1}^{n} x_i)^2\rangle} = \sqrt{n\langle x^2\rangle + 2\sum_{i\neq j}\langle x_i x_j\rangle} = \sqrt{n}. \tag{6.6}$$

Thus, it follows that the expected value of the distance of moving n steps is $\sqrt{n}$. Back to our problem, where a complete traverse for X is of distance $O(\mathcal{N})$, then the number of steps needed is $O(\mathcal{N}^2)$, which is $O(\mathcal{N}^2/N) = O(N^3)$ MCS, consistent with the 10^6 MCS observed. While all of these arguments need to be tightened quantitatively, they do paint a plausible picture, namely, that X performs an unbiased random walk in case of equal N_I and N_E. However, near the two ends of the flat distribution, an additional consideration becomes important. Focusing on the small X, we observe that a considerable fraction of introverts which have no connections at all emerges. Similarly, for large X, we find a fraction of extroverts which have all links. When these nodes are selected in the simulation, no update can occur. As a consequence, near the two boundaries, the numbers of *active* introverts and extroverts are no longer equal and the dynamics of X becomes a biased random walk. Hence, X is pushed towards the center, until the equality of *effective* N_I and *effective* N_E is restored. To confirm this argument, we measure the degree distribution in several intervals near the "walls," and examine $\rho_I(0)$ and $\rho_E(N-1)$ for small and large X, respectively. The data show that when X fluctuates around very small (large) values, non-zero values for $\rho_I(0)$ ($\rho_E(N-1)$) are observed. For instance, when $X \in [1600, 1700]$, $\rho_I(0) \simeq 1\%$, which indicates that in each MCS, one introvert does not cut links when selected. While this argument provides some insight into the *existence* of the "walls," it still cannot predict their *locations*.

The above arguments lead to a qualitative explanation for some behaviors of X, but only limited to three systems, $(N_I, N_E) = (101, 99)$, $(100, 100)$, and $(99, 101)$. In the rest of this chapter, we will consider more systems with different N_E/N_I's. To simplify our discussion, we focus on the mean, $\langle X\rangle$, instead of the whole distribution. Note that the features of X are dominated by the difference between N_I and N_E, i.e., $|N_E - N_I|$. For convenience, let us define a quantity $h \equiv (N_E - N_I)/(N_E + N_I)$, and a normalized mean $\bar{X} = \langle X\rangle/\mathcal{N}$. Next, we will study $\bar{X}$ as a function of h.

Before we present the simulation data for $\bar{X}$, let us first discuss what can be expected.

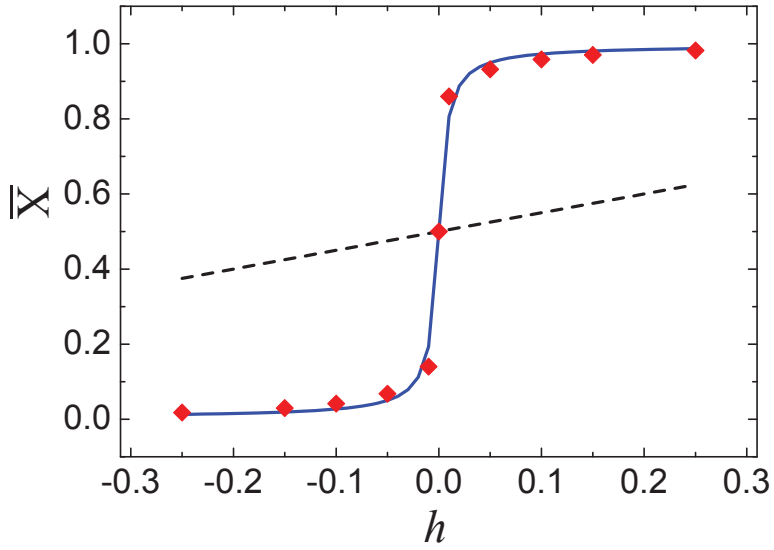

Figure 6.6 The behavior of the average number of cross links for various N_I and N_E, displayed in terms of $\bar{X}(h)$. Data points (red diamonds) are associated with $(N_I, N_E) = (125, 75), (110, 90), (101, 99), (100, 100)$, etc. The dashed line is the prediction from an "intuitively reasonable" argument. A mean-field approach leads to the solid (blue) line.

Clearly, $\bar{X}$ should be a monotonically increasing function of N_E/N. Since in each update, every node is equally likely to be chosen, a rough guess for the ratio of the numbers of creation and deletion events could be N_E/N_I. Note that in the stationary state, there are $\langle X \rangle$ links and $\mathcal{N} - \langle X \rangle$ "holes." We reach a naive guess $N_E/N_I = \langle X \rangle / (\mathcal{N} - \langle X \rangle)$, which is shown as a dashed line in Fig. 6.6. However, our simulation results (red diamonds) paint a completely different picture, i.e, instead of a linear function, $\bar{X}(h)$ exhibits a sizable jump. Although the jump of $\langle X \rangle$ suggests a first order phase transition, some other associated features, such as phase coexistence and metastability, are absent in the XIE model. Specifically, we have tested for metastability: We start the simulation with $N_I = 101$ and $N_E = 99$, run it long enough for the network to relax to its stationary state, and then suddenly change N_I and N_E to 99 and 101, respectively. In Fig. 6.7, our data show that X promptly responds to the switch, following a biased random walk with velocity of 2/MCS till it reaches the appropriate X of system with 99 I's and 101 E's. Other systems sizes have also been examined, and they all follow the same behaviors.

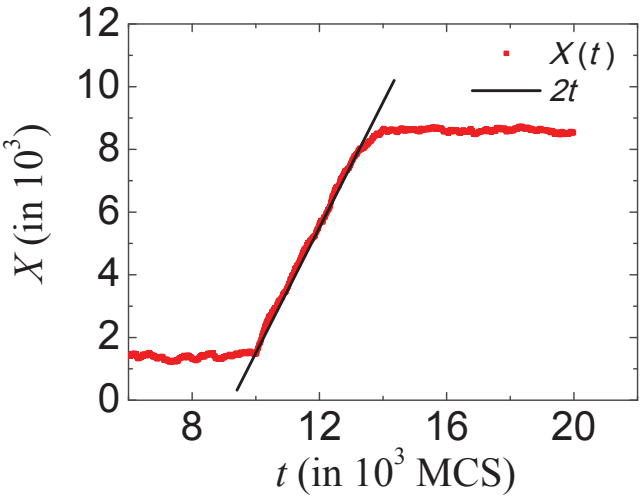

Figure 6.7 Time trace $X(t)$ (red) for a system with 200 nodes. Initially, the system has $N_I = 101$ and $N_E = 99$, after it relaxes to its stationary state, N_I and N_E are switched. The solid line is $\propto 2t$.

6.3.1 Master equation and stationary $\mathcal{P}^*$

To describe the model completely, we have to specify and solve the master equation for $\mathcal{P}(\mathbb{N}, t\ |\mathbb{N}_0, 0)$, which is the probability of finding configuration $\mathbb{N}$ at time t, with the initial configuration $\mathbb{N}_0$. We can write down the discrete master equation for $\mathcal{P}$ as follows: the change over one attempt, $\mathcal{P}(\mathbb{N}, t+1) - \mathcal{P}(\mathbb{N}, t)$ is given by

$$\sum_{\{\mathbb{N}'\}} [W(\mathbb{N}, \mathbb{N}')\mathcal{P}(\mathbb{N}', t) - W(\mathbb{N}', \mathbb{N})\mathcal{P}(\mathbb{N}, t)] \tag{6.7}$$

where $W(\mathbb{N}, \mathbb{N}')$ is the rate for configuration $\mathbb{N}'$ to change to $\mathbb{N}$. Using (6.1), $W(\mathbb{N}', \mathbb{N})$ can be written as:

$$\sum_{i,j} \frac{\Delta}{N} \left[\frac{\Theta(k_i)}{k_i} \bar{n}'_{ij} n_{ij} + \frac{\Theta(p_j)}{p_j} n'_{ij} \bar{n}_{ij} \right] \tag{6.8}$$

where $\Theta(x)$ is the Heavyside function, whose value is 1 if $x > 0$ and 0 if $x \leq 0$, and $\Delta \equiv \Pi_{k\ell \neq ij} \delta(n'_{k\ell}, n_{k\ell})$ insures that only n_{ij} may change.

Since the dynamics of the network is memoryless, it is a Markov process. In particular, we find that the dynamics obeys detailed balance (details can be found in Appendix B). Consequently, when the limit $t \to \infty$ is taken, $\mathcal{P}$ approaches its stationary distribution, $\mathcal{P}^*$. In the appendix we show that the dynamics satisfies detailed balance, and therefore all

stationary probability currents vanish. By using the detailed balance condition recursively, $\mathcal{P}^*(\mathbb{N}) = \mathcal{P}^*(\mathbb{N}')\, W(\mathbb{N}, \mathbb{N}') \,/\, W(\mathbb{N}', \mathbb{N})$, and imposing normalization, we find explicitly

$$\mathcal{P}^*(\mathbb{N}) = \frac{1}{\Omega} \prod_{i=1}^{N_I} (k_i!) \prod_{j=1}^{N_E} (p_j!) \tag{6.9}$$

where $\Omega = \Sigma_{\{\mathbb{N}\}} \Pi(k_i!)\, \Pi(p_j!)$ plays the role of the "partition function." From the form of stationary distribution, the particle-hole symmetry is obvious.

6.3.2 Mean-field approximation

With the explicit stationary distribution $\mathcal{P}^*$, in principle, $P(X)$ can be obtained by summing up the probabilities over all configurations having X cross links,

$$P(X) \equiv \sum_{\{\mathbb{N}\}} \delta(X, \Sigma_{ij} n_{ij})\, \mathcal{P}^*(\mathbb{N}). \tag{6.10}$$

Calculating Eqn. (6.10), however, is quite involved. Therefore, to make progress, we invoke a mean-field approach and find an approximate expression for Eqn. (6.10). Instead of working with the exact configuration, we replace each element n_{ij} (= 0 or 1) in $\mathbb{N}$ by the average, $X/\mathcal{N}$, so that, $k_i = \Sigma_j n_{ij} \to N_E (X/\mathcal{N})$ and $p_j = \Sigma_i \bar{n}_{ij} \to N_I (1 - X/\mathcal{N})$, while

$$\sum_{\{\mathbb{N}\}} \delta(X, \Sigma_{ij} n_{ij}) = \binom{\mathcal{N}}{X}. \tag{6.11}$$

Applying Stirling's formula, we reach a mean field approximation of P, which is referred to as $P_{MF}(X)$. In this spirit, it is natural to label

$$F(\rho) \equiv -\ln P_{MF}(X) \tag{6.12}$$

as a "free energy" for $\rho \equiv X/\mathcal{N}$ ($\rho \in [0, 1]$). In the thermodynamic limit (X, $\mathcal{N} \to \infty$ at fixed ρ), the leading order of F is linear in ρ, with slope $ln(N_I/N_E)$. Specifically, as long as $N_I \neq N_E$, the minimum of F occurs at the boundary values $\rho = 0$ or 1, and therefore, ρ can only assume the values 0 or 1. By contrast, when $N_I = N_E$, F is flat over the entire interval. This prediction qualitatively agrees with the simulation results. To avoid the extremes, we keep the next order. The result is

$$F(\rho) \propto \rho \ln N_I + [1 - \rho] \ln N_E - \frac{1}{2} \left(\frac{\ln \rho}{N_E} + \frac{\ln [1 - \rho]}{N_I} \right) + O\left(\frac{1}{\mathcal{N}} \right). \tag{6.13}$$

From here, we can find the minimum of F and plot it as $\bar{X}(h)$ for the specific case of $N = 200$. The resultant (solid blue curve in Fig. 6.6) is remarkably respectable. We should caution the reader, however, that such good agreement does not extend to the entire distribution, i.e., $P_{MF}(X)$ deviates considerably from the histograms of X.

CHAPTER 7. INTERACTING DYNAMIC NETWORKS III: OTHER MODELS

In Chapters 5 and 6, we have discussed the results for a model of interacting preferred degree networks, where the interaction is controlled by a parameter, $\chi \in [0, 1]$. When χ is 0 (1), the model describes isolated networks (coupled networks with maximal interaction). Other choices of χ lead to more general interacting network models. In Chapter 5, we explored the general parameter space of this model, while Chapter 6 focused on an extreme case (a model with maximum interaction). Other than this model, there are many possible ways to introduce an interaction between networks. Thus, in this chapter, we attempt to explore different methods to couple two networks. Of course, it is difficult to include all possibilities, and therefore, we only present two models here.

7.1 Two-κ model

In all our previous discussions, each network is assigned only a single preferred degree, which governs the total degree of each node. Subject to that constraint, the number of internal or cross links is still free to vary. However, in more realistic situations, e.g., in a social network, an individual may be part of a group, which interacts with another group, and in this context, we may wish to control the intra- and inter-group connections separately. Motivated by such considerations, we introduce a new model, in which each node is characterized by two κ's, governing its internal and cross degrees, respectively.

7.1.1 Model description

Again, we focus on the interaction between two preferred degree networks, with N_1 and N_2 nodes, respectively. The total number of nodes $N_1 + N_2$ is denoted by N. Instead of having a single preferred degree, κ_α ($\alpha = 1, 2$), each individual network is assigned two preferred degrees, the preferred internal degree κ_α^* and the preferred cross degree $\kappa_\alpha^\times$. Without a specific parameter, i.e. χ, to control the interaction strength, now $\kappa_\alpha^\times$ plays the role of governing the interaction: Ideally, the larger $\kappa^\times$ is, the more cross links exist. Of course, this ideal situation only occurs when $\kappa_1^\times \simeq \kappa_2^\times$, otherwise, if $\kappa_1^\times \gg \kappa_2^\times$ (or $\kappa_1^\times \ll \kappa_2^\times$) so that one group prefers to have far more cross links than the other, this will lead to "frustration" between two groups, and then, it is difficult to have an immediate estimate of the number of cross links.

In our simulations, we update the links in the system as follows. At each attempt, a node is selected from the two groups at random. For the sake of simplicity, in this section, we always consider two groups of the same size, so that the rate of selecting a node from either network is always 1/2. Once a node is chosen, we first decide, with equal probability, whether to take action on its cross links or internal links. In the latter case, the internal degree, k^*, of the node is noted. If $k^* < \kappa^*$, a new internal link will be established between the chosen node and a partner node randomly selected from the same group. Otherwise, we will cut one of the chosen node's existing internal links. In the former case, we update the cross links of the chosen node, in the same fashion. Note that the partner nodes have no control over the link updates. Again, self-loops or multiple connections are not allowed. In the simulations, one Monte Carlo step (MCS) consists of N such attempts, so that we can insure that, on the average, each node can be picked once.

Let us present a short discussion of the quantities of interest and our expectations for the simulation results. As seen before, there are three classes of degree distributions, ρ_α, ρ_α^*, and $\rho_\alpha^\times$. Since each node has specific preferred degrees to govern its internal and cross degrees separately, both preferred degrees play a part in managing the total degree. Thus, we expect that ρ_α might be different from the cases we studied in Chapter 5 and 6, where only the total degree of each node was specified. To understand ρ_α, we start from the detailed degree

distributions, ρ_α^* and $\rho_\alpha^\times$ first. Note that in either network, κ_α^* is the only parameter that controls the internal degrees, and therefore the internal links in one network are not affected by cross links or internal links in the other network. Hence, we expect that ρ_α^* is the same as the degree distribution of a single preferred degree network. By contrast, the cross degrees of either network should be affected by the other. If we look at the cross links only, the partial system is similar to the XIE model, except that the I's (E's) prefer moderate degrees instead of the minimum (maximum) degrees. Another difference resides that here, the internal links are still dynamic and therefore, the cross links evolve on a different time scale. When the two networks have very different $\kappa^\times$'s, it may again result in frustration, where one group keeps cutting cross links, while the other always adds. As we have learnt from Chapters 5 and 6, once there is "frustration" in the system, we expect to observe large fluctuations in the number of cross links, X. However, as we will see below, the fluctuations here are not nearly as extreme as in the XIE model.

7.1.2 Simulation results and theoretical explanations

As discussed above, systems with $\kappa_1^\times \simeq \kappa_2^\times$ and ones with $\kappa_1^\times \gg \kappa_2^\times$ ($\kappa_1^\times \ll \kappa_2^\times$) might exhibit very different behaviors, due to possible "frustration" between the networks. In the following, we first investigate the "symmetric" case, characterized by $\kappa_1^\times = \kappa_2^\times$, and later in this chapter, we turn to "asymmetric" cases (with $\kappa_1^\times \neq \kappa_2^\times$). For each case, we first analyze the degree distributions and thereafter, briefly consider the number of cross links. As before, for the degree distribution, with the first $2K$ MCS discarded, our simulation results are averaged over 10^4 measurements, each separated by 100 MCS. Turning to the cross links, we observe that X already settles down within a short run time of approximately 10^5 MCS. This allows us to shorten our runs for $X(t)$ to 10^6 MCS, within which X is measured every 100 MCS.

7.1.2.1 Symmetric networks

To have comparable data sets, we look at a system with networks of size 1000 ($N_1 = N_2 = 1000$). In Sections 3.2 and 4.2, the total preferred degree is 250, and therefore, in this section, we confine the sum of preferred internal and cross degrees, $\kappa_\alpha^\times + \kappa_\alpha^* = 250$. If the size of the

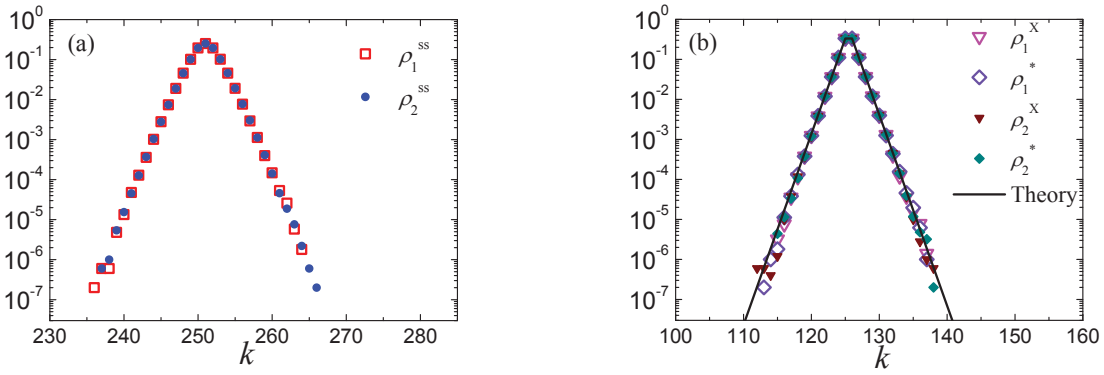

Figure 7.1 Simulation results of degree distributions for a symmetric system with $N_\alpha = 1000$ and $\kappa_\alpha^{*,\times} = 125$. (a) shows the total degree distributions, ρ_1^{ss} and ρ_2^{ss}. (b) shows four detailed degree distributions, $\rho_\alpha^{*,\times}$. Our theory is plotted as solid lines in (b).

networks is unchanged, the control parameters are just the four κ's, so we vary their values and explore how the degree distributions of the networks changes. We first look at the most symmetric system, in which $\kappa_\alpha^{\times} = \kappa_\alpha^{*} = 250/2 = 125$. The simulation results are shown in Fig. 7.1. In (a), the two total degree distributions, ρ_α^{ss}, are the same and peaked at $k = 251$. In (b), all four distributions $\rho_\alpha^{*,\times}$ fall on top of each other and peaked at $k = 125.5$. Let us consider the detailed degree distributions first. Unsurprisingly, ρ_α^{*} agrees with our expectation, consistent with a Laplacian distribution, $\propto e^{-\mu|k-\kappa|}$ (solid line in figure). Our data indicate $\mu = 1.08 \pm 0.01$. As mentioned before, ρ_α^{*} is exlusively determined by the inter-group dynamics, and therefore is identical to the total degree distribution for a single preferred degree network (see in Section 3.2). Moreover, here $\rho_\alpha^{\times}$ is also consistent with a Laplacian distribution for this parameter set. Of course, in general, this does not hold (see below); instead, it is a special feature of the symmetric case $\kappa_1^{\times} = \kappa_2^{\times}$. Let us consider a randomly selected node in group one, and let us assume that we take action on a cross link. For such an action, the chosen node needs to select a partner from all nodes in network 2. Furthermore, the chosen node and all the nodes in network 2 have the same $\kappa^{\times}$. Therefore, this set of $N_2 + 1$ nodes effectively form a single preferred degree network. Consequently, $\rho_\alpha^{\times}$ obeys a Laplacian distribution wich the same μ.

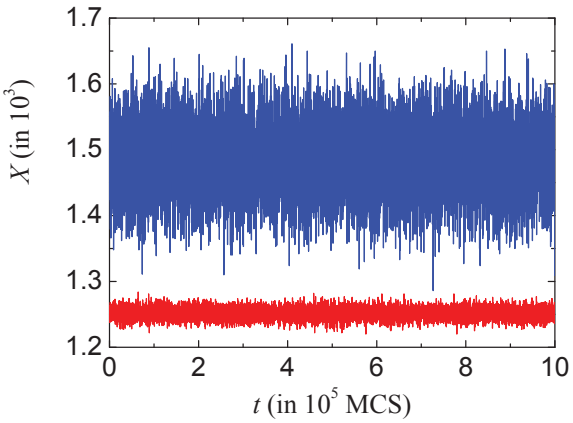

Figure 7.2 Simulation results of $X(t)$ for a symmetric system (red) with $N_\alpha = 1000$ and $\kappa_\alpha^{*,\times} = 125$, as well as a asymmetric system (blue) with $N_\alpha = 1000$, $\kappa_1^* = 50$, $\kappa_1^\times = 200$, $\kappa_2^* = 200$, and $\kappa_2^\times = 50$.

Next, we turn to the the total degree distribution ρ_α^{ss}. We first note that it cannot be obtained from ρ_α^* and $\rho_\alpha^\times$, which can be seen as follows. For convenience, let us change the notation of ρ_α^* and $\rho_\alpha^\times$ to $\rho_{\alpha\beta}\left(k_{\alpha\beta}\right)$, associated with $k_{\alpha\beta}$, denoting the number of links with which a node in community α is connected to nodes in community β. Though somewhat cumbersome, we will use the notation above, to leave no doubt about which quantity is being considered. To see how the degree distributions are related, we can proceed further and consider joint distributions, $P_1\left(k_{11}, k_{12}\right)$, the probability that a node in community 1 will be found with degrees k_{11} and k_{12}. Clearly,

$$\rho_\alpha\left(k\right) \equiv \sum_{k_{\alpha\alpha}, k_{\alpha\beta}} \delta\left(k_{\alpha\alpha} + k_{\alpha\beta} - k\right) P_\alpha\left(k_{\alpha\alpha}, k_{\alpha\beta}\right) \tag{7.1}$$

while $\rho_{\alpha\alpha}$ and $\rho_{\alpha\beta}$ are simple projections of P_α, e.g., $\rho_{\alpha\alpha}\left(k_{\alpha\alpha}\right) = \sum_{k_{\alpha\beta}} P_\alpha\left(k_{\alpha\alpha}, k_{\alpha\beta}\right)$. These remarks show that ρ_α cannot be obtained from $\rho_{\alpha\alpha}$ and $\rho_{\alpha\beta}$ in general. Looking at Fig. 7.1(a), we notice some slight curvature in the tails. This is borne out by investigating the data in more detail. Hence we conclude that ρ_α^{ss} is not a Laplacian, but its analytic form remains unknown at this point.

Next, we shift our focus to X. Again, to have data comparable to our previous studies, we focus on a smaller system, with $N_1 = N_2 = 100$ and $\kappa_\alpha^* = \kappa_\alpha^\times = 12.5$. Motivated by

our findings reported in the previous two chapters, it is natural to investigate $X(t)$ and its fluctuations. A time trace for X is shown in Fig. 7.2 (red). It is clear from the data that $X(t)$ exhibits small fluctuations around a well defined average. Another way to argue is to consider the degree distribution $\rho_\alpha^\times$, which is directly associated with X. Here, the cross degree distributions of both networks are Laplacian distributions, sharply peaked at $\kappa_\alpha^\times$. Since X is simply $\sum_0^{N_\alpha} k_\alpha^\times \rho_\alpha^\times N_\alpha$, we expect X to be stabilized. The mean, $\langle X \rangle$, and the standard deviation, σ, are $\sim 1251 (\simeq \kappa_\alpha^\times N_\alpha)$ and ~ 8.4, respectively.

7.1.2.2 Asymmetric networks

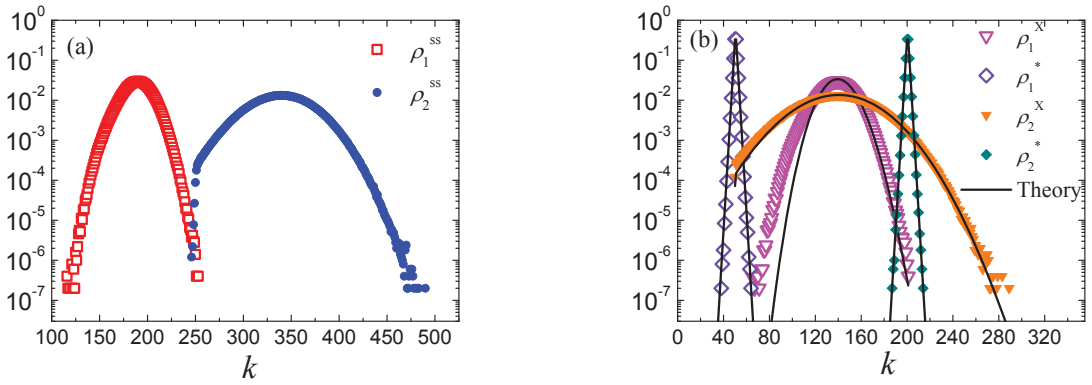

Figure 7.3 Simulation results of degree distributions for an asymmetric system with $N_\alpha = 1000$, $\kappa_1^* = 50$, $\kappa_1^\times = 200$, $\kappa_2^* = 200$, and $\kappa_2^\times = 50$. (a) shows the total degree distributions, ρ_1^{ss} and ρ_2^{ss}. (b) shows four detailed degree distributions, $\rho_\alpha^{*,\times}$. Our theory is plotted as solid lines in (b).

Let us move on to the asymmetric systems, where $\kappa_1^\times \neq \kappa_2^\times$. In the simulations, we choose $N_1 = N_2 = 1000$ and keep $\kappa_\alpha^* + \kappa_\alpha^\times = 250$. The results are shown in Fig. 7.3. As discussed above, the internal degree distribution ρ_α^* is independent from the other distributions, and therefore, it is still consistent with a Laplacian distribution. By contrast, when we turn to the other degree distributions, different behaviors are observed. Neither ρ_α^{ss} and $\rho_\alpha^\times$ are narrowly peaked any more; instead, they are broad distributions. Furthermore, since ρ_α^* is a sharply peaked distribution, ρ_α^{ss} is essentially identical to $\rho_\alpha^\times$ apart from a shift by $\langle k_\alpha^* \rangle$. Therefore,

the key is to understand $\rho_\alpha^\times$. We believe that the broad distributions can be traced to the existence of frustration. Specifically, in the system shown in the figure, each node of network 1 desires 200 cross links, while the nodes in network 2 prefer to have only 50 each. The resultant averages are $\langle k_1^\times \rangle = \langle k_2^\times \rangle \simeq 140$, which differ significantly from their preferred degrees (200 and 50). In addition to the averages, most nodes are not content with their cross degrees, $k_1^\times < \kappa_1^\times$ ($k_2^\times > \kappa_2^\times$) for nodes in network 1 (2). This feature allows us to simplify the asymmetric system: If we focus on the cross links only, the system lets network 1 add links, and network 2 cut links. (Of course, for those few in network 1 (2) with $k_1^\times = 201$ ($k_2^\times = 50$), cutting (adding) links is also possible.) This reminds us of our XIE model. Therefore, to make our life easier, we name network 1 nodes as extroverts, nodes in network 2 as introverts, and reuse some results of the XIE model to help us make progress in understanding $\rho_\alpha^\times$. For the XIE model, we arrive at a recursion relation Eqn. 6.2,

$$W[k+1,k]\rho^{ss}(k) = W[k,k+1]\rho^{ss}(k+1), \tag{7.2}$$

to calculate the total degree distribution for I and E, where $W[k',k]$ stands for the rate for a node to change its degree from k to k'. Here, we can use this equation again, for $\rho_\alpha^\times$. For convenience, we drop the superscript $\times$ on $k_\alpha^\times$, since we only discuss the cross links here. In our specific system shown in Fig. 7.3(b), clearly, introverts and extroverts are nodes in network 2 and 1, respectively. As before, our task is to determine the rates $W[k',k]$. Let us focus on $\rho_2^\times$ first. The only way for an introvert to get its degree decreased is by itself cutting one of its existing links. The probability $W_2[k_2,k_2+1]$ is simply $1/(2N)$, where $1/N$ accounts for the probability of this introvert being selected, and $1/2$ is the rate of updating the cross links. Since only extroverts not already connected to an introvert can add links to it, $W_2[k_2+1,k_2]$ is the rate of an extrovert making a new link to the chosen introvert. The probability of selecting an extrovert not already connected to it is $(N_1-k_2)/N$, and with rate $1/2$ it will add a cross link. Additionally, this action will be taken on the target introvert with probability $1/(N_2-\langle k_1\rangle)$, where $\langle k_1\rangle$ is an approximation for the degree of an extrovert. Following the argument above for $W_2[k_2+1,k_2]$, we have

$$W_2[k_2+1,k_2] = \frac{N_1-k_2}{2N(N_2-\langle k_1\rangle)}. \tag{7.3}$$

With explicit expression for W_2's, using Eqn. (7.2), we can get a recursion relation for $\rho_2^{\times}$

$$\frac{N_1 - k_2}{2N(N_2 - \langle k_1 \rangle)} \rho_2^{\times}(k_2) = \frac{1}{2N} \rho_2^{\times}(k_2 + 1). \tag{7.4}$$

Following the above analysis, a similar argument leads to $W_1[k_1 + 1, k_1] = 1/(2N)$, and $W_1[k_1, k_1 + 1] = (k_1 + 1)/(2N\langle k_2 \rangle)$, so that we obtain

$$\frac{1}{2N} \rho_1^{\times}(k_1) = \frac{k_1 + 1}{2N\langle k_2 \rangle} \rho_1^{\times}(k_1 + 1). \tag{7.5}$$

Obviously, if $\langle k_1 \rangle$ and $\langle k_2 \rangle$ are given, we can solve for $\rho_1^{\times}$ and $\rho_2^{\times}$ by using Eqn. (7.5) and (7.4), respectively. Note that in general, $\langle k_1 \rangle$ is different from $\langle k_2 \rangle$. Instead, a more general form, $N_1\langle k_1 \rangle = N_2\langle k_2 \rangle$, is always true. In our study, however, we limit ourselves to the special regime where $N_1 = N_2$, so that, we can safely say $\langle k_1 \rangle = \langle k_2 \rangle$. So far, $\langle k_1 \rangle$ and $\langle k_2 \rangle$ are unknown quantities. To obtain their values, we have to know $\rho_1^{\times}$ and $\rho_2^{\times}$ first, which seems to lead us to an endless loop. But again we can use a self-consistent approach as in the XIE model. Recall that the definitions of $\langle k_1 \rangle$ and $\langle k_2 \rangle$ are

$$\langle k_1 \rangle \equiv \sum_0^{N_2} k_1 \rho_1^{\times}(k_1), \langle k_2 \rangle \equiv \sum_0^{N_1} k_2 \rho_2^{\times}(k_2). \tag{7.6}$$

We can pretend to know $\langle k_1 \rangle$, and plug it into Eqn. (7.4) and then determine all $\rho_2^{\times}$'s. Given $\rho_2^{\times}$, it is trivial to obtain $\langle k_2 \rangle$ by definition. Then, $\rho_1^{\times}$'s can be found through Eqn. (7.5), and in turn, we can get an output for $\langle k_1 \rangle$. By adjusting the input $\langle k_1 \rangle$, we can decrease the difference between the input and output $\langle k_1 \rangle$'s, and get satisfiable $\rho_1^{\times}$ and $\rho_2^{\times}$. The result is a prediction (i.e., no fitting parameters) for $\rho_1^{\times}$ and $\rho_2^{\times}$, plotted as solid lines in Fig. 7.3(b). The predictions and simulation results agree quite well for the introverts, $\rho_2^{\times}$ in our case, as well as for the mean of $\rho_1^{\times}$ though; however, the prediction is notably satisfactory for the whole distribution of $\rho_1^{\times}$. The failure can be roughly understood by the following arguments. When we invoke Eqn. (7.4) and (7.5), we approximate k_1 and k_2, the cross degree of each extrovert and introvert, by the averages, $\langle k_1 \rangle$ and $\langle k_2 \rangle$, respectively. $\rho_1^{\times}$ is a relatively narrower distribution, so the approximation works well. By contrast, $\rho_2^{\times}$ is very broad, distributed from 50 to ~ 280. Therefore, k_2 is poorly estimated by $\langle k_2 \rangle$.

Although a improved theory will be needed to provide better quantitative agreement, most features of the degree distributions are understood. Finally, we present a brief description of

X, see Fig. 7.2 (blue). Compared to $X(t)$ of a symmetric system (red), the fluctuation here is $\sigma \simeq 51.3$, approximately 5 times larger than σ of the symmetric case. This is consistent with $\rho_1^\times$ and $\rho_2^\times$ being broader distributions.

7.2 Preferred ratio model

Starting with preferred degree networks, there are many possible ways to couple two networks together. So far, we have presented two ways to model the interaction: via χ controlling the interaction strength, or via separate preferred degrees (κ^* and $\kappa^\times$) managing the intra- and inter-group links independently. Here, we consider the case, where the nodes prefer a certain ratio of cross degree to total degree.

7.2.1 Model description

We first consider two separate preferred degree networks, of size N_1 and N_2. Of course, the sizes and preferred degrees of the two networks can vary in general. To make our simulation results comparable to our previous studies, we choose $N_\alpha = 1000$, and $\kappa_\alpha = 250$. Now we introduce the new feature of this model, namely, we specify the ratio of cross degree and total degree ($k_\alpha^\times/k_\alpha$) of each node. To realize this feature, clearly, a new parameter is needed, i.e., the *preferred ratio*, $\gamma \in [0, 1]$. All nodes in the same group are assigned the same γ, and they try to reach and maintain their preferred ratio, by adding or cutting links: If a node finds its current ratio $k^\times/k$, denoted by r, smaller than γ, it will either cut an internal link or add a cross link when it is selected to update its links. Otherwise, the node will either add an internal link or cut a cross link when chosen. In that sense, no matter the value of κ, the greater γ is, the more the nodes prefer to have cross links. Generally, the two networks may be assigned distinct γ's, and later we will see that, with $\gamma_1 = \gamma_2$, the system exhibits very interesting properties.

Let us introduce the definition of this model. In each attempt of updating a link, a node is selected amongst all N nodes at random, and its total degree k and cross degree $k^\times$ are noted. If $k < \kappa$, the node will add a link. Otherwise, it will cut a link. Whether the action is applied on an intra- or inter-group link is determined by the preferred ratio γ. Let us first look at the case of adding a link. We first compute the current ratio r $(= k^\times/k)$ of the chosen node. If

$r < \gamma$, it means this node has fewer cross links than it prefers. To reach the preferred ratio, it will need to add a cross link. Otherwise, if $r \geq \gamma$, it seeks to decrease the ratio by adding an internal link. In the situation of the selected node needing to cut a link, a similar process takes place. If $r < \gamma$, to increase r, the node has to cut an internal link, and otherwise, the node will cut a cross link. Self-loops or multiple connections are not allowed. In our simulation, one Monte Carlo step (MCS) consists of N such attempts of adding or cutting links, so that on average, each node has one chance to be selected to update its links.

With the parameter γ specifying the $k^{\times}/k$ ratio, we can easily control how the links of a node are distributed between internal and cross links. By choosing γ at extreme values, 0 and 1, we explore special cases. Clearly, when $\gamma = 0$, the nodes prefer no cross links, which in turn, leads us to two separate preferred degree networks. At the other end, where $\gamma = 1$, a system only having cross links is achieved.

Let us point out the difference of this preferred-ratio model to the other models studied in this thesis. Let us first consider the model discussed in Chapter 5. There, we introduced the parameter χ, which determines the probability with which an action is taken on cross links vs. internal links. However, χ does not imply a preference for adding as opposed to cutting cross links. By contrast, with preferred ratio γ, the model can precisely control the r of each node. Next, we turn to the two-κ model, discussed in Section 7.1. At first glance, the two model might look superficially similar, by setting $\kappa^{\times}/(\kappa^{*} + \kappa^{\times}) = \gamma$. Their underlying difference resides in the fact that the two-κ model has separate $\kappa^{\times}$ and κ^{*}, so that updates of internal degrees are independent from the cross degrees and vice versa. In contrast, in the preferred ratio model, each time when a node decides to add or cut a cross link, it needs to look at its current ratio r first, where both $k^{\times}$ and k^{*} play a role. As a result, $k^{\times}$ and k^{*} are no longer independent from each other in this model. This leads to notable differences in the observed behaviors.

7.2.2 Statistical properties of the degree distributions

To study the topological properties of this model, we focus on its degree distributions. In our simulations, the first $2K$ MCS are discarded. Our result is an average over 10^4 measurements, each separated by 100 MCS. We always fix $N_1 = N_2$ and $\kappa_1 = \kappa_2$ here, and change γ. We

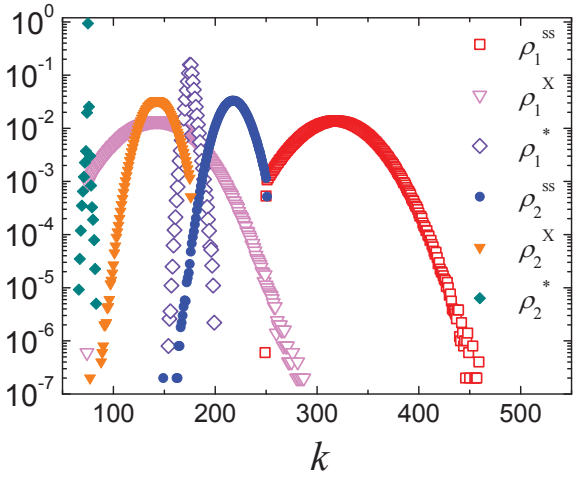

Figure 7.4 Simulation results of the degree distributions for an asymmetric system with $N_\alpha = 1000$, $\kappa_\alpha = 250$, $\gamma_1 = 0.3$, and $\gamma_2 = 0.7$.

discover that similar to the previous model, the degree distributions of the preferred ratio model also show a sensitivity to the symmetry of the system parameters ($\gamma_1 = \gamma_2$ or $\gamma_1 \neq \gamma_2$).

In Fig. 7.4, we present a typical plot of the degree distributions for systems with asymmetric parameters. γ is 0.3 and 0.7 for the two networks, respectively. The nodes in both networks prefer to have $\kappa = 250$ links in total. While each node in network 1 prefers 75 ($= 250 \times 0.3$) cross links, every node in network 2 seeks 175 ($= 250 \times 0.7$) cross links. Therefore, there is a huge difference between the preferred cross degrees of the two groups, resulting in frustration between the networks. It is very challenging to understand the total degree distributions (which are not Laplacian distributions centered at κ any more), let alone the detailed degree distributions.

The system with symmetric parameter sets, i.e., $\gamma_1 = \gamma_2$, seems much easier to understand at first glance. The simulation results are presented in Fig 7.5. When the two networks have the same preferred ratios, clearly, there is no frustration. Therefore, we can observe sharply peaked total degree distributions, i.e., Laplacians, for both networks. However, if we shift our attention to the other four degree distributions, ρ_1^*, $\rho_1^\times$, ρ_2^* and $\rho_2^\times$, interesting features are noted, some of them understandable, and others puzzling. The four subfigures correspond to different values of γ's. In each subfigure, we observe that two of the detailed degree distributions fall onto a single point, and the other two are simple Laplacians. The value of γ determines which of the

four distributions are single valued versus Laplacians.

One class of their detailed degree distributions, either internal or cross, only has one value, and the other class, is exactly like the total degree distributions, i.e., Laplacian distributions (with shifted means of course). Recall that our discussion on the relation between the total and detailed degree distributions indicates, in general, ρ_α cannot be obtained from ρ^*_α and $\rho^\times_\alpha$. In this particular case, however, ρ_α is simply $\rho^*_\alpha + \rho^\times_\alpha$. The means of the distributions agree with the preferred ratios well, e.g., for Fig. 7.5(a), $\langle k^\times \rangle \simeq 171.5$ and $\langle k \rangle \simeq 250.5$, and therefore, $\langle k^\times \rangle / \langle k \rangle \simeq 0.6846 \simeq \gamma$. Note that the systems shown in (a) and (b) ((c) and (d)) have very close γ's, i.e., $\gamma = 0.6845$ and 0.683 in (a) and (b), respectively, and $\gamma = 0.301$ and 0.299 in (c) and (d), respectively. Though the γ's in (a) and (b) are very close to each other, a significant difference between their degree distributions is noted. In (a), the ρ^*_1 and ρ^*_2 are both single valued distributions, and $\rho^\times_1$ and $\rho^\times_2$ are both Laplacian distributions. However, it is the other way around in (b). We find that the difference is due to the choices of γ: If $\gamma \in [k^\times/\kappa, (k^\times + 1)/(\kappa + 1)]$, $\rho^\times_\alpha$ will be a Laplacian distribution, and ρ^*_α will be a single valued distribution (see (a) and (c)). If $\gamma \in [k^\times/\kappa, k^\times/(\kappa + 1)]$, $\rho^\times_\alpha$ and ρ^*_α will be a single valued distribution and a Laplacian distribution, respectively (see (b) and (d)). However, a careful theoretical explanation still remains to be established.

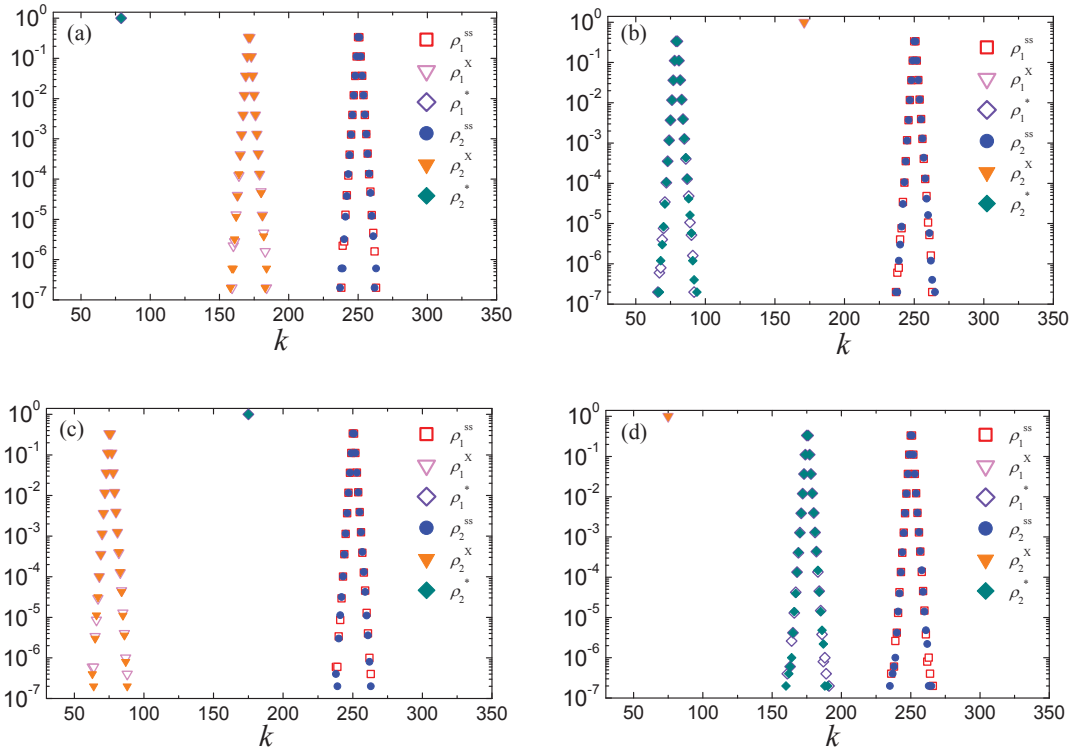

Figure 7.5 Simulation results of the degree distributions for symmetric systems with $N_\alpha = 1000$, $\kappa_\alpha = 250$, and $\gamma_1 = \gamma_2$. $\gamma_\alpha = 0.6845$ (a), 0.683 (b), 0.301 (c), and 0.299 (d).

CHAPTER 8. SUMMARY

In this thesis, we first introduce the idea of a stochastically evolving network with preferred degrees, namely the preferred degree network model, in which the nodes can dynamically form and break connections to reach and maintain a pre-assigned number of contacts (preferred degree κ). First, a homogeneous population is studied, where each node is assigned the same κ. Specifically, when selected, a node, with degree k, creates (destroys) a new (an existing) link with probability $w(k)$ $(1 - w(k))$, where $w(k)$ is referred to as the rate function, valued in $[0, 1]$. The partner node is chosen at random from all the remaining nodes. In the form of a Fermi-Dirac function, the rate function reflects how flexible an individual is, by varying β (Eqn. (3.1)). Even in such a simple model, the dynamics violates detailed balance, and as a consequence, it is quite difficult to obtain an analytically exact approach. Instead, we explore the statistical properties by Monte Carlo simulations and a variety of mean-field approaches. For a single-network model with $N = 1000$ nodes and $\kappa = 250$, we discover that the network settles into a steady state quite quickly (within $1K$ MCS). For the most rigid population (with $\beta \to \infty$), the degree distribution is found to be a symmetric exponential distribution, centered at κ. Moreover, it is found to be consistent with a Laplacian distribution: $\rho^{ss}(k) \propto e^{-\mu|k-\kappa|}$, where $\mu = 1.08 \pm 0.01$ indicated by our data. The degree distribution of a more flexible population ($\beta = 0.1$ or 0.2) is Gaussian like around κ and crosses over to two exponential tails, characterized by the same decay rate as the most rigid population. A simple mean-field argument, in the context of an approximate master equation, leads to good agreement with the simulation results. Of course, the system will not display this type of behavior for extreme values of system parameters (e.g., $\kappa \to 0$), and we believe the theory will break down in those limits. Nevertheless, for generic points in parameter space, we are confident that the main features of this dynamic network have been captured by the mean-field theory.

With knowledge of a single preferred degree network, we introduce an interaction between such networks. To characterize such coupled networks, we need to introduce additional quantities to capture the statistical properties of our models. Specifically, links are now classified in terms of their end nodes, so that we can distinguish internal links, which connect nodes in the same group, from cross links, which join nodes from different networks. Accordingly, each node is associated with an internal degree k^*, a cross degree $k^\times$, and a total degree k $(= k^* + k^\times)$, and we can study the different classes of degree distributions (ρ^*, $\rho^\times$, and ρ). Besides these distributions, another very simple measure is the total number of cross links X, which directly reflects how strongly the two networks interact. For all interdependent network models, we examine a variety of degree distributions and X.

We first introduce a simple naive model, which is treated as a baseline model of interdependent networks. This model is essentially a single homogeneous network being partitioned into two subsets, labeled red and blue. Its $red - red$ $(blue - blue)$ and $red - blue$ $(blue - red)$ connections are treated as internal and cross links, respectively. Due to its simplicity, all of its features are trivial and well explained. Its total degree distribution is exactly the same as in a single preferred degree network, and the other two detailed degree distributions (ρ^* and $\rho^\times$) are well explained by binomial distributions. We find that $P^{ss}(X)$, the stationary distribution of X, is well described by a Gaussian distribution, with an easily predicted mean, $\langle X \rangle$, and standard deviation, σ.

Next, we introduce an interacting dynamic model with a new parameter, the interaction strength χ, which is the probability that a node adds or cuts a cross link. Thus, $\chi = 0$ corresponds to two completely isolated networks, while a system with $\chi = 1$ can be regarded as maximally coupled. With two networks present, we face a much larger parameter space of 6 dimensions: system size N_1 and N_2, preferred degree κ_1 and κ_2, and interaction strength χ_1 and χ_2. Therefore, we cannot explore the whole parameter space, and instead, focus on select cases which we expect to reflect the influence of each parameter (N, κ, χ) on the system. We start with a study of the degree distributions for three cases, where the two networks differ in only one of the three parameters. With moderate difference between the parameters of the two networks (e.g., N_1 is not much larger or smaller than N_2), the simulation results indicate

that the total degree distribution of each network is not significantly affected by the interaction between networks. By generalizing the mean-field theory for the single-network model, total ρ's can be reasonably well explained. The puzzles appear when we consider more detailed degree distributions, namely ρ^* and $\rho^\times$. Similar to the distributions of the simple relabeling network, we find ρ^* and $\rho^\times$ to be approximately binomial distributions on short time scales; however, on longer time scales, the distributions are found to drift. We believe that this slow wandering is associated with similar behavior of X, and thus, we turn our attention to the exploration of X. A careful comparison of X between two similar systems, namely a relabeling network model, and a symmetric two-network model, consisting of two identical networks coupled by $\chi = 1/2$, shows drastically different behavior of X. $P^{ss}(X)$ of the former is well described by a Gaussian distribution, and by contrast, $P^{ss}(X)$ of the latter displays a very broad and flat plateau, with much larger standard deviation. This observation suggests that this way of coupling two networks has a profound effect on the system. Thereafter, a more systematic study of X is carried out, as a function of the system parameters (N, κ, χ). Focusing on two measures, the mean, $\langle X \rangle$, and the standard deviation, σ, we can qualitatively understand most features of the simulation results, although a better theory will be needed to provide acceptable quantitative predictions. Remarkably, a kind of "universal behavior" of different systems is observed in a special regime, where the number of introverts is much smaller than the number of extroverts. In that regime, the distribution of X is independent of κ. We discover that this behavior of X can be traced to the extreme frustration of introverts: introverts never add links; instead, they only cut links to compensate for the links that are continuosly being created by the extroverts. As a result, the introverts have no internal links, and their state can be specified by their cross degrees alone. By formulating an approximation scheme for the cross degree distribution, we can successfully explain this phenomenon.

Thereafter, we continue our study on interacting preferred degree networks, and specifically, focus on an extreme case, the XIE model. By fixing the preferred degree of one network at the minimum and the other one at the maximum ($\kappa_I = 0$ and $\kappa_E = \infty$), the introverts only cut connections while the extroverts keep adding links. Consequently, there are no links among introverts, while the extroverts are connected to everyone else in their own population, so that

the dynamics is restricted on the cross links. We first examine the degree distributions and find that they exhibit a symmetry when their parameters, N_I and N_E, are symmetric. Further, we discover that when $N_I = N_E$, the degree distributions are broad and flat, in contrast to the sharply peaked ones in systems with non-equal N_I and N_E. With a self-consistent mean-field approximation, we understand the behaviors of the degree distributions quite well, except for the $N_I = N_E$ system. To explore that special case in more detail, we study the number of cross links, X. The simulation results for X show that the network experiences an unusually sharp transition, as the ratio N_I/N_E crosses 1. Specifically, the transition is driven by the change of the system geometry only. Thanks to the restoration of detailed balance, we find an explicit expression for the stationary distribution $\mathcal{P}^*$, which plays the role of the Boltzmann distribution for systems in thermal equilibrium. A mean-field theory provides some insight into much of the surprising behavior.

In addition to the models we have studied, there are many other possible ways to introduce an interaction between two networks. In the final chapter, we explore some of the other possibilities, and present results for two models involving different forms of interaction. In the two-κ model, an individual is allowed to have two κ's, to govern the actions on inter- and intra-group contacts separately. In the preferred ratio model, we assign a preferred ratio of cross degree and total degree to each node. For both models, we can understand some of their topological properties.

Beyond these initial findings, there are many avenues to explore other interacting dynamic networks. Here we present a few comments on how to extend our model to more realistic cases. First, in a society, instead of a single preferred degree, there is typically a distribution of preferences, and so one should really consider a set, $\{\kappa\}$. Second, in our models, every node can make connections to anyone else, which clearly fails to capture the more complex structures of the real society, separated by spatial distances and subtle ethnic divides. Third, we should explore more realistic models of real phenomena, where dynamic degrees of freedom, e.g., opinions, wealth, or health, are associated with the nodes. The topological structures of a network determine the states of the nodes, and these degrees of freedom of nodes in turn affect the topology of the network, leading to a coevolving network model. Beyond the preferred

degree networks, a worthy extension would be the understanding of the interactions between different types of networks, such as those listed in the Introduction. In most of the models with interactions, a phenomenon coined as "frustration" is observed. Aside from the standard concepts from statistical mechanics, in the study of interacting networks, we may need to quantify the notion of "frustration," ϕ. The simplest possibility is to start with the degree distribution of a node i, $Q_i(k)$, and define ϕ of node i as $\phi_i \equiv [\Sigma_{k>\kappa} - \Sigma_{k<\kappa}]Q_i(k)$. Therefore, ϕ vanishes if the node has as many links above its preferred degree as below, while it assumes the extreme values ± 1 when the node always has degrees above/below κ.

Clearly, the studies reported in this thesis have only scratched the surface of the vast range of possible interacting networks, leaving much more work to be done. In particular, it will be interesting and important to investigate the coupled networks in the real world.

APPENDIX A. STOCHASTIC DYNAMICS OF A SINGLE NETWORK: EXACT MASTER EQUATION AND VIOLATION OF DETAILED BALANCE

A single network can be described by an $N \times N$ adjacency matrix $\mathbb{A}$ (symmetric in our case, as the links are undirected), where the elements $a_{ij} = 0$ (1) indicate the absence (presence) of the link between nodes i and j. Since self-loops are not allowed, $a_{ii} = 0$ for all $i \in [1, N]$. A complete analytical description of the stochastic evolution of our model is provided by $\mathcal{P}(\mathbb{A}, t \mid \mathbb{A}_0, 0)$, which is the probability of finding configuration $\mathbb{A}$ at time t, given an initial configuration $\mathbb{A}_0$. Since we focus on a Markov process, we can write down the discrete master equation for $\mathcal{P}$ as follows. The change over one attempt, $\mathcal{P}(\mathbb{A}, t+1) - \mathcal{P}(\mathbb{A}, t)$ is

$$\sum_{\{\mathbb{A}'\}} [W(\mathbb{A}, \mathbb{A}')\mathcal{P}(\mathbb{A}', t) - W(\mathbb{A}', \mathbb{A})\mathcal{P}(\mathbb{A}, t)] \tag{A.1}$$

where $W(\mathbb{A}, \mathbb{A}')$ is the rate for configuration $\mathbb{A}'$ to change to $\mathbb{A}$. Note that, since each $\mathbb{A}$ has $\mathcal{L} \equiv N(N-1)/2$ elements, the configuration space in which $\mathcal{P}(\mathbb{A}, t)$ evolves consists of the $2^{\mathcal{L}}$ vertices of a unit cube in $\mathcal{L}$-dimensional space. In this setting, each attempt is seen to be just a step from one vertex to another along an edge of this cube.

Explicitly, W consists of a sum over terms, each corresponding to an attempt at changing the state of a link. We begin with the probability to choose a particular node, i: $1/N$. Next, we need its degree, k_i, which is obtained by summing up all elements along the row i : $k_i = \sum_j a_{ij}$. From here, we attempt to add a link with probability $w(k_i)$, or cut with probability $1 - w(k_i)$. Consider first the later case. A cutting action can occur for one of the k_i existing links, so that the total probability for a_{ij} to change from 1 to 0 (by node i) is $(1 - w(k_i))/(Nk_i)$. Meanwhile, none of the other links changes in this attempt. Thus, the term describing this action is

$$\Delta \frac{1 - w(k_i)}{Nk_i} \left(1 - a'_{ij}\right) a_{ij} \tag{A.2}$$

where

$$\Delta \equiv \Pi_{k\ell \neq ij} \delta \left(a'_{k\ell}, a_{k\ell} \right) \tag{A.3}$$

A similar term can be written to describe the adding action. All together, we have

$$W(\mathbb{A}, \mathbb{A}') = \sum_i \frac{\Delta}{N} \sum_{j \neq i} \left[\frac{1 - w\left(k_i\right)}{k_i} \left(1 - a'_{ij}\right) a_{ij} + \frac{w\left(k_i\right)}{N - 1 - k_i} a'_{ij} \left(1 - a_{ij}\right) \right]. \tag{A.4}$$

Once the rates are known explicitly, we can check if they satisfy detailed balance or not. The Kolmogorov criterion [109] states that a set of W's satisfies detailed balance if and only if the product of W's around *any* closed loop in configuation space is equal to that around the reversed loop. In our case, all loops can be regarded as sums over "elementary closed loops," i.e., ones which goes around a plaquette (or face) on our $\mathcal{L}$-cube. Thus, we only need to focus on such elementary loops. Clearly, such a loop involves two links, e.g., by adding two links from a given $\mathbb{A}$, followed by cutting them to return to the original $\mathbb{A}$. As a specific example, we start with an $\mathbb{A}$ which has neither an ij link nor an im one, then the sequence

$$\begin{pmatrix} a_{ij} \\ a_{im} \end{pmatrix} = \begin{pmatrix} 0 \\ 0 \end{pmatrix} \to \begin{pmatrix} 1 \\ 0 \end{pmatrix} \to \begin{pmatrix} 1 \\ 1 \end{pmatrix} \to \begin{pmatrix} 0 \\ 1 \end{pmatrix} \to \begin{pmatrix} 0 \\ 0 \end{pmatrix} \tag{A.5}$$

denotes adding these two and cutting them, while the rest of $\mathbb{A}$ is left unchanged. Apart from an overall factor of N^{-4}, the product of the W's associated with this loop is

$$\begin{aligned} &\left(\frac{w(k_i)}{N-1-k_i} + \frac{w(k_j)}{N-1-k_j} \right) \left(\frac{w(k_i+1)}{N-1-(k_i+1)} + \frac{w(k_m)}{N-1-k_m} \right) \times \\ &\left(\frac{1-w(k_i+2)}{k_i+2} + \frac{1-w(k_j+1)}{k_j+1} \right) \left(\frac{1-w(k_i+1)}{k_i+1} + \frac{1-w(k_m+1)}{k_m+1} \right) \end{aligned} \tag{A.6}$$

Now, the reversed loop can be denoted as

$$\begin{pmatrix} a_{ij} \\ a_{im} \end{pmatrix} = \begin{pmatrix} 0 \\ 0 \end{pmatrix} \to \begin{pmatrix} 0 \\ 1 \end{pmatrix} \to \begin{pmatrix} 1 \\ 1 \end{pmatrix} \to \begin{pmatrix} 1 \\ 0 \end{pmatrix} \to \begin{pmatrix} 0 \\ 0 \end{pmatrix} \tag{A.7}$$

associated with the product

$$\begin{aligned} &\left(\frac{w(k_i)}{N-1-k_i} + \frac{w(k_m)}{N-1-k_m} \right) \left(\frac{w(k_i+1)}{N-1-(k_i+1)} + \frac{w(k_j)}{N-1-k_j} \right) \times \\ &\left(\frac{1-w(k_i+2)}{k_i+2} + \frac{1-w(k_m+1)}{k_m+1} \right) \left(\frac{1-w(k_i+1)}{k_i+1} + \frac{1-w(k_j+1)}{k_j+1} \right) \end{aligned} \tag{A.8}$$

We can find the difference explicitly and verify that it does not vanish in general. To appreciate this fact more easily, note that, e.g., the factor $w(k_i)w(k_m)$ appears in (A.6) but not in (A.8). From these considerations, we conclude that detailed balance is violated here.

We should re-emphasize the following. In our case, the products of W's around many elementary loops are the same as those of the reversed loops (e.g., two links involving 4 different vertices). However, detailed balance is satisfied only if *all* loops are "reversible." Thus, showing just one "failed loop" is sufficient for us to conclude that detailed balance is violated.

APPENDIX B. STOCHASTIC DYNAMICS OF XIE MODEL: THE RESTORATION OF DETAILED BALANCE

With the explicit expression of the transition rates, we can check if the dynamic process of XIE model satisfies detailed balance or not. As stated in Kolmogorov criterion [109], detailed balance holds, if the product of transition rates around every closed loop in the configuration space is independent of the direction of the loop being traversed. Thus, it seems that we have to check the product of transition rates around any closed loops in the configuration space. However, our work can be simplified by taking into account of the following two facts. First, recalling that the dynamics only occurs on $\mathcal{N}$ cross links, we can reduce the configuration space to $2^{\mathcal{N}}$ dimensions. That allows us to consider the configuration space as a $\mathcal{N}$-cube, so that adding or cutting a link is associated to traverse along the edges of the $\mathcal{N}$-cube. Second, one "elementary closed loop" involves the creation and break of two links, and all loops can be regarded as sums over such loops. For example, a closed loop of updating three links, "adding ij (where ij stands for the link between node i and j), adding jl, adding lm, cutting ij, cutting jl, and cutting lm," can be viewed as the combination of three elementary loops, one involving "adding ij, adding jl, cutting ij, and cutting jl," the second involving "adding jl, adding lm, cutting jl, and cutting lm," and the third involving "adding lm, adding ij, cut cutting lm, and cutting ij." Thus, we only need to focus on the elementary loops. That is, we select two links to update, and check whether the Kolmogorov criterion is satisfied. Suppose we start with a configuration $\mathbb{N}$, where the ij and im links are absent ($n_{ij} = n_{im} = 0$). Let the states of node be such that i has k_i links, and j and m have p_j and p_m "holes," respectively. One way around the loop is adding these two links followed by cutting them, which can be denoted as

the sequence

$$\begin{pmatrix} n_{ij} \\ n_{im} \end{pmatrix} = \begin{pmatrix} 0 \\ 0 \end{pmatrix} \to \begin{pmatrix} 1 \\ 0 \end{pmatrix} \to \begin{pmatrix} 1 \\ 1 \end{pmatrix} \to \begin{pmatrix} 0 \\ 1 \end{pmatrix} \to \begin{pmatrix} 0 \\ 0 \end{pmatrix} \tag{B.1}$$

and leave the rest of $\mathbb{N}$ unchanged. The associated product of the transition rates is, apart from an overall factor of N^4

$$\frac{1}{p_j}\frac{1}{p_m}\frac{1}{k_i+2}\frac{1}{k_i+1} \tag{B.2}$$

Now, the reversed loop can be denoted as

$$\begin{pmatrix} n_{ij} \\ n_{im} \end{pmatrix} = \begin{pmatrix} 0 \\ 0 \end{pmatrix} \to \begin{pmatrix} 0 \\ 1 \end{pmatrix} \to \begin{pmatrix} 1 \\ 1 \end{pmatrix} \to \begin{pmatrix} 1 \\ 0 \end{pmatrix} \to \begin{pmatrix} 0 \\ 0 \end{pmatrix} \tag{B.3}$$

associated with the product

$$\frac{1}{p_m}\frac{1}{p_j}\frac{1}{k_i+2}\frac{1}{k_i+1} \tag{B.4}$$

which is exactly equal to B.2, so that Kolmogorov criterion is satisfied here. Thus, the detailed balance holds and our system will eventually approach to a stationary distribution.

BIBLIOGRAPHY

[1] Albert R, Jeong H and Barabási A-L, Diameter of the world wide web, 1999 *Nature* **401** 130

[2] Barabási A-L and Albert R, Emergence of Scaling in Random Networks, 1999 *Science* **286** 509

[3] Adamic L A and Huberman B A, Power-law distribution of the world wide web, 2000 *Science* **287** 2115

[4] Strogatz S H, Exploring complex networks, 2001 *Nature* **410** 268

[5] Albert R and Barabási A-L, Statistical mechanics of complex networks, 2002 *Rev. Mod. Phys.* **74** 47

[6] Dorogovtsev S N and Mendes J F F, Evolution of networks, 2002 *Adv. Phys.* **51** 1079

[7] Newman M E J, The structure and function of complex networks, 2003 *SIAM Rev.* **45** 167

[8] Estrada E, Fox M, Higham D and Oppo G-L (eds), 2010 *Network Science: Complexity in Nature and Technology* (Springer, New York)

[9] Williams R J and Martinez N D, Simple rules yield complex food webs, 2000 *Nature* **404** 180

[10] Camacho J, Guimerá R and Amaral1 L A N, Robust patterns in food web structure, 2002 *Phys. Rev. L* **88** 22

[11] Montoya J M and Solé R V, Small world patterns in food webs, 2002 *J. theor. Biol* **214** 405

[12] Zia R K P, Liu W, Jolad S and Schmittmann B, Studies of adaptive networks with preferred degree, 2011 *Physics Procedia* **15** 102

[13] Jolad S, Liu W, Schmittmann B and Zia R K P, Epidemic spreading on preferred degree adaptive networks, 2012 *PLoS ONE* **7(11)** e48686

[14] Newman M E J, Scientific collaboration networks: I. Network construction and fundamental results, 2001 *Phys. Rev. E* **64** 016131

[15] Newman M E J, Scientific collaboration networks: II. Shortest paths, weighted networks, and centrality, 2001 *Phys. Rev. E* **64** 016132

[16] Wasserman S and Faust K (eds), 1994 *Social Network Analysis: Methods and Applications* (Cambridge: Cambridge University Press)

[17] Watts D J, Strogatz S H, Collective dynamics of small-world networks, 1998 *Nature* **393** 440

[18] Erdős P and Rényi A, On random graphs, 1959 *Publ. Math. Debrecen* **6** 290

[19] Erdős P and Rényi A, On the evolution of random graphs, 1960 *Publ. Math. Inst. Hungar. Acad. Sci.* **5** 17

[20] Erdős P and Rényi A, On the strength of connectedness of a random graph, 1961 *Acta Math. Acad. Sci. Hungar.* **12** 261

[21] Newman M E J, Strogatz S H and Watts D J, Random graphs with arbitrary degree distributions and their applications, 2001 *Phys. Rev. E* **64** 026118

[22] Milgram S, The small world problem, 1967 *Psych. Today* **2** 60

[23] Travers J and Milgram S, An experimental study of the small world problem, 1969 *Sociometry* **32** 425

[24] Garfield E, Its a small world after all, 1979 *Current Contents* **43** 5

[25] Faloutsos M, Faloutsos P and Faloutsos C, On power-law relationships of the internet topology, 1999 *Comp. Comm. Rev.* **29** 251

[26] Kleinberg J M, Kumar R, Raghavan P, Rajagopalan S and Tomkins A S, 1999 *Computing and Combinatorics* (Springer, Berlin)

[27] Watts D J, Networks, dynamics, and the small-world phenomenon, 1999 *Am. J. Sociol.* **105** 493

[28] Barabási A-L, 2002 *Linked: The New Science of Networks* (Cambridge: Perseus Publishing)

[29] Albert R, Jeong H and Barabási A-L, Mean-field theory for scale-free random networks, 1999 *Physica A* **272** 173

[30] Barabási A-L, Albert R and Jeong H, Scale-free characteristics of random networks: the topology of the world wide web, 2000 *Physica A* **281** 69

[31] Mariolis P, Interlocking directorates and control of corporations: The theory of bank control, 1975 *Social Sci. Quart.* **56** 425

[32] Mizruchi M S, 1982 *The American Corporate Network, 1904C1974* (Beverly Hills: Sage Publications)

[33] Moreno J L, 1934 *Who Shall Survive?* (Beacon House)

[34] Roethlisberger F J and Dickson W J, 1939 *Management and the Worker* (Harvard University Press)

[35] Liljeros F, Edling C R, Amaral L A N, Stanley H E and Åberg Y, The web of human sexual contacts, 2001 *Nature* **411** 907

[36] Grossman J W and Ion P D F, On a portion of the well-known collaboration graph, 1995 *Congr. Numer.* **108** 129

[37] Melin G and Persson O, Studying research collaboration using co-authorships, 1996 *Scientometrics* **36** 363

[38] Castro R D and Grossman J W, Famous trails to Paul Erdős, 1999 *Math. Intelligencer* **21** 51

[39] Batagelj V and Mrvar A, Some analyses of Erdős collaboration graph, 2000 *Social Networks* **22** 173

[40] Newman M E J, The structure of scientific collaboration networks, 2001, *Proc. Natl Acad. Sci. USA* **98** 404

[41] Barabási A-L, Jeong H, Ravasz E, Schuberts Z N A and Vicsek T, Evolution of the social network of scientific collaborations, 2002 *Phys. A* **311** 590

[42] Watts D J, 1999 *Small Worlds* (Princeton University Press)

[43] Amaral L A N, Scala A, Barthélémy M and Stanley H E, Classes of small-world networks, 2000 *Proc. Natl. Acad. Sci. USA* **97** 11149

[44] Price D J D S, Networks of scientific papers, 1965 *Science* **149** 510

[45] Egghe L and Rousseau R, 1990 *Introduction to Informetrics : quantitative methods in library, documentation and information science* (Elsevier, Amsterdam)

[46] Seglen P O, The skewness of science, 1992, *J. Am. Soc. Inform. Sci.* **43** 628

[47] Redner S, How popular is your paper? An empirical study of citation distribution, 1998, *Eur. Phys. J. B* **4** 131

[48] Krapivsky P L, Redner S and Leyvraz F, Connectivity of growing random network, 2000 *Phys. Rev. Lett.* **85** 4629

[49] Tsallis C and De Albuquerque M P, Are citations of scientific papers a case of nonextensivity?, 2000, *Eur. Phys. J. B* **13** 777

[50] Jeong H, Néda Z and Barabási A-L, Measuring preferential attachment for evolving networks, 2001 *EPL* **61** 567

[51] Krapivsky P L and Redner S, Organization of growing random networks, 2001 *Phys. Rev. E* **63** 066123

[52] Vázquez A, Statistics of citation networks, 2001 *arXiv preprint* **arXiv:cond-mat/0105031**

[53] White H D, Wellman B and Nazer N, Does citation reflect social structure? Longitudinal evidence from the "Globenet" interdisciplinary research group, 2004 *J. Am. Soc. Inform. Sci. Tech.* **55** 111

[54] Broder A, Kumar R, Maghoul F, Raghavan P, Rajagopalan S, Stata R, Tomkins A and Wiener J, Graph structure in the web, 2000 *Computer Networks* **33** 309

[55] Huberman B A, 2001 *The Laws of the Web* (MIT Press, Cambridge)

[56] Flake G W, Lawrence S R, Giles C L and Coetzee F M, Self-organization and identification of Webc ommunities, 2002 *IEEE Computer* **35** 66

[57] Fell D A and Wagner A, The small world of metabolism, 2000 *Nature Biotechnology* **18** 1121

[58] Jeong H, Tombor B, Albert R, Oltvai Z N and Barabási A-L, The large-scale organization of metabolic networks, 2000 *Nature* **407** 651

[59] Podani J, Oltvai Z N, Jeong H, Tombor B, Barabási A-L and Szathmary E, Comparable system-level organization of Archaea and Eukaryotes, 2001 *Nature Genetics* **29** 54

[60] Wagner A and Fell D, The small world inside large metabolic networks, 2001 *Proc. Roy. Soc. London Ser. B* **268** 1803

[61] Stelling J, Klamt S, Bettenbrock K, Schuster S and Gilles E D, Metabolic network structure determines key aspects of functionality and regulation,2002 *Nature* **420** 190

[62] Solé R V and Montoya J M, Complexity and fragility in ecological networks, 2001 *Proc. Roy. Soc. London Ser. B* **268** 2039

[63] Dunne J A, Williams R J and Martinez N D, Food-web structure and network theory: The role of connectance and size, 2002 *Proc. Natl. Acad. Sci. USA* **99** 12917

[64] Dunne J A, Williams R J and Martinez N D, Network structure and biodiversity loss in food webs: Robustness increases with connectance, 2002 *Ecology Lett.* **5** 558

[65] Williams R J, Berlow E L, Dunne J A, Barabási A-L and Martinez N D, Two degrees of separation in complex food webs, 2002 *Proc. Natl. Acad. Sci. USA* **99** 12913

[66] Sporns O, Tononi G and Edelman G M, Theoretical neuroanatomy: Relating anatomical and functional connectivity in graphs and cortical connection matrices, 2000 *Cerebral Cortex* **10** 127

[67] Sporns O, Network analysis, complexity, and brain function, 2002 *Complexity* **8** 56

[68] Dorogovtsev S N, Goltsev A V and Mendes J F F, Critical phenomena in complex networks, 2008 *Rev. Mod. Phys.* **80** 1275

[69] Dornic I, Chaté H, Chave J and Hinrichsen H, Critical Coarsening without Surface Tension: The Universality Class of the Voter Model, 2001 *Phys. Rev. Lett.* **87** 045701

[70] Galam S, Minority opinion spreading in random geometry, 2002 *Eur. Phys. J. B* **25** 403

[71] Pastor-Satorras R and Vespignani A, Epidemic dynamics and endemic states in complex networks,2001 *Phys. Rev. E* **63** 066117

[72] Conservation laws for the voter model in complex networks Suchecki K, Eguiluz V M and San Miguel M, 2005 *EPL* **69** 228

[73] Moore C and Newman M E J, Epidemics and percolation in small-world networks, 2000 *Phys. Rev. E* **61** 5678

[74] Castellano C, Vilone D and Vespignani A, Incomplete ordering of the voter model on small-world networks, 2003 *EPL* **63** 153

[75] Vilone D and Castellano C, Solution of voter model dynamics on annealed small-world networks, 2004 *Phys. Rev. E* **69** 016109

[76] Gross R, D'Lima C J D and Blasius B, Epidemic Dynamics on an Adaptive Network, 2006 *Phys. Rev. Lett.* **96** 208701

[77] Gross T and Blasius B, Adaptive coevolutionary networks: a review, 2008 *J. R. Soc. Interface* **5** 259

[78] Vazquez F, Eguíluz V M and Miguel M S, Generic absorbing transition in coevolution dynamics, 2008 *Phys. Rev. Lett.* **100** 108702

[79] Nardini C, Kozma B and Barrat A, Whos Talking First? Consensus or lack thereof in coevolving opinion formation models, 2008 *Phys. Rev. Lett.* **100** 158701

[80] Fu F and Wang L, Coevolutionary dynamics of opinions and networks: From diversity to uniformity, 2008 *Phys. Rev. E* **78** 016104

[81] Gil S and Zanette D, Coevolution of agents and networks: Opinion spreading and community disconnection, 2006 *Phys. Lett. A* **356** 89

[82] Benczik I J, Benczik S Z, Schmittmann B and Zia R K P, Lack of consensus in social systems, 2008 *EPL* **82** 48006

[83] Benczik I J, Benczik S Z, Schmittmann B and Zia R K P, Opinion dynamics on an adaptive random network, 2009 *Phys. Rev. E* **79** 046104

[84] Jolad S, Liu W, Schmittmann B, Zia R K P, Epidemic spreading on preferred degree adaptive networks, 2011 *PloS one* **7** e48686

[85] Peerenboom J, Fischer R and Whitfield R, Recovering from disruptions of interdependent critical infrastructures, 2001 *Proc. CRIS/DRM/IIIT/NSF Workshop Mitigat. Vulnerab. Crit. Infrastruct. Catastr. Failures*

[86] Rinaldi S., Peerenboom J and Kelly T, Identifying, understanding, and analyzing critical infrastructure interdependencies, 2001 *IEEE Contr. Syst. Mag.* **21** 11

[87] Kurant M and Thiran P, Layered complex networks, 2006 *Phys. Rev. Lett.* **96** 138701

[88] Laprie J C, Kanoun K and Kaniche M, Modeling interdependencies between the electricity and information infrastructures, 2007 *SAFECOMP-2007* **4680** 54

[89] Panzieri S and Setola R, Failures propagation in critical interdependent infrastructures, 2008 *Int. J. Model. Ident. Contr.* **3** 69

[90] Rosato V, Issacharoff L, Tiriticco F, Meloni S, Porcellinis S and Setola R, Modelling interdependent infrastructures using interacting dynamical models, 2008 *Interna- tional Journal of Critical Infrastructures* **4** 63

[91] Uetz P, Giot L, Cagney G, Mansfield T A, Judson R S, Knight J R, Lockshon D, Narayan V, Srinivasan M, Pochart P, Qureshi-Emili A, Li Y, Godwin B, Conover D, Kalbfleisch T, Vijayadamodar G, Yang M, Johnston M, Fields S and Rothberg J M, A comprehensive analysis of proteinCprotein interactions in saccharomyces cerevisiae, 2000 *Nature* **403** 623

[92] Ito T, Chiba T, Ozawa R, Yoshida M, Hattori M and Sakaki Y, A comprehensive two-hybrid analysis to explore the yeast protein interactome, 2001 *Proc. Natl. Acad. Sci. USA* **98** 4569

[93] Jeong H, Mason S, Barabási A-L and Oltvai Z N, Lethality and centrality in protein networks, 2001 *Nature* **411** 41

[94] Maslov S and Sneppen K, Specificity and stability in topology of protein networks, 2002 *Science* **296** 910

[95] Solé R V and Pastor-Satorras R, Complex networks in genomics and proteomics, 2003 *Handbook of Graphs and Networks* 145 (S. Bornholdt and H. G. Schuster (eds), Wiley-VCH, Berlin)

[96] Buldyrev S V, Parshani R, Paul G, Stanley H E and Havlin S, Catastrophic cascade of failures in interdependent networks, 2010 *Nature (London)* **464** 1025

[97] Parshani R, Buldyrev S V and Havlin S, Interdependent networks: Reducing the coupling strength leads to a change from a first to second order percolation transition, 2010 *Phys. Rev. Lett.* **105** 48701

[98] Buldyrev S V, Shere N W and Cwilich G A, Interdependent networks with identical degrees of mutually dependent nodes, 2011 *Phys. Rev. E* **83** 016112

[99] Huang X, Shao S, Wang H, Buldyrev S V, Stanley H E and Havlin S, The Robustness of Interdependent Clustered Networks, 2013 *EPL* **101** 18002

[100] Huang X, Vodenska I, Havlin S and Stanley H E, Cascading failures in bi-partite graphs: Model for systemic risk propagation, 2013 *Scientific Reports* **3** 1219

[101] Leicht E A and D'Souza R M, Percolation on interacting networks, 2009 *arXiv preprint* **arXiv:0907.0894**

[102] Vespignani A, Complex networks: The fragility of interdependency, 2010 *Nature (London)* **464** 984

[103] Parshani R, Rozenblat C, Ietri D, Ducruet C and Havlin S, Inter-similarity between coupled networks, 2010 *EPL* **92** 68002

[104] Pocock M J O, Evans D M and Memmott J, The robustness and restoration of a network of ecological networks, 2012 *Science* **335** 973

[105] Platini T and Zia R K P, Network evolution induced by the dynamical rules of two populations, 2010 *J. Stat. Mech. Theory Exp.* **2010** P10018

[106] Zia R K P, Liu W and Schmittmann B, An extraordinary transition in a minimal adaptive network of introverts and extroverts, 2012 *Physics Procedia* **34** 124

[107] Liu W, Schmittmann B and Zia R K P, Extraordinary variability and sharp transitions in a maximally frustrated dynamic network, 2012 *EPL* **100** 66007

[108] Liu W, Jolad S, Schmittmann B and Zia R K P, Modeling interacting dynamic networks: I. Preferred degree networks and their characteristics, 2013 *J. Stat. Mech. Theory Exp.* **2013** P08001

[109] Kolmogorov A N, 1936 *Math. Ann.* **112** 155